CHALMERS
UNIVERSITY OF TECHNOLOGY

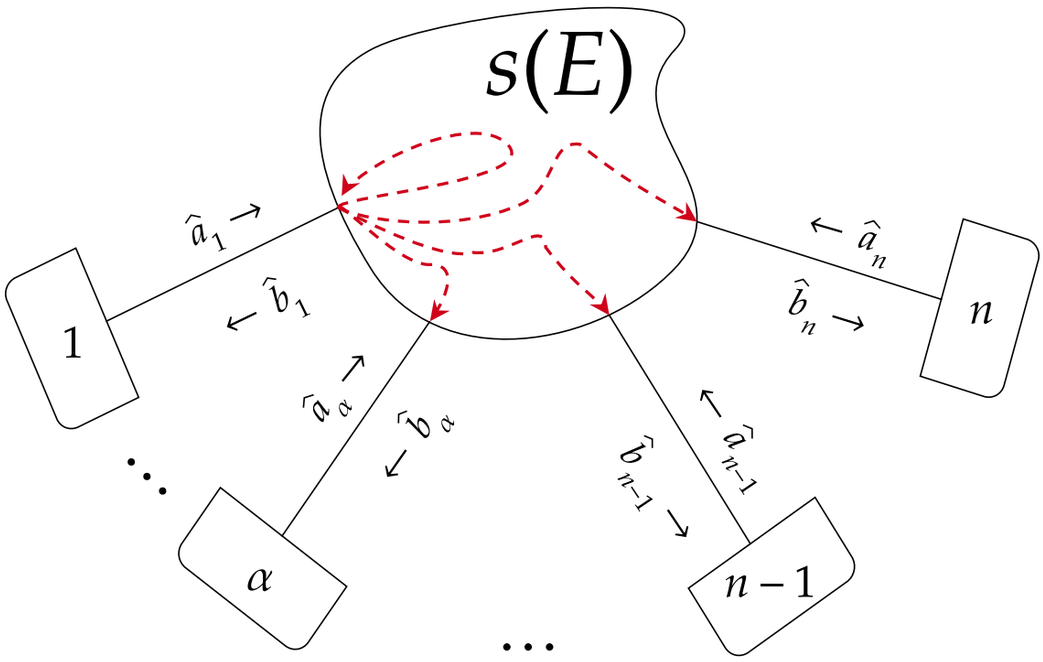


$$\left(S^{(0)}_{\alpha\alpha} - \frac{2h}{B_\alpha}\left|I^{(0)}_\alpha\right|^2\right) \geq \frac{4\left|I^{(\nu)}_\alpha\right|^2}{\left(S^{(\nu)}_{\alpha\alpha} - \frac{2h}{B_\alpha}\left|I^{(\nu)}_\alpha\right|^2\right)}$$

$$\sum_{\alpha=1}^{n}\sqrt{\left(S^{(0)}_{\alpha\alpha} - \frac{2h}{B_\alpha}\left|I^{(0)}_\alpha\right|^2\right)\left(S^{(\Sigma)}_{\alpha\alpha} - \frac{2h}{B_\alpha}\left|I^{(\Sigma)}_\alpha\right|^2\right)} \geq 2\sigma \geq 4k_{\mathrm{B}}\frac{|I^{(0)}_\alpha|^2}{\left(S^{(0)}_{\alpha\alpha} - \frac{2h}{B_\alpha}\left|I^{(0)}_\alpha\right|^2\right)}$$

# Bounds on entropy production and its noise in bosonic systems

## Thermodynamic constraints on noise in the coherent transport of particles

Master's thesis in Physics

Didrik Palmqvist

Department of Microtechnology and Nanoscience
CHALMERS UNIVERSITY OF TECHNOLOGY
Gothenburg, Sweden 2024
www.chalmers.se

Master's thesis 2024

# Bounds on entropy production and its noise in bosonic systems

Thermodynamic constraints on noise in the coherent transport of particles

Didrik Palmqvist


CHALMERS
UNIVERSITY OF TECHNOLOGY

Department of Microtechnology and Nanoscience - MC2
*Applied Quantum Physics Laboratory*
Dynamics and Thermodynamics of Nanoscale devices group
Chalmers University of Technology
Gothenburg, Sweden 2024

Bounds on entropy production and its noise in bosonic systems
Thermodynamic constraints on noise in the coherent transport of particles
DIDRIK PALMQVIST



Supervisor: Prof. Janine Splettstößer [1], Ludovico Tesser [1]
Examiner: Prof. Janine Splettstößer [1]

Master's Thesis 2024
[1] Department of Microtechnology and Nanoscience - MC2
Applied Quantum Physics Laboratory
Dynamics and Thermodynamics of Nanoscale devices group
Chalmers University of Technology
SE-412 96 Gothenburg
Telephone +46 31 772 1000

Cover: Sketch of generic scattering theory setup, where reservoirs are connected by a central scattering region. Below are two central results of this thesis, constraints on precision of a current in coherent transport, and a bound on the total entropy production.

Typeset in LaTeX
Printed by Chalmers Reproservice
Gothenburg, Sweden 2024

Bounds on entropy production and its noise in bosonic systems
Thermodynamic constraints on noise in the coherent transport of particles
DIDRIK PALMQVIST
Department of Microtechnology and Nanoscience - MC2
Chalmers University of Technology

# Abstract

When describing the thermodynamics of a device we are often interested in quantifying its performance, e.g. by its efficiency in converting a resource into useful output. In a general setting this is characterized by the entropy production in a resource and entropy reduction in the working substance [26]. The efficiency is often a good measure of performance when working with macroscopic machines, but when we are interested in describing nanoscale devices other aspects of performance are important aswell. This is due to phenomena such as nonthermal resources being more common due to the typical thermalization scales [26], and quantum phenomena in the transport of particles such as coherence, interference and superposition [6]. A key difference is the presence of fluctuations, which can often be of the same magnitude as average quantities in nanoscale devices. Fluctuations or noise can limit the achievable precision in the thermodynamic performance of a device, and by extension its useful applications. To understand precision in nanoscale devices is thus of crucial importance when characterising performance.

In this thesis we consider multitermal nanoscale devices that can be described by scattering theory and the role fluctuations plays in their performance. The devices are modelled as reservoirs of particles connected to one dimensional leads where particles propagate coherently as waves. The leads are strongly coupled to each other in a scattering region [6]. Recently so called *trade-off relations* have been derived for such systems where the particles are fermions [2, 8], constraining precision. Fermions are a type of fundamental particle, obeying the Pauli exclusion principle, which states that two fermions can never occupy the same state at once. Examples of fermions are electrons and protons. In this thesis we are mainly concerned with another type of fundamental particle, namely bosons. In contrast to fermions, there is no limit to the number of bosons that can occupy the same state. This difference has multiple implications for quantum statistical mechanics and transport of the two particle types. One such difference is that bosons display bunching, they tend to "stick" together during transport which increases fluctuations, while fermions display anti-bunching, they stay apart which decreases fluctuations. In this thesis we extend the trade-off relations of Ref. [2, 8] to bosonic systems. Furthermore we make improvements to the relations of Ref. [2] which applies to both bosonic and fermionic systems. We are also able to include more quantum effects in the trade-off relations which can naturally be interpreted as bunching in the bosonic case and anti-bunching in the fermionic case. By doing this we see in which way bunching decreases precision in bosonic systems, while increasing it in fermionic systems. Finally we combine the two different types of relations to find an upper and lower bound on the total entropy production in a multiterminal device with thermal reservoirs described by scattering theory.

Keywords: Quantum thermodynamics, Quantum transport, Scattering theory, Condensed matter physics

# Acknowledgements

I want express my sincerest gratitude to my supervisors Ludovico Tesser and Janine Splettstößer, for their guidance and many interesting discussions. Without your support this project would truly not have been possible and I could not have wished for better supervisors. I also want to thank the Dynamics and Thermodynamics of Nanoscale devices group as a whole, which has always been welcoming and including and inspiring. I also want to thank Janine Splettstößer for allowing me to continue studying as a PhD in the her group, investigating the fundamental physics of nanoscale devices.

Didrik Palmqvist, Gothenburg, June 2024

# List of Acronyms

Below is the list of acronyms that have been used throughout this thesis:

| | |
|---|---|
| BE | Bose Einstein |
| TUR | Thermodynamic Uncertainty Relation |
| QTUR | Quantum Thermodynamic Uncertainty Relation |
| KUR | Kinetic Uncertainty Relation |
| FEB | Fluctuation Entropy production Bound |
| DFB | Dynamical Fluctuation Bound |
| QDFB | Quantum Dynamical Fluctuation Bound |
| CSI | Cauchy-Schwarz inequality |
| PSI | Pólya and Szegö's Inequality |
| HOM | Hong-Ou-Mandel |

# Nomenclature

Below is the nomenclature of indices, sets, parameters, and variables that have been used throughout this thesis.

## Indices

| | |
|---|---|
| $i$,$j$ | Channel indices |
| $\alpha, \beta$ | Reservoir indices |
| $\nu$ | c-weighted current index |

## Parameters

| | |
|---|---|
| $B_\alpha$ | Bandwidth of transport |
| $T_\alpha$ | Temperature of reservoir $\alpha$ |
| $\mu_\alpha$ | Chemical potential of reservoir $\alpha$ |
| $f_\alpha(E)$ | Average occupation of reservoir $\alpha$, at energy $E$ |
| $s_{\alpha i,\beta j}(E)$ | Scattering matrix |
| $C_\alpha^{(\nu)}(E, E')$ | Generalized charge |

## Variables

| | |
|---|---|
| $I_\alpha^{(\nu)}$ | Bosonic c-weighted current |
| $S_{\alpha\alpha}^{(\nu)}$ | Bosonic fluctuations |
| $S_{\alpha\alpha,\mathrm{cl}}^{(\nu)}$ | Bosonic classical fluctuations |
| $S_{\alpha\alpha,\mathrm{qu}}^{(\nu)}$ | Bosonic quantum fluctuations |
| $\tilde{S}_{\alpha\alpha}^{(\nu)}$ | Bunching-compensated fluctuations |
| $\mathcal{I}_\alpha^{(\nu)}$ | Fermionic c-weighted current |
| $\mathcal{S}_{\alpha\alpha}^{(\nu)}$ | Fermionic fluctuations |
| $\mathcal{S}_{\alpha\alpha,\mathrm{cl}}^{(\nu)}$ | Fermionic classical fluctuations |
| $\mathcal{S}_{\alpha\alpha,\mathrm{qu}}^{(\nu)}$ | Fermionic quantum fluctuations |
| $\tilde{\mathcal{S}}_{\alpha\alpha}^{(\nu)}$ | Anti-bunching-compensated fluctuations |
| $\Sigma$ | Entropy |
| $\sigma$ | Total entropy production |

# Contents

# List of Figures

# 1
# Introduction

## 1.1 The thermodynamics of nanoscale devices

Thermodynamics was an essential theoretical framework in the industrial revolution, during which it saw much of its development. It was used to describe the physics of steam and combustion engines by dealing with heat transfer and work production. These concepts are not exclusive to engines, and thermodynamics has since been applied to many fields, such as chemistry, biology, information theory, and meteorology, among others [24]. In general, thermodynamics has been extremely successful in describing macroscopic devices, and in today's age, it is more relevant than ever with the ever-increasing power consumption of modern technology. The deeper underlying theory behind thermodynamics is statistical mechanics, where one applies statistics to ensembles of a large number of microscopic degrees of freedom. Thermodynamics can be derived from statistical mechanics [24]. The success of thermodynamics and statistical mechanics lies in being able to treat systems consisting of a large number of degrees of freedom such that the interesting observables of the system are the average quantities and how they evolve. For example, if one considers a container full of gas, the interesting quantities to calculate would be its temperature, the volume it occupies, and how much pressure it is exerting on its environment, not the individual position and momentum of every single gas molecule. Partly because it would be an impossible task to either measure or calculate, but also because such detailed knowledge hardly would help in constructing technology, e.g., a heat engine from the system. The thermodynamic concept that encapsulates the statistical treatment of a system the best might be entropy. Originally coined by physicist Rudolf Clausius in the nineteenth century, the word entropy comes from combining energy with the Greek word tropē, which means change [16]. Clausius investigated how the usable energy of a steam engine decreased from the inlet to the outlet and used entropy to describe this. Later, Ludwig Boltzmann gave a definition of entropy based on statistical mechanics. In this definition, the entropy $\Sigma$, of a system is the product of the Boltzmann constant $k_{\mathrm{B}}$ and the logarithm of the number of microstates $\Omega$ compatible with a given macrostate of the system,

$$\Sigma = k_{\mathrm{B}} \log[\Omega]. \tag{1.1}$$

In this view, entropy can be associated with a degree of uncertainty in the specific state a system is in. Returning to the canister of gas, if this system is cooled, the average kinetic energy of the molecules would decrease, leading to fewer available microstates compared to if one were to heat the system. In both cases, the macrostates of the system would still be characterized by only its temperature, volume, and pressure, but the heated canister would have a larger number of microstates available compatible with the macrostate, thus a higher entropy. For closed systems, the change in entropy can be used as the most general way of characterizing the performance of a resource and its output. This follows from the famous second law of thermodynamics, which states that total entropy of a closed system always increases [24],

$$\frac{d}{dt}\Sigma \geq 0. \tag{1.2}$$

Dividing the system into a resource $R$ with entropy $\Sigma_{\mathrm{R}}$ that is performing work by producing entropy and a working substance $WS$ with entropy $\Sigma_{\mathrm{WS}}$ where work is performed and entropy is reduced, the second law tells us that

$$\frac{d}{dt}\Sigma_{\mathrm{R}} \geq -\frac{d}{dt}\Sigma_{\mathrm{WS}}. \tag{1.3}$$

Thus, if the entropy production in the resource is large, it potentially provides a lot of power, and if the entropy reduction is large, the energy conversion would be efficient. In thermal systems the entropy change is given by heat flows, however this line of thought is also applicable to nonthermal systems where there is not a well defined temperature for example. These types of nonthermal states are more common in small scale systems since they can be smaller than thermalization scales [26]. A common way to characterize the performance of a thermodynamic machine is through its efficiency $\eta$,

$$1 \geq \eta = \frac{|\Delta\Sigma_{\mathrm{WS}}|}{|\Delta\Sigma_{\mathrm{R}}|}, \tag{1.4}$$

which is a measure of how much of the provided work by the resource is being used to perform a useful output. Here $\Delta\Sigma_{\mathrm{WS}}$ and $\Delta\Sigma_{\mathrm{R}}$ are the total changes in entropy of the working substance and

resource, respectively. Such a measure is useful since it can give insight into the performance of a thermodynamic machine and how it could be improved, if at all possible. An example of this is the Carnot efficiency, which is the theoretical maximum efficiency for a classical heat engine using a hot and cold reservoir with temperatures $T_{\mathrm{H}}$ and $T_{\mathrm{C}}$ [24],

$$\eta = 1 - \frac{T_{\mathrm{C}}}{T_{\mathrm{H}}}. \tag{1.5}$$

The Carnot efficiency is interesting since a two-terminal heat engine could never outperform it, so it can serve as a guideline for the possibility of improving the realization of a proposed heat engine. Similarly, one can formulate other trade-off relations for telling us how technology can be improved, and a particularly relevant one to *nanoscale devices* is the trade-off between power and noise.

The thermodynamics of nanoscale devices which is the main focus of this masters thesis are conceptually different from their macroscopic counterparts for multiple reasons. Classical thermodynamics is based on describing systems consisting of such a large number of particles that only their average quantities matter. This obviously breaks down for nanoscale devices, where the number of particles is relatively small. To understand this, we can simply imagine an ensemble of $N$ independent constituent elements. We consider some observable $O$ of the ensemble defined by

$$O = \sum_{i}^{N} o_i, \tag{1.6}$$

where $o_i$ denotes the value of this observable for each individual element. We assume that each $o_i$ is independent and identically distributed. Under these assumptions, $O$ is distributed according to a normal distribution due to the central limit theorem,

$$\rho(O) = \frac{1}{\sqrt{\langle \Delta O^2 \rangle}\sqrt{2\pi}} \exp\left\{ -\frac{1}{2} \left( \frac{O - \langle O \rangle}{\sqrt{\langle \Delta O^2 \rangle}} \right)^2 \right\}. \tag{1.7}$$

Here $\langle O \rangle$ is the ensemble average and $\sqrt{\langle \Delta O^2 \rangle}$ is the standard deviation of $O$, quantifying how much the value of $O$ fluctuates. Importantly, the fluctuations and average value scale differently as functions of the size of the system. To see this, we calculate

$$\langle O \rangle = \sum_{i}^{N} \langle o_i \rangle = N \langle o \rangle . \tag{1.8}$$

Here we used the assumption of $o_i$ being identically distributed. Using this again, together with the assumption that they also are independent, we find

$$\left\langle \Delta O^2 \right\rangle = \sum_{i}^{N} \sum_{j}^{N} \langle \Delta o_i \Delta o_j \rangle = N \left\langle \Delta o^2 \right\rangle . \tag{1.9}$$

This implies that

$$\frac{\langle \Delta O^2 \rangle}{\langle O \rangle^2} \propto \frac{1}{N}. \tag{1.10}$$

This means that in the so-called *thermodynamic limit* valid for macroscopic devices, where one takes $N \to \infty$, the fluctuations vanish relative to the average of $O$. This is illustrated in Fig. (1.1), where the distribution of $O$ in Eq. (1.7) is plotted. Conversely, the reason why this approximation of neglecting fluctuations is valid for macroscopic devices is exactly why it is not at the nanoscale, where the number of particles is relatively small. In fact, the average value of an observable can often be of the same order of magnitude as its fluctuations for nanoscale devices. In such systems, not only is the efficiency of converting the provided resource into useful output interesting, but so is the precision with which one is able to do this. This is the main focus of this master's thesis: deriving trade-off relations for precision in nanoscale devices.

While important, the presence of fluctuations is not the only difference between working with the thermodynamics of macro- and nanoscale devices. Often, the process of thermalization occurs on scales larger than the nanoscale devices themselves, and unusual nonthermal resources can be present. A very important difference is the fact that at these scales, quantum effects can become important, e.g. in the transport of particles. Thus, thermodynamics has to be modified to take this into account.

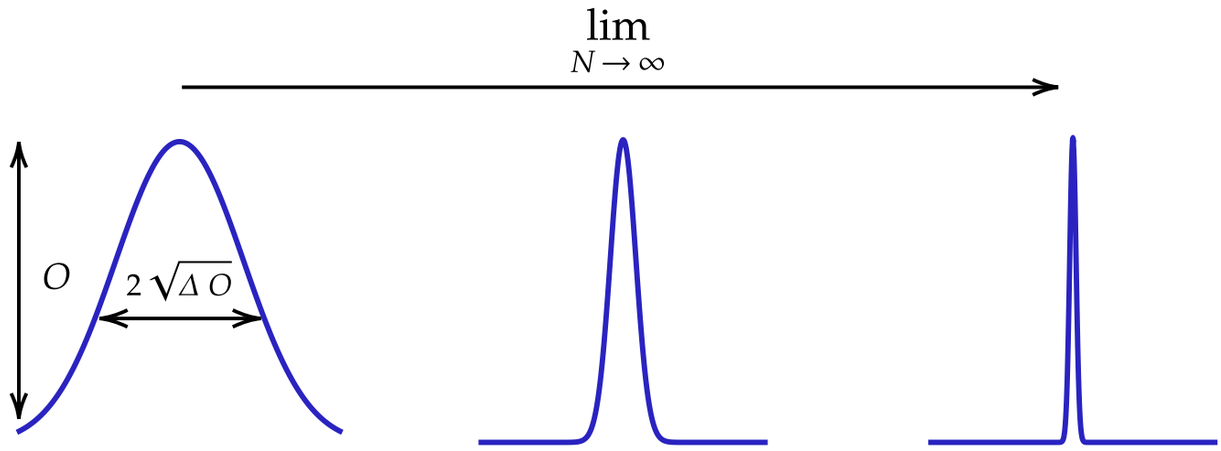


**Figure 1.1:** The distribution of an observable $O$, approximated as Gaussian in the thermodynamic limit. The relative fluctuations vanishes as the number of particles increase, and in the thermodynamic limit, the distribution becomes a Dirac delta function.

## 1.2 Quantum mechanics

Fittingly enough, quantum mechanics saw its birth in the failure of classical thermodynamics to describe the emission spectrum of black bodies, in what is now dubbed the ultraviolet catastrophe. To accurately describe the observations, light had to come in discrete quanta, or photons, as we know them now [5]. Nonetheless, quantum mechanics is not limited to photons but also applies to systems such as atoms, superconductors, and elementary particles, to mention a few. Even though all of these systems are different, in quantum mechanics, their state is described by a wavefunction, $|\psi\rangle$, which encodes all possible knowledge about the state [25]. The systems of interest in this thesis are quantum mechanical particles in multitermal nanoscale devices and their transport. However, these particles, e.g., electrons or photons, are indistinguishable, i.e., there is no way to tell two electrons apart. This indistinguishability has interesting implications for the exchange of particles in 3+1-dimensional spacetime. We define the joint wavefunction of two particles as

$$|\psi_1\psi_2\rangle\,. \tag{1.11}$$

Because the particles are indistinguishable, it is required that when exchanging the particles, the wavefunction only differs by a complex phase $e^{i\theta}$, where $\theta$ is a real number,

$$|\psi_1\psi_2\rangle = e^{i\theta}\,|\psi_2\psi_1\rangle\,. \tag{1.12}$$

This additional phase is possible because a global complex phase has no physical meaning, and the wavefunctions of Eq.(1.12) describes the exact same physical state of the system. This is a consequence of our inability to tell which of the two particles is occupying which state. While this phase in principle could take any value, the spin-statistics theorem tells us that for half-integer spin particles, fermions, it is $e^{i\theta} = -1$, and for integer spin particles, bosons, it is $e^{i\theta} = 1$ [14]. Examples of fermions are electrons and protons, and examples of bosons are photons and phonons. While the spin-statistics theorem is simple to state, there is no elementary proof without the use of relativity and Lorentz invariance, which is outside the scope of this thesis [23, 14]. A consequence of the fermionic wavefunction being antisymmetric with respect to the exchange of particles is that two fermions can never occupy the same state since

$$|\psi_1\psi_1\rangle = -\,|\psi_1\psi_1\rangle = 0. \tag{1.13}$$

This is the Pauli exclusion principle, and it has widespread consequences for both quantum statistical mechanics and the transport of fermions. On the other hand, there is no limit to the number of bosons able to occupy the same state, and when treating the transport of particles, this leads to *bunching* of bosons and *anti-bunching* of fermions. This is simplest illustrated by a Hong-Ou-Mandel (HOM) setup shown in Fig. (1.2), where two beams of particles are aimed at a 50% beam splitter and there are two particle detectors, one for each transmitted beam [18]. We represent the state of this system in the Fock basis, $|n_{a1}, n_{a2}, n_{b1}, n_{b2}\rangle$, where the first two numbers count how many particles are in each input mode and the last two numbers count the particles in the output modes. With creation operators for incoming particles, $\hat{a}_1^\dagger$, $\hat{a}_2^\dagger$ and outgoing particles, $\hat{b}_1^\dagger$, $\hat{b}_2^\dagger$, we have

$$(\hat{a}_1^\dagger)^{n_{a1}}(\hat{a}_2^\dagger)^{n_{a2}}(\hat{b}_1^\dagger)^{n_{b1}}(\hat{b}_2^\dagger)^{n_{b2}}\,|0,0,0,0\rangle = |n_{a1}, n_{a2}, n_{b1}, n_{b2}\rangle\,. \tag{1.14}$$

Assuming that each pair of incoming particles is in the same state, and that they arrive at the beam splitter perfectly synchronized, the ladder operators are related by the following unitary transformation

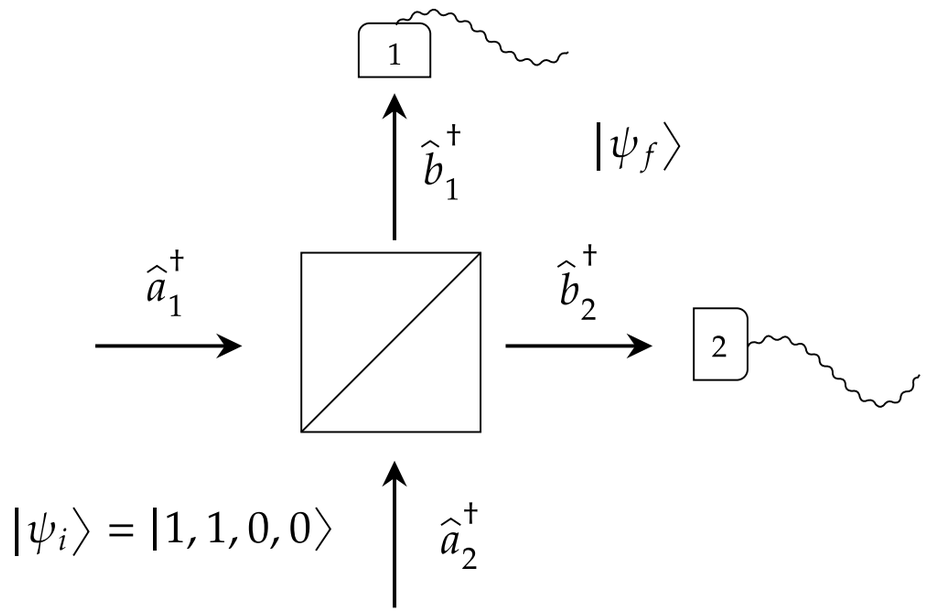


**Figure 1.2:** Hong-Ou-Mandel setup, where particles from two sources are fired at a beam splitter and then detected by two detectors. Fermions anti-bunch due to the Pauli exclusion principle and the variance in the number of detected particles is suppressed. Bosons bunch together, increasing the variance. This effect has implications for the precision of transport in nanoscale devices.

[3]:

$$\hat{a}_1^\dagger \mapsto \frac{\hat{b}_1^\dagger + \hat{b}_2^\dagger}{\sqrt{2}},\ \hat{a}_2^\dagger \mapsto \frac{\hat{b}_1^\dagger - \hat{b}_2^\dagger}{\sqrt{2}}. \tag{1.15}$$

From this, one would observe different correlations in detection of fermionic and bosonic particles. For bosons, the initial state $|1,1,0,0\rangle$ with one particle in each incoming beam would evolve as

$$\begin{aligned} |\psi_i\rangle = |1,1,0,0\rangle = \hat{a}_1^\dagger \hat{a}_2^\dagger |0,0,0,0\rangle \mapsto \frac{\hat{b}_1^\dagger + \hat{b}_2^\dagger}{\sqrt{2}} \frac{\hat{b}_1^\dagger - \hat{b}_2^\dagger}{\sqrt{2}} |0,0,0,0\rangle = \\ = \frac{\hat{b}_1^\dagger \hat{b}_1^\dagger - \hat{b}_2^\dagger \hat{b}_2^\dagger}{\sqrt{2}} |0,0,0,0\rangle = \frac{|0,0,2,0\rangle - |0,0,0,2\rangle}{\sqrt{2}} = |\psi_f\rangle , \end{aligned} \tag{1.16}$$

since bosonic ladder operators fulfill commutation relations. The state after the beam splitter is an even superposition of having two particles in output mode $b_1$ and none in $b_2$ and having two particles in $b_2$ and none in $b_1$. This is the Hong-Ou-Mandel effect, where by measuring the number of particles arriving at a detector after the beam splitter, one would *always* find either zero or two particles, which would come in pairs. This is what is meant by bunching: the particles arrive in correlated pairs. This increases the variance and thus the fluctuations one measures in the transmitted currents of particles, which is typical in the transport of bosonic particles. To see this, one can calculate the average number of particles one detects using detector 1, which is given by the number operator $\hat{b}_1^\dagger \hat{b}_1$ and its variance $\left\langle (\Delta \hat{b}_1^\dagger \hat{b}_1)^2 \right\rangle$. Doing this one finds

$$\left\langle \hat{b}_1^\dagger \hat{b}_1 \right\rangle = \langle \psi_f | \, \hat{b}_1^\dagger \hat{b}_1 \, | \psi_f \rangle = 1, \tag{1.17}$$

$$\left\langle (\Delta \hat{b}_1^\dagger \hat{b}_1)^2 \right\rangle = \left\langle \left( \hat{b}_1^\dagger \hat{b}_1 - \left\langle \hat{b}_1^\dagger \hat{b}_1 \right\rangle \right)^2 \right\rangle = 1. \tag{1.18}$$

On average, one measures one particle at the detector, but doing so, one would always measure a second particle since they are perfectly correlated. The variance becomes large since the system is in a superposition up until measurement, and the outcome is random at each event.

Considering the setup of Fig. (1.2) for fermionic particles, the result is different. Fermions, which obey the Pauli exclusion principle, have ladder operators that fulfill anticommutation relations. This implies

$$\begin{aligned} |\psi_i\rangle = |1,1,0,0\rangle = \hat{a}_1^\dagger \hat{a}_2^\dagger |0,0,0,0\rangle \mapsto \frac{\hat{b}_1^\dagger + \hat{b}_2^\dagger}{\sqrt{2}} \frac{\hat{b}_1^\dagger - \hat{b}_2^\dagger}{\sqrt{2}} |0,0,0,0\rangle = \\ = \frac{\hat{b}_1^\dagger \hat{b}_2^\dagger - \hat{b}_2^\dagger \hat{b}_1^\dagger}{\sqrt{2}} |0,0,0,0\rangle = |0,0,1,1\rangle = |\psi_f\rangle . \end{aligned} \tag{1.19}$$

For the fermionic setup, one *always* measures one particle at each detector, so the fluctuations in the measured currents are suppressed. This is what is meant by anti-bunching. One can understand this by again calculating the average number of particles detected at detector 1 and the fluctuations,

$$\left\langle \hat{b}_1^\dagger \hat{b}_1 \right\rangle = \langle \psi_f | \, \hat{b}_1^\dagger \hat{b}_1 \, | \psi_f \rangle = 1, \tag{1.20}$$

$$\left\langle (\Delta \hat{b}_1^\dagger \hat{b}_1)^2 \right\rangle = \left\langle \left( \hat{b}_1^\dagger \hat{b}_1 - \left\langle \hat{b}_1^\dagger \hat{b}_1 \right\rangle \right)^2 \right\rangle = 0. \tag{1.21}$$

One always measures one particle, but never a second particle at the same time. This causes the variance to vanish. The effect of anti-bunching has been experimentally observed in fermionic systems [7, 13]. The setup discussed here is, of course, highly idealized: the incoming particles could have different momenta or arrive at different times, which would weaken this effect, but in general, the effect of bunching or anti-bunching is highly relevant to describing fluctuations and transport in quantum devices since this effect increases or decreases the fluctuations measured on average.

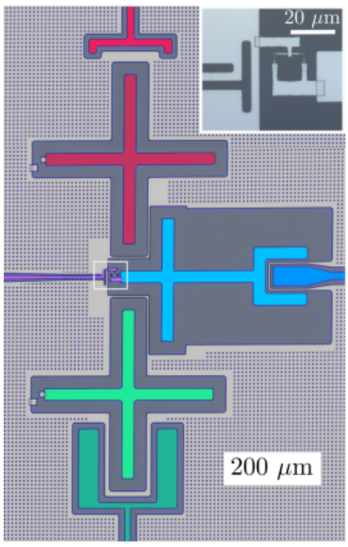


**(a)** On-chip absorption fridge used for resetting qubits, implemented using superconducting circuits and thermal photons [1].

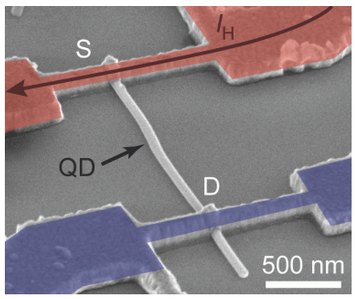


**(b)** An lnAS nanowire containing a quantum dot connected to cold and hot metallic contact, for thermopower measurements [15].

**Figure 1.3:** Examples of multiterminal devices, where the transport of particles from reservoirs through a central region is utilized to perform some tasks, e.g., cooling. The left image shows transmission lines supporting thermal photons connected via a superconducting circuit. Such a device might occur in certain realizations of quantum computers. The right figure shows a thermoelectric device where electrons are transported.

We have seen that, when describing transport in quantum mechanical systems, non-classical phenomena affect interesting quantities, such as the fluctuations one measures in the currents and therefore their precision. Not only are fluctuations important in nanoscale devices because of the relatively small currents, but quantum effects such as superpositions and interference also play important roles. Furthermore, how this manifests even crucially depends on the type of system investigated, i.e., fermions versus bosons.

How should one describe these effects? One could, of course, try to model each device from a microscopic perspective, derive some Hamiltonian, and use it to solve for interesting thermodynamic quantities such as particle currents, energy currents, entropy productions, and their respective fluctuations. While this has the potential to give detailed knowledge about the quantum thermodynamics of a specific system, it is typically an extremely challenging task that requires either heavy numerics or various approximations.

Furthermore, one would like to be able to make more general statements about fluctuations in the two types of systems, in a similar manner as the second law of thermodynamics, for example. If one were to calculate currents and their fluctuations for a system, e.g., waveguides acting as reservoirs of thermal photons connected to some superconducting circuit, could one gain more general physics

knowledge from this? If one were to exchange the specific superconducting circuit for another, could one still say something about the system from a thermodynamics perspective? Even further, if one were to instead consider a nanoscale electronic device where the particles are fermions instead of bosons, would one need to change the approach completely?

An alternative to modelling the devices of interest from a microscopic model is to use scattering theory, or, as it is also called, Landauer-Büttiker theory [6, 21]. In scattering theory, one investigates a more general system of reservoirs connected by leads to a central scattering region, described by a scattering matrix. The reservoirs contain particles that enter the leads, where they propagate coherently as waves and enter the scattering region. In the scattering region, the particles are scattered into the different leads in some general superposition, which would depend on the specific scattering matrix. In this view, the device of interest can be modelled by the scattering matrix, e.g., the earlier superconducting circuit. With this approach, one is able to calculate different thermodynamic quantities and their fluctuations by defining quantum fields in the leads, and the exact mathematics of doing this would depend on whether one is considering bosonic or fermionic systems. While it is possible to derive specific scattering-matrices for systems, the power of the scattering theory approach is to use the scattering matrix as a placeholder for a system. With this approach, we can make general statements for bosonic or fermionic systems by calculating currents and fluctuations. For this reason, we employ the scattering theory framework to investigate the thermodynamics and precision of nanoscale devices.

## 1.3 Thesis goal

The main goal of this thesis is to investigate precision of coherent transport in nanoscale devices. This includes extending the trade-off relations derived for fermionic systems in a paper written by M. Acciai et. al. [2] to bosonic systems. There, it was proven that classical fluctuations limit the absolute value of the entropy change, implementing a trade-off relation for thermodynamic work in fermionic systems described by scattering theory. To extend this to bosonic systems, one needs to calculate currents, entropy productions and their fluctuations. Furthermore, it is desired to include the quantum part of fluctuations in the bounds, since this allows one to make statements for the full physical fluctuations that would be measured experimentally. Hence, extending the bounds to include the full noise is the second main goal of the thesis. Additionally, we improve the classical bounds of [2] and establish constraints on the precision for a variety of currents. This is a key result of this thesis, which we compare to constraints obtained with a different approach. The latter are called thermodynamic uncertainty relations, and in this thesis, we prove their validity for bosonic systems within the scattering theory formalism, in analogy to the fermionic results of a paper written by K. Brandner et. al. [8]. Similarly to the trade-off relations first derived in Ref. [2], we extend the thermodynamic uncertainty relation to include the full noise, not just the classical fluctuations. The inclusion of quantum fluctuations in bosonic systems turns out to be naturally interpreted as the effect of bunching. Following this intuition, we are able to also include the fermionic quantum fluctuations in the bounds, which include the effect of anti-bunching. This is a key result in the thesis since it also allows us to handle the quantum noise in both the new relations for bosons and the old fermionic relations of Refs. [2, 8] in a similar way. Finally, we combine the trade-off relations to be able to bound the total entropy production from below and from above in systems described by scattering theory.

The remainder of this thesis is structured as follows: In chapter 2, we lay out basic theory for thermodynamics and quantum mechanics, and we present classical trade-off relations for precision in Section 2.1.1. Furthermore, in Section 2.2, we introduce the theoretical framework of scattering theory and employ it to calculate particle, energy, heat and entropy currents together with their fluctuations. Next, we show earlier results for fermionic systems derived using scattering theory.

After this, we present our results in Chapter 3. We begin by showing the extension of the bounds of Ref. [2] to bosonic systems in Section 3.1.2. After this, we find a way to improve both the fermionic and bosonic versions of this bound in Sections 3.1.3 and 3.1.4. Next, we investigate the quantum part of the fluctuations and manage to extend the bounds to concern the full fluctuations in Sections 3.1.5 and 3.1.6. Furthermore, we extend the thermodynamic uncertainty relation to bosonic systems in Section 3.2. Finally, in Section 3.3, we compare these bounds by combining them into two-sided bounds on entropy production. The thesis ends with making some general conclusions in Chapter 4 and some suggestions for future work in Chapter 5.

# 2

# Theory

This chapter will lay out the theoretical concepts used in this master's thesis to describe the thermodynamics of nanoscale devices. We begin by recounting some basic thermodynamic concepts, with a focus on entropy. We compare the classical notion of entropy to the quantum mechanical Von Neumann entropy, which is more general. After this, we introduce scattering theory, which is used to calculate currents and their fluctuations. Scattering theory allows us to make calculations for strongly coupled systems, but at the cost of not being able to treat strongly interacting particles. We show earlier results that have been derived for fermionic systems that this thesis will extend to bosonic systems. Then, we apply the scattering theory to a two-terminal system of coupled reservoirs and calculate its steady-state thermodynamics. With this concrete example, we illustrate both an applications of scattering theory and some differences between bosonic and fermionic systems.

## 2.1 Thermodynamics

Thermodynamics as a subject has traditionally dealt with the behaviour of systems consisting of a large number of degrees of freedoms in equilibrium. The macroscopic state of such a system is parameterized by state variables, which come in pairs of extensive and intensive quantities such as particle number and the chemical potential $\mu$, entropy, and temperature. A thermodynamic system is in equilibrium if its thermodynamic potential is minimized. For a closed system, this corresponds to the state with maximum entropy. Standard thermodynamics is based on four laws [24],

- Zeroth law: If two systems are both in thermal equilibrium with a third system, then they are in thermal equilibrium with each other.
- First law: Energy is conserved.
- Second law: Heat flows spontaneously from high temperature to low temperature.
- Third law: It is not possible to reach the coldest temperature using a finite set of reversible steps.

For closed system, the second law states that the total entropy $\Sigma$ always increases

$$\frac{d}{dt}\Sigma \geq 0. \tag{2.1}$$

Considering a system of $n$ reservoirs each in internal equilibrium, an important result dealing with the second law is Clausius' relation [26],

$$\sum_{\alpha=1}^{n} \frac{I_\alpha^{(J)}}{T_\alpha} = \sum_{\alpha=1}^{n} \frac{I_\alpha^{(E)} - \mu_\alpha I_\alpha^{(0)}}{T_\alpha} = \frac{d}{dt}\Sigma \equiv \sigma \geq 0. \tag{2.2}$$

Here $I_\alpha^{(J)}$ and $T_\alpha$ are the heat current into and temperature of the reservoir $\alpha$, respectively, defined through the energy current $I_\alpha^{(E)}$, particle current $I_\alpha^{(0)}$ and chemical potential $\mu_\alpha$. Thus, if one is able to calculate these currents in a system of coupled thermal reservoirs, the entropy productions are known. Entropy can be interpreted as a lack of information about a system. A definition of entropy that holds for both classical thermal and nonthermal resources is the Gibbs entropy

$$\Sigma = -k_\mathrm{B} \sum_{i=1}^{\Omega} p_i \log[p_i], \tag{2.3}$$

where $\Omega$ is the number of microstates, and $p_i$ are the probabilities associated with occupying each microstate. A microstate includes all information about a system, for example, every particle's momentum and position in a gas, while a macrostate is characterized by state variables such as pressure and temperature. Useful work can be done by allowing, for example, heat to flow from a warm reservoir into a cold one. There are, however, other more exotic possible resources. If one of the reservoirs is out of equilibrium internally, it can perform useful work without an average flow of heat or particles by producing entropy [26]. Such resources become relevant in the context of quantum thermodynamics, where non-equilibrium systems are common. In this view, entropy production is the fundamental quantity needed to characterize the performance and outcome of a resource's work.

For quantum systems, instead of microstates, we have the quantum state vectors $|\psi\rangle$ of a Hilbert space. The quantum mechanical state of a system can generally be described by a density matrix $\rho$ [9], which must fulfill

$$\rho = \rho^\dagger, \;\; \mathrm{Tr}\{\rho\} = 1, \;\; \langle\psi|\,\rho\,|\psi\rangle \geq 0, \; \forall\,|\psi\rangle\,. \tag{2.4}$$

The density matrix allows for the treatment of quantum systems where the state is a statistical mixture, and representing a system of particles in a basis $\{|k\rangle\}$, one can generally express $\rho$ as

$$\rho = \sum_{k,l=0}^{\infty} \rho_{kl}\,|k\rangle\langle l|\,, \tag{2.5}$$

where $\rho_{kl}$ are complex numbers. The off-diagonal elements contain non-classical correlations, which are called coherences. The density matrix can be represented as diagonal in some basis $\{|\psi_i\rangle\}$ since it is hermitian,

$$\rho = \sum_i p_i\,|\psi_i\rangle\langle\psi_i|\,, \tag{2.6}$$

where the $p_i$ are occupation probabilities associated with each state $|\psi_i\rangle$. If more than one $p_i$ is nonzero, the state is *mixed*. It should be noted here that there are two distinct notions of probabilities in quantum mechanics. The first one is the uncertainty that comes from having a system in a state of superposition, where a system is truly in two states at the same time, up until measurement. When a system in a superposition is measured, it is projected into the eigenbasis of the measured observable. Even if we know the state of the system perfectly, we cannot predict the measurement outcome if we measure it in a basis where the state is not included. The second uncertainty is the one associated with the probabilities $p_i$ of the density matrix. These can be thought of as classical probabilities resulting from either non-perfect state preparation or decoherence through interaction with the environment. This uncertainty could be reduced by having better knowledge of or control over a system. This distinction is important since they play different roles in quantum thermodynamics. This is simplest illustrated by considering a two-level system with the basis $|0\rangle$ and $|1\rangle$. One can imagine two different density matrices

$$\rho_1 = \frac{1}{2}\,|0\rangle\langle 0| + \frac{1}{2}\,|1\rangle\langle 1|\,, \;\; \rho_2 = \frac{1}{2}(|0\rangle + |1\rangle)(\langle 0| + \langle 1|) = \frac{1}{2}(|0\rangle\langle 0| + |1\rangle\langle 1| + |1\rangle\langle 0| + |0\rangle\langle 1|). \tag{2.7}$$

Here $\rho_1$ is a statistical mixture of the states $|0\rangle$ and $|1\rangle$, each with probability 1/2. On the other hand, $\rho_2$ is a pure density matrix, corresponding to the even superposition of the two states: $\frac{|0\rangle+|1\rangle}{\sqrt{2}}$. For both these systems, the probability of measuring each state is 1/2, but for $\rho_1$, this uncertainty comes from statistical uncertainty and for $\rho_2$, it comes from the state being a superposition. A way to distinguish between these to types of uncertainties is by means of the von Neumann entropy, which is defined as

$$\Sigma_{\mathrm{VN}}[\rho] = -k_{\mathrm{B}}\,\mathrm{Tr}\{\rho\log[\rho]\}. \tag{2.8}$$

Indeed, calculating the Von Neumann entropy for the two states $\rho_1$ and $\rho_2$, one finds,

$$\Sigma_{\mathrm{VN}}[\rho_1] = -\frac{k_{\mathrm{B}}}{2}(-\log[1/2] - \log[1/2]) = k_{\mathrm{B}}\log[2], \tag{2.9}$$

$$\Sigma_{\mathrm{VN}}[\rho_2] = -k_{\mathrm{B}}\log[1] = 0. \tag{2.10}$$

While seemingly having similar measurement statistics at first glance, $\rho_1$ is in fact a maximum entropy state, while $\rho_2$ has zero entropy. The second law of thermodynamics is still true, and we quantify a resource by how much entropy it produces. Thus, $\rho_1$ and $\rho_2$ could behave very differently from a quantum thermodynamics perspective. The difference between the states can be made more clear by choosing a different basis. If we instead use the basis

$$|+\rangle = \frac{1}{\sqrt{2}}(|0\rangle + |1\rangle), \;\; |-\rangle = \frac{1}{\sqrt{2}}(|0\rangle - |1\rangle), \tag{2.11}$$

our density matrices is represented by

$$\rho_1 = \frac{1}{2}\,|+\rangle\langle +| + \frac{1}{2}\,|-\rangle\langle -|\,, \;\; \rho_2 = |+\rangle\langle +|\,. \tag{2.12}$$

If we measure in this basis, there would still be the same statistical uncertainty when measuring $\rho_1$, but when measuring $\rho_2$, we would always find the state $|+\rangle$. Therefore, the von Neumann entropy, which is independent of the basis used to represent the state, quantifies the statistical uncertainty of a state.

In general, the Von Neumann entropy coincides with the classical Gibbs entropy for density matrices that are diagonal in the Fock basis. Furthermore, for a thermal state of particles [9]

$$\rho_{\text{th}} = \frac{1}{Z} e^{-(\hat{H}-\mu\hat{N})/k_{\text{B}}T}, \tag{2.13}$$

where $Z = \text{Tr}\left\{e^{-(\hat{H}-\mu\hat{N})/k_{\text{B}}T}\right\}$ is the partition function, $\hat{H}$ is the Hamiltonian and $\hat{N}$ is the number operator, the production of Von Neumann entropy reduces to the Clausius' relation, i.e.

$$\frac{d}{dt}\Sigma_{\text{VN}}[\rho_{\text{th}}] = \frac{1}{T}\frac{d}{dt}\left(\left\langle \hat{H} \right\rangle - \mu \left\langle \hat{N} \right\rangle\right). \tag{2.14}$$

The entropy production in quantum mechanical systems simplifies considerably when working with states diagonal in the number basis, thus we will focus on these situations in this thesis. However, we still allow for nonthermal states. In other words we treat states where the Von Neumann entropy reduces to the Gibbs entropy.

In recent work, much focus has been put on the study of fluctuations in thermodynamics, specifically in out-of-equilibrium systems. In the next section, we introduce two trade-off relations dealing with noise.

### 2.1.1 Thermodynamic and kinetic uncertainty relations

The relation between fluctuations and dissipation is an important field of study, exemplified by the fluctuation-dissipation theorems that hold for equilibrium systems [24]. Fluctuations in observables are also relevant quantities in the study of the thermodynamics of nanoscale devices and out-of-equilibrium systems. As discussed in the introduction, it is not only interesting to make statements about the efficiency of a thermodynamic process but also about how noisy it is. This is often quantified by the *relative fluctuations* of an observable $O$

$$\frac{\langle \Delta O^2 \rangle}{\langle O \rangle^2} = \frac{\left\langle (O - \langle O \rangle)^2 \right\rangle}{\langle O \rangle^2}, \tag{2.15}$$

or the *precision*

$$\frac{\langle O \rangle^2}{\langle \Delta O^2 \rangle} = \frac{\langle O \rangle^2}{\left\langle (O - \langle O \rangle)^2 \right\rangle}. \tag{2.16}$$

The intuition behind these expressions is that if the average of an observable is large and the variance is small, the precision is large. In a device, we could generate a strong current, but if the fluctuations in the currents are very large, the use of the device might be limited. Therefore, an area of research that has received much focus in recent years, both experimentally and theoretically, is trade-off relations for precision. A famous type of trade-off relation is the Thermodynamic Uncertainty Relation, or TUR for short, where the precision is bounded by the entropy production of a system. The most simple version of a TUR was derived for a classical Markovian system [4] and reads:

$$\Delta\Sigma \geq 2k_{\text{B}} \frac{\langle O \rangle^2}{\langle \Delta O^2 \rangle}. \tag{2.17}$$

Here, entropy change $\Delta\Sigma$ serves as the thermodynamic cost of precision in the accumulation of the quantity $O$. Assuming that the system is in a steady state, we can divide the left-hand side by the time over which we are measuring, which gives us

$$\frac{\Delta\Sigma}{t} \geq 2k_{\text{B}} \left(\frac{\langle O \rangle}{t}\right)^2 \left(\frac{t}{\langle \Delta O^2 \rangle}\right). \tag{2.18}$$

Now the relation can be interpreted in terms of an average entropy production on the left-hand side and an average precision in the current of the quantity $O$.

Another type of trade-off relation is the Kinetic Uncertainty Relation, or KUR for short. The KUR involves the *dynamical activity* $\mathcal{K}$, which for a discrete state system is the average number of jumps between states observed. A kinetic uncertainty relation for a discrete-state continuous-time Markov jump process is

$$\mathcal{K} \geq \frac{\langle I \rangle^2}{\langle \Delta I^2 \rangle}, \tag{2.19}$$

where $I$ is a current [12, 29]. While the TUR and KUR are similar, they are fundamentally different statements. The TUR involves dissipation, while the KUR involves the amount of activity in the system. In a sense, the TUR characterises the irreversibility of a process, while the KUR is a statement

about the time scales of a process [29].

An important point is that the TUR and KUR do not hold for all systems, and violations often occur as a result of quantum effects [8]. Investigating this is interesting since it can highlight the possible advantages of quantum technology over its classical counterparts. Often, when deriving TURs and KURs, an important assumption is that the system is Markovian. There are realisations of nanoscale devices where the assumption of markovianity is not valid since different reservoirs could be strongly coupled. Establishing TURs and KURs for strongly coupled systems is thus interesting since this is extending trade-off relations to a new class of physically important systems. A framework for treating quantum transport in these strongly coupled systems is scattering theory. The introduction of scattering theory is the focus of the next section, where we use it to derive currents and their fluctuations for strongly coupled systems.

## 2.2 Second quantization and scattering theory

In the previous section, we saw that currents and their fluctuations are important quantities from a thermodynamics perspective. This section will focus on the calculation of these quantities. We are interested in describing multiterminal nanoscale devices thermodynamically, where there is the possibility of strong coupling between reservoirs. The systems of interest in this thesis can be pictured as shown in Fig. (2.1), where particle reservoirs, enumerated by Greek letters, are connected through one-dimensional leads. The leads are strongly coupled through a central region described by an energy-dependent scattering matrix $s(E)$. In this way of modeling a nanoscale device, the reservoirs serve as boundary conditions, supplying particles to the leads, where they coherently propagate towards the central region as waves. The central region serves as a coherent scatterer, scattering the incoming particles into the different leads in some superposition. The particles then propagate back towards the reservoirs. This is the basis of scattering theory, where we are able to treat strongly coupled systems at the expense of not being able to treat strong interactions between propagating particles. Nonetheless, weak interactions between particles can still be treated using mean-field theory [6, 21, 28]. Before we can treat the quantum transport of such systems, we need to define field operators and introduce the second quantization formalism.

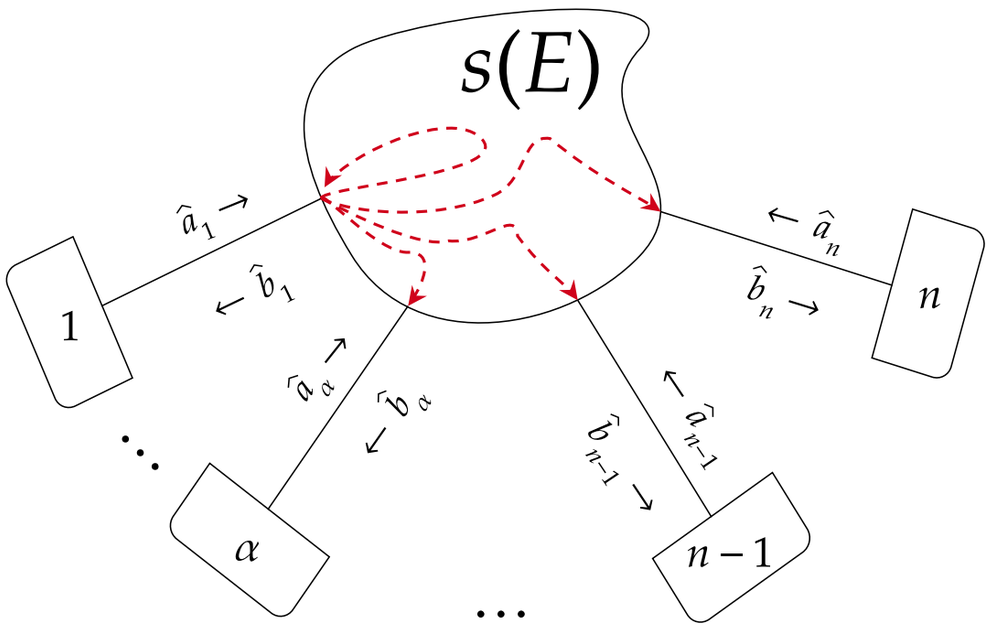


**Figure 2.1:** Sketch of reservoirs of particles connected through leads to a conductor with scattering matrix $s(E)$. The reservoirs contain particles distributed according to possibly non-equilibrium distributions. Particles propagate through their leads, scatter in the conductor and enter the lead. In scattering theory, we are able to treat interactions between particles using mean field theory, but not strong particle-particle interactions.

When treating quantum many-body problems, it is often natural to work within the second quantization formalism. In this formalism, indistinguishable particles are treated as excitations in quantum fields, represented in Fock states. These excitations are created and destroyed by so-called ladder operators. The state containing no particles is called the vacuum state and is denoted by $|0\rangle$. As discussed

in the introduction, in three-dimensional configuration space, there are two types of indistinguishable particles: fermions with half-integer spin and bosons with integer spin. Mathematically, the different particle types are implemented by letting the ladder operators for fermions fulfill anticommutation relations

$$\begin{aligned}\left\{\hat{a}_{\alpha i}(E), \hat{a}^\dagger_{\beta j}(E')\right\} &= \delta_{\alpha\beta}\delta_{ij}\delta(E-E'),\\ \left\{\hat{a}^\dagger_{\alpha i}(E), \hat{a}^\dagger_{\beta j}(E')\right\} &= 0,\\ \{\hat{a}_{\alpha i}(E), \hat{a}_{\beta j}(E')\} &= 0,\end{aligned} \tag{2.20}$$

while the bosonic ladder operators fulfill commutation relations

$$\begin{aligned}\left[\hat{a}_{\alpha i}(E), \hat{a}^\dagger_{\beta j}(E')\right] &= \delta_{\alpha\beta}\delta_{ij}\delta(E-E'),\\ \left[\hat{a}^\dagger_{\alpha i}(E), \hat{a}^\dagger_{\beta j}(E')\right] &= 0,\\ [\hat{a}_{\alpha i}(E), \hat{a}_{\beta j}(E')] &= 0.\end{aligned} \tag{2.21}$$

Here, $\hat{a}_{\alpha i}(E)$ is the annihilation operator for the particles in channel $i$ of the lead connected to reservoir $\alpha$, removing a particle with energy $E$ and $\hat{a}^\dagger_{\alpha i}(E)$ is the creation operator for the particles in channel $i$ of the lead connected to reservoir $\alpha$, creating a particle with energy $E$ [6, 21, 28]. The different channels enumerated by letters of the Latin alphabet refer to different modes of propagation in a lead, e.g., different conduction bands. A consequence of the fermionic ladder operators fulfilling anticommutation relations is the Pauli exclusion principle. This can be seen from $\hat{a}^\dagger_{\alpha i}(E_1)\hat{a}^\dagger_{\beta j}(E_2)\left|\psi\right\rangle = -\hat{a}^\dagger_{\beta j}(E_2)\hat{a}^\dagger_{\alpha i}(E_1)\left|\psi\right\rangle$, for fermions and any state $\left|\psi\right\rangle$, which implies that the wavefunction of two fermions is antisymmetric under exchange of the particles. From this, it follows that

$$\hat{a}^\dagger_{\alpha i}(E_1)\hat{a}^\dagger_{\alpha i}(E_1)\left|\psi\right\rangle = -\hat{a}^\dagger_{\alpha i}(E_1)\hat{a}^\dagger_{\alpha i}(E_1)\left|\psi\right\rangle = 0. \tag{2.22}$$

Thus, two fermions can never occupy the same state, while there is no limit to the number of bosons occupying the same state [23]. This leads to fundamental differences when treating the statistics and thermodynamics of fermionic and bosonic systems. Indeed, the average number of particles at energy $E$ in an equilibrium reservoir at temperature $T$ and chemical potential $\mu$ is described by the Fermi distribution [24]

$$f_{\mathrm{F}}(E) = \frac{1}{e^{(E-\mu)/(k_{\mathrm{B}}T)}+1}, \tag{2.23}$$

for fermions and the Bose-Einstein (BE) distribution for bosons

$$f_{\mathrm{BE}}(E) = \frac{1}{e^{(E-\mu)/(k_{\mathrm{B}}T)}-1}. \tag{2.24}$$

The difference between the particle types is also reflected in the properties of the chemical potential: it can be positive for fermions, while it is always zero or negative for bosons [10] (see Appendix [A.1]). An important special case is non-conserved bosons, such as photons, which are of fundamental importance in many areas of quantum technology, such as superconducting circuits, quantum optics and optomechanics. A system of non-conserved particles at equilibrium adjusts their number to minimize the free energy $F$, which implies that [10]

$$\mu = \left.\frac{\partial F}{\partial N}\right|_{\Sigma} = 0. \tag{2.25}$$

Setting $\mu = 0$ causes the BE distribution of Eq. (2.24) to diverge as its energy argument goes to zero. This is, however, not physically relevant since the distribution is only valid for

$$\frac{E-\mu}{k_{\mathrm{B}}T} > 0. \tag{2.26}$$

Furthermore, the energy of a photon is given by the Planck-Einstein relation

$$E = \frac{hc}{\lambda}, \tag{2.27}$$

where $c$ is the speed of light, $h$ is Planck's constant, and $\lambda$ is the wavelength of the photon [25]. This implies that for a photon to have zero energy, it must have an infinite wavelength and cannot be supported inside a system of finite size. Treating non-conserved particles is important since photons have zero rest mass and are fundamentally relativistic particles that can annihilate. Photons are specifically important for many areas of quantum technology, such as superconducting circuits,

quantum optics, and optomechanics. These distributions are important when calculating expectation values of the ladder operators for equilibrium reservoirs since

$$\left\langle \hat{a}^\dagger_{\alpha i}(E)\hat{a}_{\beta j}(E')\right\rangle = \delta_{\alpha\beta}\delta_{ij}f_\alpha(E)\delta(E-E'), \tag{2.28}$$

where $f_\alpha(E)$ is the BE or Fermi distribution for reservoir $\alpha$ depending on the particle type [6, 21]. For nonthermal reservoirs, $f_\alpha(E)$ can be some general distribution, it must however less or equal to one for fermions due to the Pauli exclusion principle. In the nanoscale transport setup considered here, see Fig. (2.1), this distribution describes the average occupation of particles propagating toward the central scattering region. There, quantum effects play an important role and scattering theory takes them into account. The scattering process is described by a unitary matrix $s(E)$, which relates the incoming particles to the scattered particles. The ladder operators for particles traveling out of reservoir $\alpha$ in channel $i$ are denoted by $\hat{a}_{\alpha i}(E)$, $\hat{a}^\dagger_{\alpha i}(E)$ while $\hat{b}_{\alpha i}(E)$, $\hat{b}^\dagger_{\alpha i}(E)$ are the ladder operators for the scattered particles. These operators are related by

$$\hat{b}_{\alpha i}(E) = \sum_{\beta j} s_{\alpha i,\beta j}(E)\hat{a}_{\beta j}(E), \tag{2.29}$$

$$\hat{b}^\dagger_{\alpha i}(E) = \sum_{\beta j} s^*_{\alpha i,\beta j}(E)\hat{a}^\dagger_{\beta j}(E). \tag{2.30}$$

The unitary of $s(E)$ i.e. Eq. (2.31) stems from the conservation of particle currents by the scattering process,

$$\sum_{\beta j} s_{\alpha i,\beta j}(E)[s(E)]^\dagger_{\beta j,\gamma k} = \sum_{\beta j} s_{\alpha i,\beta j}(E)s^*_{\gamma k,\beta j}(E) = \delta_{\alpha\gamma}\delta_{ik}. \tag{2.31}$$

In addition, for systems with time-reversal symmetry, the scattering matrix is also symmetric,

$$s_{\alpha i,\beta j}(E) = s_{\beta j,\alpha i}(E). \tag{2.32}$$

It is common to define the *transmission probability* of a particle in lead $\beta$ travelling in channel $j$ with energy $E$ to enter channel $i$ of lead $\alpha$ as

$$D_{\alpha i,\beta j}(E) \equiv |s_{\alpha i,\beta j}(E)|^2. \tag{2.33}$$

Again, the system we are interested in can be schematically described by Fig. (2.1), where reservoirs are connected by leads to a coherent conductor, scattering propagating particles. The interesting quantities to calculate for such a system are current operators, their expectation values, and fluctuations. These are formulated in terms of field operators for the propagating particles. The propagation is assumed to be one-dimensional, such that the coefficients for the field operators can be written as products of transversal and longitudinal wavefunctions. The transversal wavefunction of reservoir $\alpha$ and channel $i$ with energy $E$ are denoted as $\chi_{\alpha i}(E)$. We assume that the length of a lead is much longer than its width, which causes the transversal wavefunctions to be frozen out of the propagation. Instead, the longitudinal wave functions are assumed to take the form of plane waves. By expanding in Fourier modes, the field operators are expressed as

$$\hat{\Psi}_\alpha(\mathbf{r},t) = \sum_i \int dE e^{-iEt/\hbar}\frac{\chi_{\alpha i}(E,r_\perp)}{\sqrt{hv(E)}}\left[\hat{a}_{\alpha i}(E)e^{-ik(E)x} + \hat{b}_{\alpha i}(E)e^{ik(E)x}\right], \tag{2.34}$$

$$\hat{\Psi}^\dagger_\alpha(\mathbf{r},t) = \sum_i \int dE e^{iEt/\hbar}\frac{\chi^*_{\alpha i}(E,r_\perp)}{\sqrt{hv(E)}}\left[\hat{a}^\dagger_{\alpha i}(E)e^{ik(E)x} + \hat{b}^\dagger_{\alpha i}(E)e^{-ik(E)x}\right]. \tag{2.35}$$

Here, $k(E)$ is the wave number, $h$ is Plank's constant and $v(E)$ is the particle speed. The factor $1/\sqrt{hv(E)}$ implements unit flux normalization [6, 28].

We have introduced the basics of scattering theory, such as the scattering matrix and the quantum fields of the particles inside the leads. In the next section, we utilize this framework to calculate currents in our system.

### 2.2.1 Current operators

Current operators are defined through continuity equations. Here we derive the particle and energy current operators. Beginning from the probability density for a wavefunction of a free particle, $|\psi(\mathbf{r},t)|^2$, we find its evolution by taking a time derivative [28]

$$\begin{aligned}\frac{\partial}{\partial t}|\psi(\mathbf{r},t)|^2 &= (\partial_t\psi^*)\psi + \psi^*\partial_t\psi = \frac{i}{\hbar}\left((\hat{H}\psi^*)\psi - \psi^*(\hat{H}\psi)\right) = \\ &= \frac{i}{2m\hbar}\left((\hat{\mathbf{p}}^2\psi^*)\psi - \psi^*(\hat{\mathbf{p}}^2\psi)\right) = \frac{i\hbar}{2m}\boldsymbol{\nabla}\left(-(\boldsymbol{\nabla}\psi^*)\psi + \psi^*\boldsymbol{\nabla}\psi\right) \equiv -\boldsymbol{\nabla}\boldsymbol{\mathcal{J}}^{(0)}.\end{aligned} \tag{2.36}$$

Here we used the Hamiltonian of a free particle, $\hat{\mathbf{p}}^2/2m$, in the position basis, and we interpret $\boldsymbol{\mathcal{J}}^{(0)}$ as a probability current. To generalize the current to the second quantization formalism, the wavefunctions are replaced by field operators, and the particle current operator is defined [6, 21, 28] as

$$\begin{aligned}\hat{I}_\alpha^{(0)}(t,x) &= \frac{i\hbar}{2m}\int dr_\perp \left\{\frac{\partial\hat{\Psi}_\alpha^\dagger(t,\mathbf{r})}{\partial x}\hat{\Psi}_\alpha(t,\mathbf{r}) - \hat{\Psi}_\alpha^\dagger(t,\mathbf{r})\frac{\partial\hat{\Psi}_\alpha(t,\mathbf{r})}{\partial x}\right\} \\ &= \sum_{i,i'}\frac{i\hbar}{2m}\int dr_\perp dE dE' e^{-i(E-E')t/\hbar}\frac{\chi_{\alpha i}(E,r_\perp)\chi^*_{\alpha i'}(E',r_\perp)}{\sqrt{hv(E)hv(E')}}\times \\ &\quad\Big\{ik(E)[\hat{a}^\dagger_{\alpha i'}(E')e^{ik(E')x} + \hat{b}^\dagger_{\alpha i'}(E')e^{-ik(E')x}][\hat{a}_{\alpha i}(E)e^{-ik(E)x} - \hat{b}_{\alpha i}(E)e^{ik(E)x}] \\ &\quad + ik(E')[\hat{a}^\dagger_{\alpha i'}(E')e^{ik(E')x} - \hat{b}^\dagger_{\alpha i'}(E')e^{-ik(E')x}][\hat{a}_{\alpha i}(E)e^{-ik(E)x} + \hat{b}_{\alpha i}(E)e^{ik(E)x}]\Big\}. \end{aligned} \tag{2.37}$$

Here, the area perpendicular to the propagation is integrated over. We also assumed that the transversal wavefunctions are stationary, such that one only needs to take a spatial derivative in $x$. The coordinates $x$ and $r_\perp$ inside the lead are shown in figure (2.2). With this definition, the particle

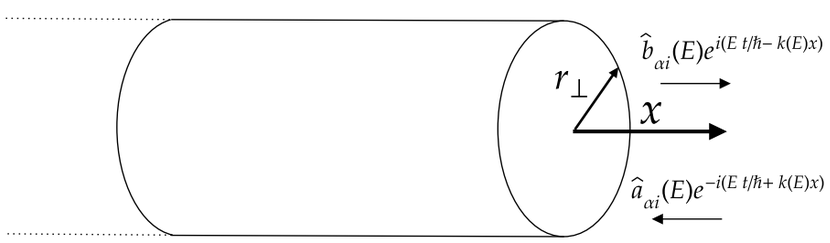


**Figure 2.2:** Figure depicting the coordinates in lead connected to reservoir. The particles are propagating along the $x$-coordinate and the current is integrated over the area perpendicular to propagation, denoted by $r_\perp$.

flow is positive for a flow into reservoir $\alpha$. This expression can be simplified by using the wideband approximation, where it is assumed that quantities depending on the energy vary slowly compared to the energy scale $E - E'$ [6, 28]. Under this approximation, $k(E') \approx k(E) = v(E)m/\hbar$, $v(E') \approx v(E)$ and $\chi_{\alpha i}(E) \approx \chi_{\alpha i}(E')$. This assumption allows us to use the orthonormality of the wavefunctions, i.e.

$$\int dr_\perp \chi^*_{\alpha i}(E,r_\perp)\,\chi_{\alpha j}(E,r_\perp) = \delta_{ij}, \tag{2.38}$$

which reduces the current operator to

$$\hat{I}_\alpha^{(0)}(t,x) = \frac{1}{h}\sum_i \int dE dE' e^{-i\frac{E-E'}{\hbar}t}\left\{\hat{b}^\dagger_{\alpha i}(E')\hat{b}_{\alpha i}(E) - \hat{a}^\dagger_{\alpha i}(E')\hat{a}_{\alpha i}(E)\right\}. \tag{2.39}$$

This expression has an intuitive interpretation as the difference between the number of in- and outflowing particles in a terminal. To evaluate expectation values of this operator, one has to take expectation values of the number operators $\langle\hat{a}^\dagger_{\alpha i}(E')\hat{a}_{\alpha i}(E)\rangle$ and $\langle\hat{b}^\dagger_{\alpha i}(E')\hat{b}_{\alpha i}(E)\rangle$. This is simple for the former case since the incident particles follow distributions of the reservoir they were emitted from, but this is generally not true for the scattered particles. However since the operators are related by the scattering matrix through Eq. (2.30), the current operator can be written as

$$\hat{I}_\alpha^{(0)} = \frac{1}{h}\sum_{i,\beta j,\gamma k}\int dE dE' e^{-i\frac{E-E'}{\hbar}t}\boldsymbol{\mathcal{A}}^{E',E}_{\alpha i,\beta j,\gamma k}a^\dagger_{\beta j}(E')a_{\gamma_k}(E), \tag{2.40}$$

where we define $\boldsymbol{\mathcal{A}}^{E',E}_{\alpha i,\beta j,\gamma k}$ [6], which we denote as the *scattering symbol*

$$\boldsymbol{\mathcal{A}}^{E',E}_{\alpha i,\beta j,\gamma k} \equiv s^*_{\alpha i,\beta j}(E')s_{\alpha i,\gamma k}(E) - \delta_{\alpha i,\beta j}\delta_{\alpha i,\gamma k}. \tag{2.41}$$

Taking the expectation value of Eq. (2.40), the average current is calculated using Eq. (2.28) and the unitarity of the scattering matrix which leads to

$$I_\alpha^{(0)} = \left\langle\hat{I}_\alpha^{(0)}\right\rangle = \frac{1}{h}\sum_{i,\beta j,\gamma k}\int dE dE' e^{-i\frac{E-E'}{\hbar}t}\boldsymbol{\mathcal{A}}^{E',E}_{\alpha i,\beta j,\gamma k}\delta_{\beta j\gamma k}\delta(E'-E)f_\beta(E) = \tag{2.42}$$

$$= \frac{1}{h}\sum_{i,\beta j}\int dE\sum_\beta |s_{\alpha i,\beta j}(E)|^2(f_\beta(E) - f_\alpha(E)). \tag{2.43}$$

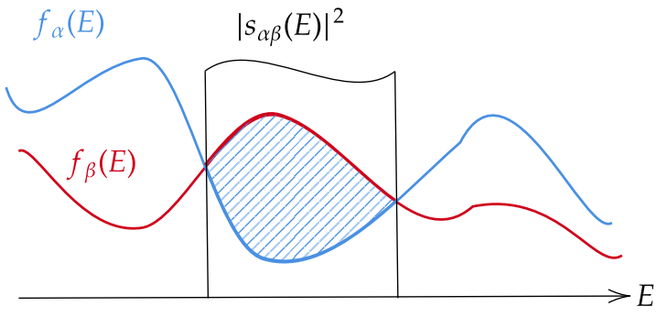


**Figure 2.3:** Illustration of the structure of the integral of the average particle current. We weight the difference in the average occupations between the reservoirs by the transmission probability and integrate over energy. In this figure the average occupations are nonthermal.

For reservoirs in internal equilibrium, $f_\alpha(E)$ is the Fermi distribution for fermions and the BE distribution for bosons. This expression has an intuitive explanation, the average current into reservoir $\alpha$ is the integral over energy, of the sum of differences in average occupations weighted by the probability of transmission between the reservoirs. This is illustrated in Fig. (2.3) for nonthermal average occupations.

Similarly, we can define the energy current operator through a continuity equation. Beginning from the energy density and assuming that the Hamiltonian is time-independent and $\left[\hat{H}, \hat{\mathbf{p}}\right] = 0$, we find

$$\frac{\partial}{\partial t}\left(\psi(\mathbf{r},t)^*\hat{H}\psi(\mathbf{r},t)\right) = (\partial_t\psi^*)\hat{H}\psi + \psi^*\hat{H}(\partial_t\psi) = \frac{i}{2m\hbar}\left((\hat{\mathbf{p}}^2\psi^*)\hat{H}\psi - \psi^*\hat{H}(\hat{\mathbf{p}}^2\psi)\right) = \tag{2.44}$$

$$= \frac{i\hbar}{2m}\boldsymbol{\nabla}\left(-(\boldsymbol{\nabla}\psi^*)\hat{H}\psi + \psi^*\hat{H}(\boldsymbol{\nabla}\psi)\right) \equiv -\boldsymbol{\nabla}\boldsymbol{\mathcal{J}}^{(E)}. \tag{2.45}$$

As earlier, to generalize to the second quantization formalism, the energy current operator is defined through replacing the wavefunction by the quantum fields

$$\hat{I}_\alpha^{(E)}(t,x) = \frac{i\hbar}{2m}\int dr_\perp \left\{\frac{\partial\hat{\Psi}_\alpha^\dagger(t,\mathbf{r})}{\partial x}\hat{H}\hat{\Psi}_\alpha(t,\mathbf{r}) - \hat{\Psi}_\alpha^\dagger(t,\mathbf{r})\hat{H}\frac{\partial\hat{\Psi}_\alpha(t,\mathbf{r})}{\partial x}\right\}, \tag{2.46}$$

for a time-independent Hamiltonian $\hat{H}$, commuting with the momentum operator. By using

$$\hat{H}\hat{\Psi}_\alpha(t,\mathbf{r}) = i\hbar\frac{\partial}{\partial t}\hat{\Psi}_\alpha(t,\mathbf{r}) = \sum_i\int dE E e^{\frac{-iEt}{\hbar}}\frac{\chi_{\alpha i}(E,r_\perp)}{\sqrt{hv(E)}}[\hat{a}_{\alpha i}e^{-ik(E)x} + \hat{b}_{\alpha i}e^{ik(E)x}], \tag{2.47}$$

and

$$\left(\hat{H}\hat{\Psi}_\alpha(t,\mathbf{r})\right)^\dagger = \hat{\Psi}_\alpha^\dagger(t,\mathbf{r})\hat{H}, \tag{2.48}$$

together with the broadband approximation we find

$$\hat{I}_\alpha^{(E)}(t,x) = \frac{1}{2h}\int dE dE' e^{-i(E-E')t/\hbar}(E+E')\sum_{i,\beta j,\gamma k}\left\{\boldsymbol{\mathcal{A}}_{\alpha i,\beta j,\gamma k}^{E',E}\hat{a}_{\beta j}^\dagger(E')\hat{a}_{\gamma_k}(E)\right\}. \tag{2.49}$$

This expression again has a simple interpretation: the energy flow into/out of reservoir $\alpha$ is the energy carried by the incoming/outgoing particles. This expression for the energy current operator will later be used to calculate its fluctuations. Taking the expectation value in the same manner as before we find

$$I_\alpha^{(E)} = \left\langle\hat{I}_\alpha^{(E)}\right\rangle = \frac{1}{h}\int dE E\sum_{i,\beta j}|s_{\alpha i,\beta j}(E)|^2(f_\beta(E) - f_\alpha(E)). \tag{2.50}$$

Other currents can be defined in an analogous way by replacing $\hat{H}$ in Eq.(2.46) by other operators. Using the results for the particle and energy currents, it is straightforward to calculate the heat current operator and its expectation value

$$\hat{I}_\alpha^{(J)} = \hat{I}_\alpha^{(E)}(t,x) - \mu_\alpha\hat{I}_\alpha^{(0)}(t,x), \tag{2.51}$$

and

$$I_\alpha^{(J)} = \left\langle\hat{I}_\alpha^{(E)} - \mu_\alpha\hat{I}_\alpha^{(0)}\right\rangle = \frac{1}{h}\int dE(E-\mu_\alpha)\sum_{i,\beta j}|s_{\alpha i,\beta j}(E)|^2(f_\beta(E) - f_\alpha(E)). \tag{2.52}$$

Importantly, for thermal reservoirs, the local entropy production is given by the heat flow into the reservoir. This means that the fluctuations in entropy production are also caused by the fluctuations

in the heat currents. We are, however, interested in treating entropy production more generally for nonthermal reservoirs where particles are distributed according to non-equilibrium average occupations. For such reservoirs, the entropy production is no longer given by Clausius' relation, and one must treat it more generally. To treat the entropy production of nonthermal reservoirs, we need to make assumptions. Firstly, we assume that the state of the reservoirs is diagonal in the number basis; doing this, the entropy is the classical Gibbs entropy. We also assume that the reservoirs are large or kept fixed by an external source, such that the average occupations are not affected by the transport of particles. Under these assumptions, the results of [11] are applicable and the average entropy production of reservoir $\alpha$ becomes

$$I_\alpha^{(\Sigma)} = \frac{k_\mathrm{B}}{h}\int dE \log\left[\frac{f_\alpha(E)}{1\mp f_\alpha(E)}\right]\sum_{i,\beta j}|s_{\alpha i,\beta j}(E)|^2[f_\alpha(E)-f_\beta(E)], \tag{2.53}$$

where the plus sign is for bosons and the minus sign is for fermions. This expression can be understood as how much the multiplicity, and therefore entropy, is changed by the flow of particles into and out of the reservoir. While this expression is used to calculate entropy productions, it should be thought of more as an entropy current. And while the entropy production isn't given by an operator (since the operator itself would depend on the state of a system), one still wishes to calculate the fluctuations in entropy currents. To do this, we define an entropy current through operators as

$$\hat{I}_\alpha^{(\Sigma)}(t,x) = \frac{-k_\mathrm{B}}{h}\int dE dE' e^{-i(E-E')t/\hbar}\log\left[\frac{f_\alpha(E)}{1\mp f_\alpha(E)}\right]\sum_{i,\beta j,\gamma k}\left\{\boldsymbol{\mathcal{A}}^{E',E}_{\alpha i,\beta j,\gamma k}\hat{a}^\dagger_{\beta j}(E')\hat{a}_{\gamma_k}(E)\right\}. \tag{2.54}$$

An important property of these entropy currents is that they reduce to the expressions for the heat currents for thermal reservoirs. This can be seen by inserting either the Fermi or BE distributions in

$$\log\left[\frac{f_\alpha(E)}{1\mp f_\alpha(E)}\right] = \log\left[\frac{\frac{1}{e^{(E-\mu_\alpha)/(k_\mathrm{B}T_\alpha)}\pm 1}}{1\mp\frac{1}{e^{(E-\mu_\alpha)/(k_\mathrm{B}T_\alpha)}\pm 1}}\right] = \frac{\mu_\alpha - E}{k_\mathrm{B}T_\alpha}, \tag{2.55}$$

which implies

$$\hat{I}_\alpha^{(\Sigma)}(t,x) = \frac{\hat{I}_\alpha^{(J)}(t,x)}{T_\alpha} \implies I_\alpha^{(\Sigma)} = \frac{I_\alpha^{(J)}}{T_\alpha}, \tag{2.56}$$

for thermal reservoirs, recovering Clausius' relation [11].

We have seen that multiple interesting currents, from a thermodynamics perspective, can be written in the form of a double integral over energy of a product of the scattering symbol, ladder operators, and a *real number*. We denote a current operator that can be written on this form as a classically weighted current, or a *c-weighted current* for short, and by defining the *generalized charge* coefficients

$$\begin{aligned} &C_\alpha^{(0)}(E,E') = 1,\ C_\alpha^{(E)}(E,E') = \frac{E+E'}{2}, \\ &C_\alpha^{(\Sigma)}(E,E') = -k_\mathrm{B}\log\left[\frac{f_\alpha(E)}{1\mp f_\alpha(E)}\right],\ C_\alpha^{(J)}(E,E') = (E-\mu_\alpha), \end{aligned} \tag{2.57}$$

we can compactly write the current operators as

$$\hat{I}_\alpha^{(\nu)} = \frac{1}{h}\sum_{i,\beta j,\gamma k}\int dE dE' C_\alpha^{(\nu)}(E,E')e^{-i\frac{E-E'}{\hbar}t}\boldsymbol{\mathcal{A}}^{E',E}_{\alpha i,\beta j,\gamma k}a^\dagger_{\beta j}(E')a_{\gamma_k}(E), \tag{2.58}$$

and its expectation value as

$$I_\alpha^{(\nu)} = \frac{1}{h}\int dE C_\alpha^{(\nu)}(E,E)\sum_{i,\beta j}|s_{\alpha i,\beta j}(E)|^2(f_\beta(E)-f_\alpha(E)). \tag{2.59}$$

We will often drop the second energy argument $C_\alpha^{(\nu)}(E,E)$ when working with the expectation values of the current operators, since they are always the same. We introduce the notion of c-weighted currents since multiple of the results derived in this thesis hold for c-weighted currents in general. Thus, if one is able to derive a new current on this form using scattering theory, one does not need to rederive the results that will later be presented in this thesis. While we have shown that multiple currents can be written in this form, it should be noted that the particle current is the central one, since the transport of a quantity is mediated by the particle current itself: The energy currents can be understood as the flow of energy due to the transported particles carrying energy, the heat flow due to the heat carried by particles, and the entropy current, which is caused by the flowing particles changing the multiplicity in different reservoirs. This might seem trivial, but if there are, for example,

states with quantum coherence then the entropy production would not be given by only the flow of particles but also by decoherence.

In this section, scattering theory has been employed to calculate multiple current operators and their expectation value. We introduced c-weighted currents, which allow one to compactly refer to a number of interesting currents. In the next section, we continue using scattering theory to calculate fluctuations in these currents, which will later be used to derive trade-off relations.

### 2.2.2 Correlators and noise

Fluctuations and uncertainties are fundamental features of quantum mechanics. These stem from classical phenomena such as thermal fluctuations, imperfect state preparation, as well as from quantum mechanical effects such as superpositions and decoherence. The most famous example of a relation between uncertainties in quantum mechanics is the Heisenberg uncertainty relation. Introducing the deviation from the average of an operator

$$\Delta\hat{A} = \hat{A} - \left\langle \hat{A} \right\rangle, \tag{2.60}$$

the Heisenberg uncertainty relation states that for two operators, $\hat{A}$ and $\hat{B}$ the following inequality holds [25]

$$\sqrt{\left\langle \Delta\hat{A}^2 \right\rangle}\sqrt{\left\langle \Delta\hat{B}^2 \right\rangle} = \sqrt{\left\langle \hat{A}^2 \right\rangle - \left\langle \hat{A} \right\rangle^2}\sqrt{\left\langle \hat{B}^2 \right\rangle - \left\langle \hat{B} \right\rangle^2} \geq \frac{1}{2}\left|\left\langle \left[\hat{A}, \hat{B}\right] \right\rangle\right|. \tag{2.61}$$

This inequality states that the product of the standard deviations of the two operators is bound from below by the expectation value of the commutator between the operators. Thus, the two observables can only be measured perfectly simultaneously if they commute. This is the famous result for position and momentum. It should be noted that this is a much more fundamental feature of quantum theory compared to the relations we derive in this thesis.

Focusing on nanoscale devices, we have already derived average currents. The magnitude of these currents is, however, not the only way to characterize performance: we also care about precision. For the rest of this section, we will focus on introducing fluctuations and how to calculate them.

To start, we define the deviation from the average of a current operator

$$\Delta\hat{I}_\alpha^{(\nu)}(t,x) = \hat{I}_\alpha^{(\nu)}(t,x) - \left\langle \hat{I}_\alpha^{(\nu)}(t,x) \right\rangle, \tag{2.62}$$

which is exactly the type of expression used in the Heisenberg uncertainty relation. Using this, we introduce the notion of noise in a current as the *symmetrized fluctuations* through the following correlator, in the absence of external time-dependent fields [28, 6, 21]:

$$S_{\alpha\beta}^{(\nu)}(t,t') = S_{\alpha\beta}^{(\nu)}(t-t') = \left\langle \Delta\hat{I}_\alpha^{(\nu)}(t)\Delta\hat{I}_\beta^{(\nu)}(t') + \Delta\hat{I}_\beta^{(\nu)}(t')\Delta\hat{I}_\alpha^{(\nu)}(t) \right\rangle = \left\langle \left\{ \Delta\hat{I}_\alpha^{(\nu)}(t), \Delta\hat{I}_\beta^{(\nu)}(t') \right\} \right\rangle. \tag{2.63}$$

We choose to study the fluctuations in the frequency domain, which is often called the *noise power*. To do this, we take the Fourier transform

$$\begin{aligned}\int_{-\infty}^{\infty} dt' e^{-i\omega' t'} \int_{-\infty}^{\infty} dt e^{-i\omega t} S_{\alpha\beta}^{(\nu)}(t-t') &= 2\pi\delta(\omega+\omega')S_{\alpha\beta}^{(\nu)}(\omega) \\ &= \left\langle \left\{ \Delta\hat{I}_\alpha^{(\nu)}(\omega), \Delta\hat{I}_\beta^{(\nu)}(\omega') \right\} \right\rangle = \left\langle \left\{ \hat{I}_\alpha^{(\nu)}(\omega), \hat{I}_\beta^{(\nu)}(\omega') \right\} \right\rangle. \end{aligned} \tag{2.64}$$

The last equality holds for $\omega \neq \omega'$. Next, we evaluate the expectation values of Eq. (2.64). This involves taking the expectation value of quartic products of ladder operators. For non-interacting particles, this can be done using Wick's theorem [23], which tells us that

$$\left\langle \hat{a}_{\alpha i}^\dagger \hat{a}_{\beta j} \hat{a}_{\gamma k}^\dagger \hat{a}_{\delta l} \right\rangle = \left\langle \hat{a}_{\alpha i}^\dagger \hat{a}_{\beta j} \right\rangle \left\langle \hat{a}_{\gamma k}^\dagger \hat{a}_{\delta l} \right\rangle \pm \left\langle \hat{a}_{\alpha i}^\dagger \hat{a}_{\gamma k}^\dagger \right\rangle \langle \hat{a}_{\beta j} \hat{a}_{\delta l} \rangle + \left\langle \hat{a}_{\alpha i}^\dagger \hat{a}_{\delta l} \right\rangle \left\langle \hat{a}_{\beta j} \hat{a}_{\gamma k}^\dagger \right\rangle - (1 \pm 1) \left\langle \hat{a}_{\alpha i}^\dagger \right\rangle \langle \hat{a}_{\beta j} \rangle \left\langle \hat{a}_{\gamma k}^\dagger \right\rangle \langle \hat{a}_{\delta l} \rangle. \tag{2.65}$$

For states diagonal in the number basis, all terms not containing the same number of creation and annihilation operators drop and we find

$$\begin{aligned}\left\langle \hat{a}_{\alpha i}^\dagger(E_1)\hat{a}_{\beta j}(E_2)\hat{a}_{\gamma k}^\dagger(E_3)\hat{a}_{\delta l}(E_3) \right\rangle &= \left\langle \hat{a}_{\alpha i}^\dagger(E_1)\hat{a}_{\beta j}(E_2) \right\rangle \left\langle \hat{a}_{\gamma k}^\dagger(E_3)\hat{a}_{\delta l}(E_4) \right\rangle \\ &\quad + \left\langle \hat{a}_{\alpha i}^\dagger(E_1)\hat{a}_{\delta l}(E_4) \right\rangle \left\langle \hat{a}_{\beta j}(E_2)\hat{a}_{\gamma k}^\dagger(E_3) \right\rangle \\ &= \delta_{\alpha\beta}\delta_{ij}\delta_{\gamma\delta}\delta_{kl} f_\alpha(E_1) f_\gamma(E_3)\delta(E_1-E_2)\delta(E_3-E_4) \\ &\quad \pm \delta_{\alpha\delta}\delta_{il}\delta_{\gamma\beta}\delta_{jk} f_\alpha(E_1) f_\gamma(E_3)\delta(E_1-E_4)\delta(E_2-E_3), \end{aligned} \tag{2.66}$$

where the plus signs correspond to bosons and the minus sign to fermions. Using this, we finally find

$$S^{(\nu)}_{\alpha\beta}(\omega) = \frac{1}{2h}\sum_{\gamma\delta}\sum_{ij}\sum_{mn}\int dE \boldsymbol{\mathcal{A}}^{E,E+\hbar\omega}_{\alpha i,\gamma m,\delta n}\boldsymbol{\mathcal{A}}^{E+\hbar\omega,E}_{\beta j,\delta n,\gamma m}C^{(\nu)}_{\alpha}(E)C^{(\nu)}_{\beta}(E+\hbar\omega) \times \{f_\gamma(E)(1\pm f_\delta(E+\hbar\omega)+(1\pm f_\gamma(E))f_\delta(E+\hbar\omega)\}\,. \tag{2.67}$$

We restrict ourselves to working with the *zero-frequency noise*, which takes the following form [6, 28]:

$$S^{(\nu)}_{\alpha\beta} = S^{(\nu)}_{\alpha\beta}(0) = \int_{-\infty}^{\infty} dt \left\langle \{\Delta\hat{I}^{(\nu)}_{\alpha}(t), \Delta\hat{I}^{(\nu)}_{\beta}(0)\} \right\rangle \tag{2.68}$$

$$= \frac{1}{2h}\sum_{\gamma\delta}\sum_{ij}\sum_{mn}\int dE \boldsymbol{\mathcal{A}}^{E,E}_{\alpha i,\gamma m,\delta n}\boldsymbol{\mathcal{A}}^{E,E}_{\beta j,\delta n,\gamma m}C^{(\nu)}_{\alpha}(E)C^{(\nu)}_{\beta}(E) \times \{f_\gamma(E)(1\pm f_\delta(E))+(1\pm f_\gamma(E))f_\delta(E)\}\,. \tag{2.69}$$

Here again, the plus signs are for bosons and minus signs for fermions. This expression has a natural interpretation, it is the integral over time of the symmetrized products of the deviations, and it sums up all the correlations in the fluctuations between two currents. This expression is the cross-correlator between the fluctuations of two currents, and while interesting, we will focus the *auto-correlator* of the deviations in a current. Dropping the frequency argument since it is always zero from here on, the noise in a current becomes

$$S^{(\nu)}_{\alpha\alpha} = \int_{-\infty}^{\infty} dt \left\langle \{\Delta\hat{I}^{(\nu)}_{\alpha}(t), \Delta\hat{I}^{(\nu)}_{\alpha}(0)\} \right\rangle \tag{2.70}$$

$$= \frac{1}{2h}\sum_{\gamma\delta}\sum_{ij}\sum_{mn}\int dE \boldsymbol{\mathcal{A}}^{E,E}_{\alpha i,\gamma m,\delta n}\boldsymbol{\mathcal{A}}^{E,E}_{\alpha j,\delta n,\gamma m}[C^{(\nu)}_{\alpha}(E)]^2 \times \{f_\gamma(E)(1\pm f_\delta(E))+(1\pm f_\gamma(E))f_\delta(E)\}\,. \tag{2.71}$$

This is the quantity relevant for studying the fluctuations in a steady-state c-weighted current. It is, however, complicated to work with and will later be split up into different parts, which are more manageable. We will study how to do this for fermions in the next section, where we go through some earlier fermionic scattering theory results that we will extend to bosonic systems in Sections 3.1 and 3.2.

### 2.2.3 Earlier fermionic trade-off relations

In this section, we will discuss two previous papers where bounds between currents and fluctuations for fermionic systems were derived using scattering theory. From now on, to make it clear whether or not we are discussing fermions or bosons, different fonts will be used. For fermions, we will use

$$\mathcal{I}^{(\nu)}_{\alpha} = \left\langle \hat{\mathcal{I}}^{(\nu)}_{\alpha} \right\rangle = \frac{1}{h}\int dE C^{(\nu)}_{\alpha}(E)\sum_{i,\beta j}|s_{\alpha i,\beta j}(E)|^2(f_\beta(E)-f_\alpha(E)), \tag{2.72}$$

to refer to the currents and

$$\mathcal{S}^{(\nu)}_{\alpha\beta} = \frac{1}{2h}\sum_{\gamma\delta}\sum_{ij}\sum_{mn}\int dE \boldsymbol{\mathcal{A}}^{E,E}_{\alpha i,\gamma m,\delta n}\boldsymbol{\mathcal{A}}^{E,E}_{\beta j,\delta n,\gamma m}C^{(\nu)}_{\alpha}(E)C^{(\nu)}_{\beta}(E) \times \{f_\gamma(E)(1-f_\delta(E))+(1-f_\gamma(E))f_\delta(E)\}\,, \tag{2.73}$$

to refer to the fluctuations, while keeping

$$I^{(\nu)}_{\alpha} = \left\langle \hat{I}^{(\nu)}_{\alpha} \right\rangle = \frac{1}{h}\int dE C^{(\nu)}_{\alpha}(E)\sum_{i,\beta j}|s_{\alpha i,\beta j}(E)|^2(f_\beta(E)-f_\alpha(E)), \tag{2.74}$$

and

$$S^{(\nu)}_{\alpha\beta} = \frac{1}{2h}\sum_{\gamma\delta}\sum_{ij}\sum_{mn}\int dE \boldsymbol{\mathcal{A}}^{E,E}_{\alpha i,\gamma m,\delta n}\boldsymbol{\mathcal{A}}^{E,E}_{\beta j,\delta n,\gamma m}C^{(\nu)}_{\alpha}(E)C^{(\nu)}_{\beta}(E) \times \{f_\gamma(E)(1+f_\delta(E))+(1+f_\gamma(E))f_\delta(E)\}\,, \tag{2.75}$$

to refer to the bosonic expressions. Here it should be noted that for fermions

$$C^{(\Sigma)}_{\alpha}(E,E') = -k_{\mathrm{B}}\log\left[\frac{f_\alpha(E)}{1-f_\alpha(E)}\right] \tag{2.76}$$

while

$$C^{(\Sigma)}_{\alpha}(E,E') = -k_{\mathrm{B}}\log\left[\frac{f_\alpha(E)}{1+f_\alpha(E)}\right] \tag{2.77}$$

for bosons. From now on, we will also keep the summation over channel indices implicit for brevity, and the results we now go through will hold for multichannel leads. The full expressions, including the explicit channel indices, are shown in the appendix [B.1]. With this notation in place, we are ready to examine the previous fermionic results.

#### 2.2.3.1 Bounds on entropy production set by fluctuations

Earlier, in a paper by Acciai et. al. [2], a bound on entropy production set by fluctuations was derived using scattering theory. In the paper, the noise of Eq. (2.69) was split into a "classical" part, quadratic in the scattering matrix, and a "quantum" part, quartic in the scattering matrix.

$$\mathcal{S}^{(\nu)}_{\alpha\beta} = \mathcal{S}^{(\nu)}_{\alpha\beta,\mathrm{cl}} - \mathcal{S}^{(\nu)}_{\alpha\beta,\mathrm{qu}}. \tag{2.78}$$

By dropping energy arguments for the occupations and scattering matrix elements the classical part of the fluctuations are written as

$$\mathcal{S}^{(\nu)}_{\alpha\beta,\mathrm{cl}} = \frac{2}{h}\int dE[C^{(\nu)}_{\alpha}(E)C^{(\nu)}_{\beta}(E)]\Big\{ - F_{\alpha\alpha}|s_{\beta\alpha}|^2 - F_{\beta\beta}|s_{\alpha\beta}|^2 + \delta_{\alpha\beta}\sum_{\gamma}|s_{\alpha\gamma}|^2[F_{\alpha\gamma}+F_{\gamma\alpha}]\Big\}, \tag{2.79}$$

where $F_{\alpha\beta} = f_\alpha(1-f_\beta)$ is the Pauli factor, implementing the Pauli exclusion principle for fermions. The quantum part of the noise can be written as

$$\mathcal{S}^{(\nu)}_{\alpha\beta,\mathrm{qu}} = \frac{2}{h}\int dE[C^{(\nu)}_{\alpha}(E)C^{(\nu)}_{\beta}(E)]\,\mathrm{Re}\Big\{\sum_{\gamma\delta} s^*_{\alpha\gamma}s_{\beta\gamma}s_{\alpha\delta}s^*_{\beta\delta}(f_\alpha - f_\gamma)(f_\beta - f_\delta)\Big\}. \tag{2.80}$$

The classical part of the noise can be seen as a generalization of the classical expression for fluctuations [8]. This part of the noise describes transfers of single particles, while the quantum part describes correlated transfers of two particles. It is important to note that this division is by no means unique but useful [2]. To study the noise of different currents, the authors used the autocorrelators

$$\mathcal{S}^{(\nu)}_{\alpha\alpha} = \mathcal{S}^{(\nu)}_{\alpha\alpha,\mathrm{cl}} - \mathcal{S}^{(\nu)}_{\alpha\alpha,\mathrm{qu}}, \tag{2.81}$$

where

$$\mathcal{S}^{(\nu)}_{\alpha\alpha,\mathrm{cl}} = \frac{2}{h}\int dE[C^{(\nu)}_{\alpha}(E)]^2\Big\{\sum_{\gamma\neq\alpha}|s_{\alpha\gamma}|^2(F_{\alpha\gamma}+F_{\gamma\alpha})\Big\} \geq 0, \tag{2.82}$$

$$\mathcal{S}^{(\nu)}_{\alpha\alpha,\mathrm{qu}} = \frac{2}{h}\int dE[C^{(\nu)}_{\alpha}(E)]^2\Big\{\sum_{\gamma\neq\alpha}|s_{\alpha\gamma}|^2(f_\alpha - f_\gamma)\Big\}^2 \geq 0. \tag{2.83}$$

Using the following two inequalities

$$\begin{cases} x^2 + 1/4 \geq |x|, \\ F_{\alpha\gamma} + F_{\gamma\alpha} \geq |f_\alpha - f_\gamma|, \end{cases} \tag{2.84}$$

it was proven for fermionic systems described by scattering theory that the classical fluctuations bound the local entropy production/reduction of a reservoir through

$$\mathcal{S}^{(\Sigma)}_{\alpha\alpha,\mathrm{cl}} + \frac{k_\mathrm{B}^2}{4}\mathcal{S}^{(0)}_{\alpha\alpha,\mathrm{cl}} \geq 2k_\mathrm{B}\big|\mathcal{I}^{(\Sigma)}_{\alpha}\big|. \tag{2.85}$$

This result tells us there has to be a minimum amount of classical fluctuations present in a fermionic reservoir to produce or reduce entropy, effectively bounding the precision of a thermodynamic process [2]. However, due to the minus sign in front of the fermionic quantum noise in Eq. (2.81), this bound doesn't hold for the full fluctuations, and the bound is broken when trying to extend it to the quantum noise. In Ref. [2], the authors also proved that

$$\mathcal{S}^{(\Sigma)}_{\alpha\alpha} \geq \frac{2k_\mathrm{B}^2}{h}\int dE[C^{(\Sigma)}]^2|s_{\alpha\alpha}|^2\sum_{\gamma\neq\alpha}|s_{\alpha\gamma}|^2|f_\alpha - f_\gamma|, \tag{2.86}$$

which together with the first bound of Eq. (2.84) implies the following bound for the full noise

$$\mathcal{S}^{(\Sigma)}_{\alpha\alpha} + \frac{k_\mathrm{B}^2}{4}\mathcal{S}^{(0)}_{\alpha\alpha} \geq 2k_\mathrm{B}\big|\mathcal{I}^{(\Sigma)}_{\alpha}\big|\inf_{E\in A}|s_{\alpha\alpha}(E)|^2. \tag{2.87}$$

where $A$ is the support of the integrand in Eq. (2.72). In this thesis, we will derive the corresponding relations for bosons and treat the quantum mechanical part of the noise in a new way. We also make further improvements to the bound of Eq. (2.85) which also apply to fermions. However, this is not the only result we extend to bosonic systems: in the next section, we will go through a thermodynamic uncertainty relation that has been derived for fermionic systems using scattering theory.

#### 2.2.3.2 Thermodynamic uncertainty relation

In a paper by K. Brandner et. al. [8], thermodynamic uncertainty relations for fermionic systems were derived using scattering theory. In this paper, the same division into classical and quantum noise, as previously shown in Eq. (2.82) and Eq. (2.83), was used. In Ref. [8], TURs were derived for multiterminal devices of thermal reservoirs where each reservoir was at the same temperature but different chemical potentials. To do this, K. Brandner defined quadratic forms parametrized by real numbers $x$ and $\psi$

$$\mathcal{A}_\alpha = \frac{\sigma}{k_\mathrm{B}} - 2\psi x \mathcal{I}_\alpha^{(0)} + \psi x^2 \mathcal{S}_{\alpha\alpha,\mathrm{cl}}^{(0)}. \tag{2.88}$$

Here $\sigma$ is the total entropy production of the system, which is calculated using Clausius' relation for reservoirs at equal temperature $T$,

$$\sigma = \sum_\alpha \frac{\mathcal{I}_\alpha^{(J)}}{T}. \tag{2.89}$$

Brandner then continued to find values of $\psi$ such that the function is semidefinite positive $\mathcal{A}_\alpha \geq 0$. The quadratic form was semidefinite positive for $\psi = 2$ for systems with time reversal symmetry and for systems without this symmetry, $\psi \approx 0.89612$. This difference boils down to if the scattering matrix is symmetric or not. Using this and minimizing the quadratic form with respect to $x$ the following inequality was proven

$$\sigma \geq \psi k_\mathrm{B} \frac{\left|\mathcal{I}_\alpha^{(0)}\right|^2}{\mathcal{S}_{\alpha\alpha,\mathrm{cl}}^{(0)}}, \tag{2.90}$$

with different values of $\psi$ depending on whether or not there is time reversal symmetry. This is a thermodynamic uncertainty relation for fermionic systems described by scattering theory. It should, however be noted that it only holds for the classical part of the noise, and the TUR is generally broken when considering the full fluctuations, since the quantum fluctuations are negative for fermions. In this thesis, we will derive the corresponding TUR for bosonic systems with time reversal symmetry and extend it to the quantum part of the fluctuations. We will also find a way to include the quantum part of the fluctuations for fermionic systems. Brandner also derived TURs for classical system using a classical version of scattering theory in [8]. While the formalism is different, the expressions for currents and fluctuations remain similar to the quantum versions [8].

We have now seen the general setup for scattering theory and some trade-off relations that have been derived using it. In the next section, we show a minimal example of a system where we can apply scattering theory. The system we will investigate consists of two thermal reservoirs, connected by a scattering region.

## 2.3 Two-terminal conductor

It is instructive to see the theory applied to a system, and the simplest case illustrating important concepts is a two-terminal system consisting of two reservoirs connected by a mesoscopic conductor. In this example the transport is assumed to take place in a single channel in each lead. The system can be seen represented in Fig. (2.4), where the left (right) reservoir is denoted by L (R). The particle current for a reservoir is defined to be positive if it is flowing into the reservoir, and each reservoir has a temperature $T_\alpha$ and chemical potential $\mu_\alpha$ with $\alpha =$ L,R. The BE distributions are plotted in solid red lines and Fermi distributions as dashed blue lines. These distributions describe the average occupation numbers in each reservoir. The sign of biases in potential and temperature can be seen defined in the figure, $\Delta\mu = \mu_\mathrm{L} - \mu_\mathrm{R}$ and $\Delta T = T_\mathrm{L} - T_\mathrm{R}$.

Defining the transition probability $D_{\alpha\beta}(E) = |s_{\alpha\beta}(E)|^2$ where $s(E)$ is the scattering matrix, the expectation values of the currents for this system becomes

$$\begin{aligned}
I_L &= -I_R = \frac{q}{h}\int dE D_{LR}(E)(f_R(E) - f_L(E)),\\
I_L^E &= -I_R^E = \frac{1}{h}\int dE E D_{LR}(E)(f_R(E) - f_L(E)),\\
J_L &= \frac{1}{h}\int dE (E-\mu_L) D_{LR}(E)(f_R(E) - f_L(E)),\\
J_R &= \frac{1}{h}\int dE (E-\mu_R) D_{LR}(E)(f_L(E) - f_R(E)).
\end{aligned} \tag{2.91}$$

Note that charge and energy conservation holds due to $I_\mathrm{L} + I_\mathrm{R} = I_\mathrm{L}^E + I_\mathrm{R}^E = 0$, but heat is generally not conserved $J_\mathrm{L} + J_\mathrm{R} \neq 0$. The linear response of the system can be calculated by considering small biases in temperature and potential away from the averages $T_0$, $\mu_0$, $T_\alpha = T_0 + \Delta T_\alpha$, $\mu_\alpha = \mu_0 + \Delta\mu_\alpha$

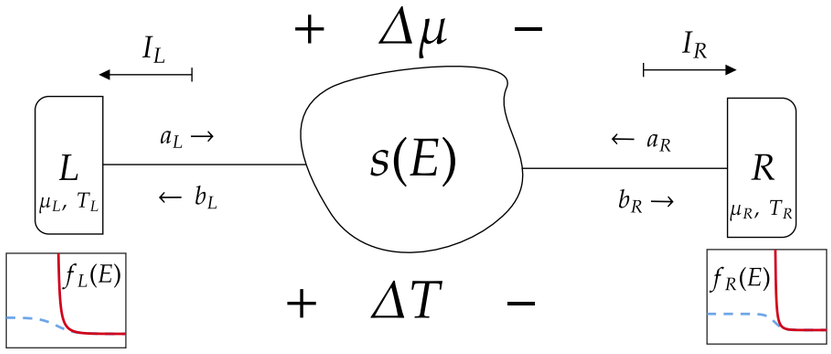


**Figure 2.4:** Figure depicting two-terminal system. The system consists of a left ($L$) and a right ($R$) reservoir connected by a mesoscopic conductor described by a scattering matrix $s(E)$. BE distributions can be seen plotted in the solid red lines and Fermi distributions as dashed blue lines. These distributions describe the average occupation numbers in each reservoir.

and expanding the average occupations. The following expansion holds for both the BE and Fermi distributions

$$\begin{aligned} f_\alpha(E) \approx & f_0(E;T_0,\mu_0) + \Delta\mu_\alpha \frac{\partial f_0}{\partial \mu} + \Delta T_\alpha \frac{\partial f_0}{\partial T} + \mathcal{O}\left(\Delta\mu_\alpha^2, \Delta T_\alpha^2\right) \\ = & f_0(E;T_0,\mu_0) - \Delta\mu_\alpha \frac{\partial f_0}{\partial E} - \Delta T_\alpha \frac{E-\mu_0}{T_0}\frac{\partial f_0}{\partial E} + \mathcal{O}\left(\Delta\mu_\alpha^2, \Delta T_\alpha^2\right). \end{aligned} \tag{2.92}$$

Using this expansion and defining $\Delta\mu \equiv -\Delta\mu_{\mathrm{R}} = \Delta\mu_{\mathrm{L}}$ and $\Delta T \equiv -\Delta T_{\mathrm{R}} = \Delta T_{\mathrm{L}}$ the linear response for the charge and energy current become

$$I \equiv -I_{\mathrm{L}} \approx -\frac{q}{h}\int dE D_{\mathrm{LR}}(E)\left\{\frac{\partial f_0}{\partial E}\Delta\mu + \frac{E-\mu_0}{T_0}\frac{\partial f_0}{\partial E}\Delta T\right\} \equiv G\Delta\mu + \kappa\Delta T, \tag{2.93}$$

$$I^E \equiv -I_{\mathrm{L}}^E \approx -\frac{1}{h}\int dE E D_{\mathrm{LR}}(E)\left\{\frac{\partial f_0}{\partial E}\Delta\mu + \frac{E-\mu_0}{T_0}\frac{\partial f_0}{\partial E}\Delta T\right\} \equiv \Gamma\Delta\mu + \Phi\Delta T. \tag{2.94}$$

With this choice of $I$ the conductances are positive. In the linear response regime it is possible to achieve a thermo-"electric" effect, where a current of particles is driven from a reservoir with lower chemical potential to one with a higher potential using a temperature bias and thus performing useful work. With the present definitions of currents and biases, this means driving a negative current with a positive potential bias

$$I = G\Delta\mu + \kappa\Delta T < 0 \implies -\Delta T\frac{\kappa}{G} > \Delta\mu. \tag{2.95}$$

For fermions this is only possible by breaking electron-hole symmetry. This is because $\frac{\partial f_{\mathrm{F}}}{\partial E}$ is an even function around $\mu_0$ while $(E-\mu_0)$ is odd causing the coefficient $\kappa$ to be zero for any transmission probability even around $\mu_0$. This is not required for bosons. Setting the transmission probability constant $D_{LR}(E) = D_{LR}$, the coefficients become

$$G = -\frac{q}{h}\int_0^\infty dE D_{LR}\frac{\partial f_{\mathrm{BE}}}{\partial E} = \frac{qD_{LR}}{h}\frac{1}{e^{-\beta_0\mu_0}-1}, \tag{2.96}$$

$$\kappa = -\frac{1}{h}\int_0^\infty dE D_{LR}(E-\mu_0)\frac{\partial f_{\mathrm{BE}}}{\partial E} = \frac{qD_{LR}}{hT_0}\left[\frac{e^{\beta_0\mu_0}\mu_0}{1-e^{\beta_0\mu_0}} - \frac{\log\left(1-e^{\beta_0\mu_0}\right)}{\beta_0}\right], \tag{2.97}$$

where $\beta_0 = 1/k_{\mathrm{B}}T_0$. These are both positive functions and the ratio is plotted in Fig. (2.5), work can be performed without the need for a specific transmission probability by setting a negative temperature bias, as suggested by Eq. (2.95).

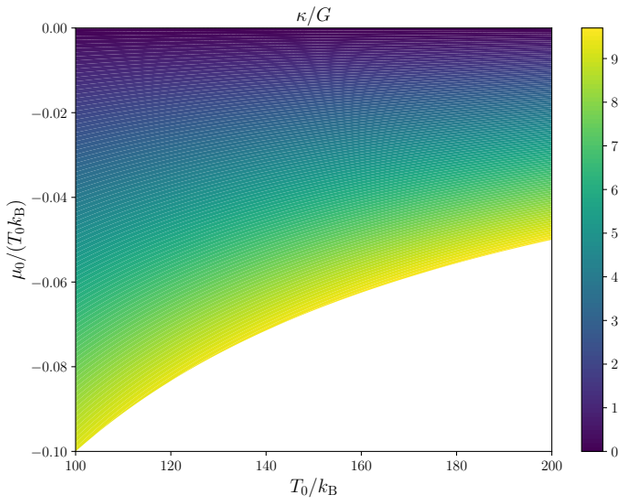


**Figure 2.5:** Ratio of thermal conductivity and chemical conductivity as functions of average chemical potential and temperature of a two-terminal system. A non-zero value of the ratio indicates that it is possible to perform useful work by setting a temperature bias that drives particles into a reservoir with a higher chemical potential.

It is also interesting to compare the currents for bosons and fermions outside of the linear regime. This can be done by again assuming an energy-independent transmission and evaluating integrals. The currents in the bosonic case become

$$I_{\mathrm{L}} = -I_{\mathrm{R}} = \frac{q k_{\mathrm{B}} D_{\mathrm{LR}}}{h} \left[ T_{\mathrm{R}} \log\left( \left| 1 - e^{\mu_{\mathrm{R}}/k_{\mathrm{B}} T_{\mathrm{R}}} \right| \right) - T_{\mathrm{L}} \log\left( \left| 1 - e^{\mu_{\mathrm{L}}/k_{\mathrm{B}} T_{\mathrm{L}}} \right| \right) \right], \tag{2.98}$$

$$I^E_{\mathrm{L}} = -I^E_{\mathrm{R}} = \frac{D_{\mathrm{LR}} k_{\mathrm{B}}^2}{h} \left[ T_{\mathrm{L}}^2 \mathrm{Li}_2(e^{\mu_{\mathrm{L}}/k_{\mathrm{B}} T_{\mathrm{L}}}) - T_{\mathrm{R}}^2 \mathrm{Li}_2(e^{\mu_{\mathrm{R}}/k_{\mathrm{B}} T_{\mathrm{R}}}) \right], \tag{2.99}$$

where $\mathrm{Li}_2(x)$ is the second order polylogarithmic function. For the fermionic case the corresponding expressions are

$$\mathcal{I}_{\mathrm{L}} = -\mathcal{I}_{\mathrm{R}} = \frac{q k_{\mathrm{B}} D_{\mathrm{LR}}}{h} \left[ T_{\mathrm{L}} \log\left( 1 + e^{\mu_{\mathrm{L}}/k_{\mathrm{B}} T_{\mathrm{L}}} \right) - T_{\mathrm{R}} \log\left( 1 + e^{\mu_{\mathrm{R}}/k_{\mathrm{B}} T_{\mathrm{R}}} \right) \right], \tag{2.100}$$

$$\mathcal{I}^E_{\mathrm{L}} = -\mathcal{I}^E_{\mathrm{R}} = \frac{D_{\mathrm{LR}} k_{\mathrm{B}}^2}{h} \left[ T_{\mathrm{R}}^2 \mathrm{Li}_2(-e^{\mu_{\mathrm{R}}/k_{\mathrm{B}} T_{\mathrm{R}}}) - T_{\mathrm{L}}^2 \mathrm{Li}_2(-e^{\mu_{\mathrm{L}}/k_{\mathrm{B}} T_{\mathrm{L}}}) \right]. \tag{2.101}$$

A comparison between the expressions for the particle current for bosons and fermions is plotted in Fig. (2.6). Here the currents are plotted as functions of chemical potential bias. It should be noted that the chemical potential is negative for bosons and positive for fermions. The bosonic currents diverge as the chemical potential of the right reservoir approaches zero, reminiscent of Bose-Einstein condensation.

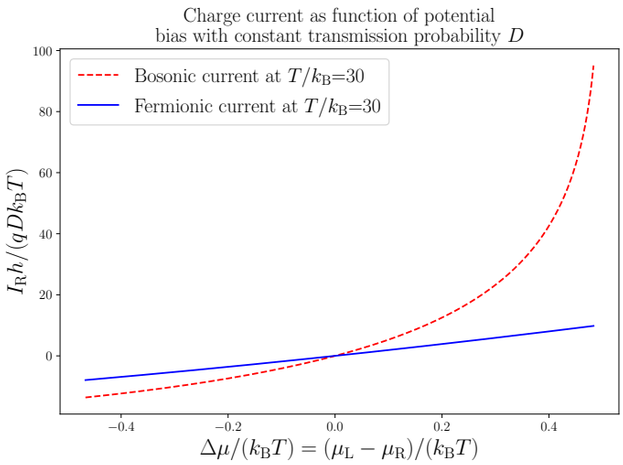


**Figure 2.6:** Plot comparing the charge current of bosons and fermions as functions of voltage bias. Both terminals have the same temperature, and the bosonic current diverges as one of the chemical potentials approaches zero.

# 3
# Results

In this chapter, we present the results derived in this thesis. These include trade-off relations for precision of both fermionic and bosonic reservoirs. In the first part of this chapter, we extend the bounds of Ref. [2] to bosonic systems and make further improvements, both by finding a tighter bound for the classical noise and by including the quantum noise. In the second part of this chapter, we extend the thermodynamic uncertainty relation derived in Ref. [8] to bosonic systems. In the third part of this chapter, we compare the results derived in the first two parts to each other and combine them to bound entropy production from both below and above for multiterminal devices with coherent transport.

This chapter is structured by first deriving a result for bosonic systems, then the fermionic counterpart. After this, the results presented are summarized, and some differences between the fermionic and bosonic cases are discussed.

## 3.1 Bounds on entropy production and currents for nonthermal reservoirs

In this section, we extend the bound on the local entropy production of Ref. [2], set by classical systems, to bosonic multiterminal systems with weakly interacting, coherently propagating particles with nonthermal occupations, diagonal in the number basis. In addition, we establish similar bounds for other c-weighted currents, such as particle and energy currents. Moreover, we are able to make improvements to the bounds of Ref. [2] that apply to both fermionic and bosonic systems. These are the first key results of this thesis. Moreover, we are able to extend the bounds to include the quantum noise. This is an important improvement since it allows us to establish bounds on the full physical fluctuations. By doing this, we gain more insight into the role of bunching and anti-bunching in the coherent transport of bosons and fermions. This is another key result of the thesis.

We begin this part of the results by presenting the expressions for the bosonic noise that will be used for the rest of the thesis.

### 3.1.1 Expressions for fluctuations in bosonic systems

There are multiple ways of writing the zero-frequency fluctuations of Eq. (2.69), e.g., splitting it into thermal and shot noise. Here we instead use the same decomposition into a "classical" part and a "quantum" part, as in Refs. [2, 8]. The classical part contains terms that are quadratic in scattering-matrix elements, while the quantum part contains terms that are quartic. In this decomposition, we write

$$S^{(\nu)}_{\alpha\beta} = S^{(\nu)}_{\alpha\beta,\mathrm{cl}} + S^{(\nu)}_{\alpha\beta,\mathrm{qu}}. \tag{3.1}$$

The classical noise can be interpreted as containing single-particle transfers across the scattering region while also including the bunching of bosons. The quantum noise can be interpreted as describing correlated two-particle transfers across the scattering region [6, 2]. We again emphasize that this is not a unique way of dividing the noise into different parts, but a practical one. By doing this, leaving the tracing over channel indices implicit and dropping the energy arguments of the scattering-matrix elements and average occupations for brevity, the classical noise becomes

$$S^{(\nu)}_{\alpha\beta,\mathrm{cl}} = \frac{2}{h}\int dE[C^{(\nu)}_{\alpha}(E)C^{(\nu)}_{\beta}(E)]\Big\{ - K_{\alpha\alpha}|s_{\beta\alpha}|^2 - K_{\beta\beta}|s_{\alpha\beta}|^2 + \delta_{\alpha\beta}\sum_{\gamma}|s_{\alpha\gamma}|^2[K_{\alpha\gamma}+K_{\gamma\alpha}]\Big\}, \tag{3.2}$$

where $K_{\alpha\beta} = f_\alpha(1+f_\beta)$, analogous to the Pauli factors in the fermionic noise, $F_{\alpha\beta} = f_\alpha(1-f_\beta)$. The Pauli factors can be interpreted as implementing the Pauli exclusion principle, while $K_{\alpha\beta}$ can be interpreted as implementing the bunching of bosons, and we therefore denote them as *bunching factors*. The quantum part of the noise can be written as

$$S^{(\nu)}_{\alpha\beta,\mathrm{qu}} = \frac{2}{h}\int dE[C^{(\nu)}_{\alpha}(E)C^{(\nu)}_{\beta}(E)]\,\mathrm{Re}\Big\{\sum_{\gamma\delta} s^*_{\alpha\gamma}s_{\beta\gamma}s_{\alpha\delta}s^*_{\beta\delta}(f_\alpha - f_\gamma)(f_\beta - f_\delta)\Big\}. \tag{3.3}$$

It is clear from comparing Eq. (2.79) and Eq. (2.80) to the expressions of Eq. (3.2) and Eq. (3.3) that the expressions for the bosonic and fermionic fluctuations are quite similar, apart from some minus signs. These are however very important, and here the first main difference to the fermionic case appears: when writing down the full noise in Eq. (3.1), the bosonic quantum noise is positive, unlike the fermionic case of Eq. (2.78). Not having this minus sign in front of the bosonic quantum noise will greatly simplify the analysis of the autocorrelators that will later be performed to characterize fluctuations in a given reservoir. Full derivations of these expressions are detailed in Appendix [B.1].

The expressions of Eq. (3.2) and Eq. (3.3) are cross-correlators between deviations in currents of different reservoirs. To analyze the fluctuations in the currents of one given reservoir, we use the autocorrelators. Using the same decompositions into quantum and classical parts, they become $S^{(\nu)}_{\alpha\alpha} = S^{(\nu)}_{\alpha\alpha,\mathrm{cl}} + S^{(\nu)}_{\alpha\alpha,\mathrm{qu}}$ where

$$S^{(\nu)}_{\alpha\alpha,\mathrm{cl}} = \frac{2}{h}\int_0^\infty dE[C^{(\nu)}_\alpha(E)]^2\left\{\sum_{\gamma\neq\alpha}|s_{\alpha\gamma}|^2(K_{\alpha\gamma}+K_{\gamma\alpha})\right\} \geq 0, \tag{3.4}$$

$$S^{(\nu)}_{\alpha\alpha,\mathrm{qu}} = \frac{2}{h}\int_0^\infty dE[C^{(\nu)}_\alpha(E)]^2\left\{\sum_{\gamma\neq\alpha}|s_{\alpha\gamma}|^2(f_\alpha-f_\gamma)\right\}^2 \geq 0. \tag{3.5}$$

It is worth pointing out that the integrand in the quantum autocorrelator is the square of the integrand of the corresponding currents of Eq. (2.59), up to multiplication by constants. From this, it follows that the quantum part of the noise vanishes when the different reservoirs are at equilibrium, i.e., $f_\alpha = f_\gamma$ for all $\gamma$. The quantum noise is also negligible in the tunneling regime, where the transmission probabilities between reservoirs are small:

$$1 \gg |s_{\alpha\gamma}(E)|^2. \tag{3.6}$$

Thus, close to equilibrium or in the tunneling regime, the classical contributions to the fluctuations dominate. In the next section, we focus on trade-off relations of such classical fluctuations, and we extend the fermionic results of Ref [2], presented in Sec. 2.2.3.1 to bosonic systems.

### 3.1.2 Bosonic bounds set by classical fluctuations

We begin by treating the classical part of the fluctuations of Eq. (3.4). To do this, we will make use of the following two inequalities:

$$\begin{cases} x^2 + 1/4 \geq |x|, \\ K_{\alpha\gamma} + K_{\gamma\alpha} \geq |f_\alpha - f_\gamma|. \end{cases} \tag{3.7}$$

Notice that the first of the two bounds holds for a general real number $x$ [2]. Combining the two inequalities, we find

$$\frac{2k_\mathrm{B}^2}{h}\int_0^\infty dE\left(\left[\frac{C^{(\Sigma)}_\alpha(E)}{k_\mathrm{B}}\right]^2+\frac{1}{4}\right)\left\{\sum_{\gamma\neq\alpha}|s_{\alpha\gamma}|^2(K_{\alpha\gamma}+K_{\gamma\alpha})\right\} \geq \frac{2k_\mathrm{B}^2}{h}\int_0^\infty dE\frac{|C^{(\Sigma)}_\alpha(E)|}{k_\mathrm{B}}\left\{\sum_{\gamma\neq\alpha}|s_{\alpha\gamma}|^2|f_\alpha-f_\gamma|\right\}, \tag{3.8}$$

which implies the following bound for the local entropy production of a reservoir:

$$S^{(\Sigma)}_{\alpha\alpha,\mathrm{cl}} + \frac{k_\mathrm{B}^2}{4}S^{(0)}_{\alpha\alpha,\mathrm{cl}} \geq 2k_\mathrm{B}\left|I^{(\Sigma)}_\alpha\right|. \tag{3.9}$$

This bound is the first key result of this thesis, and it is an extension of Eq. (2.85) found in Ref. [2] to bosonic systems. This particular combination of fluctuations in entropy production and particle currents will reappear often enough to deserve a name. We define the *resource fluctuations* [2] as

$$R_{\alpha,\mathrm{cl}} \equiv S^{(\Sigma)}_{\alpha\alpha,\mathrm{cl}} + \frac{k_\mathrm{B}^2}{4}S^{(0)}_{\alpha\alpha,\mathrm{cl}}, \tag{3.10}$$

$$R_{\alpha,\mathrm{qu}} \equiv S^{(\Sigma)}_{\alpha\alpha,\mathrm{qu}} + \frac{k_\mathrm{B}^2}{4}S^{(0)}_{\alpha\alpha,\mathrm{qu}}, \tag{3.11}$$

$$R_{\alpha} \equiv S^{(\Sigma)}_{\alpha\alpha} + \frac{k_\mathrm{B}^2}{4}S^{(0)}_{\alpha\alpha}. \tag{3.12}$$

A feature of the bound in Eq. (3.9) is that it holds on the level of integrand, not only for the full entropy production and noises. We name the inequality of Eq. (3.9) the Fluctuation Entropy production Bound or FEB for short. What this bound tells us is that if entropy is either produced or reduced in a reservoir, this sets a minimum limit on the combined fluctuations of the entropy

production and particle current. An important difference from the fermionic case is that here we are able to make the same statement for the total noise since the quantum part of the autocorrelators is positive in Eq. (3.5), unlike the fermionic case, since

$$S^{(\nu)}_{\alpha\alpha} = S^{(\nu)}_{\alpha\alpha,\mathrm{cl}} + S^{(\nu)}_{\alpha\alpha,\mathrm{qu}} \geq S^{(\nu)}_{\alpha\alpha,\mathrm{cl}}. \tag{3.13}$$

This allows us to write

$$S^{(\Sigma)}_{\alpha\alpha} + \frac{k_\mathrm{B}^2}{4} S^{(0)}_{\alpha\alpha} \geq 2k_\mathrm{B}\left|I^{(\Sigma)}_\alpha\right|. \tag{3.14}$$

This is the second key result of this thesis, where we are able to make the same statement for the complete noise as for the classical noise, unlike the fermionic case. To visualize the bound of Eq. (3.9) we can divide the left-hand side by the right-hand side. This expression is then bounded by 1 and reaches this value when the bound is tight. For the rest of the thesis, this is what is meant when we say that we plot an inequality or bound. This is shown in Fig. (3.1) for two terminals, $\alpha$ and $\gamma$, at the level of the integrands, where we defined the ratio

$$\varphi_{\alpha\gamma} \equiv \frac{|C^{(\Sigma)}_\alpha(E)|}{[C^{(\Sigma)}_\alpha(E)]^2 + k_\mathrm{B}^2/4} \frac{|f_\gamma - f_\alpha|}{K_{\alpha\gamma} + K_{\gamma\alpha}}. \tag{3.15}$$

Indeed, the inequalities of Eq. (3.7) hold at every energy in the integrals, which also allows for possibly nonthermal average occupations $f_\alpha$ and $f_\gamma$. Here one notices that the bound is non-symmetric with respect to exchanging the occupations of the reservoir, which is not surprising since entropy is not in general conserved. This is illustrated in panels (b,c). In particular, in panel (b), the ratio goes to zero as $f_\alpha - f_\gamma \to \infty$, while in panel (c) it saturates at

$$\frac{|\log\left[\frac{f_\alpha}{1+f_\alpha}\right]|}{\log\left[\frac{f_\alpha}{1+f_\alpha}\right]^2 + 1/4} \frac{1}{1+2f_\alpha} \tag{3.16}$$

as $f_\gamma - f_\alpha \to \infty$. It is clear from Fig. (3.1) that the classical FEB can be satisfied for specific average

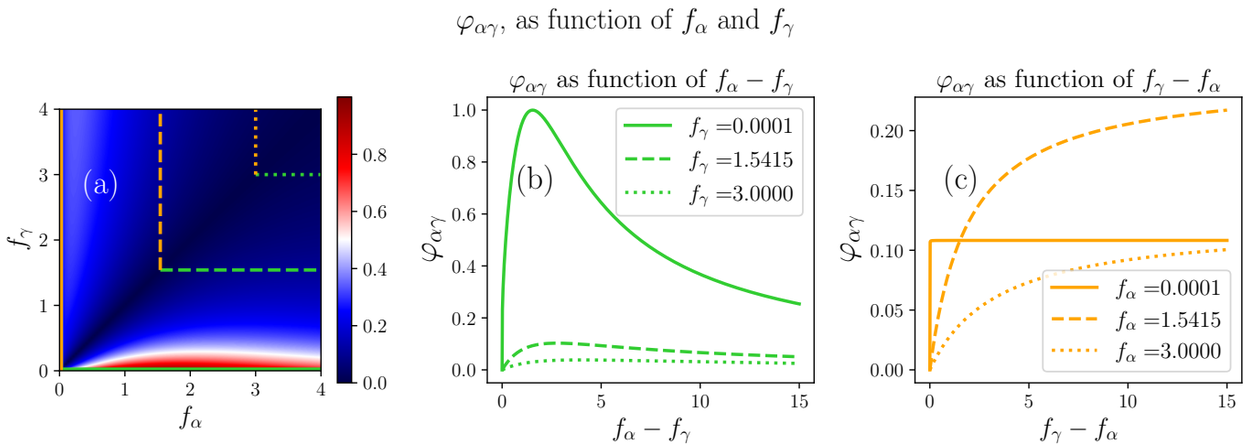


**Figure 3.1:** Figures displaying how the bound of Eq. (3.9) depends on the occupations of two reservoirs. Notice that the bound of Eq. (3.8) holds for every energy argument of the integrands. Here it is clear that there is an asymmetry in the dependence of the different occupations. This is illustrated in the two line plots, which display segments of the left plot where one of the occupations has been fixed. The bound saturates when $f_\alpha = \frac{1}{\sqrt{e}-1} \approx 1.5415$ and $f_\gamma = 0$.

occupations. To calculate when this happens, we begin from

$$[C^{(\nu)}_\alpha(E)]^2 + \frac{k_\mathrm{B}^2}{4} - |C^{(\nu)}_\alpha(E)| = 0 \implies C^{(\nu)}_\alpha(E) = \pm\frac{k_\mathrm{B}}{2}. \tag{3.17}$$

With the restriction that occupations must be positive, we find

$$\log\left[\frac{f_\alpha}{1+f_\alpha}\right] = -\frac{1}{2} \implies f_\alpha = \frac{1}{\sqrt{e}-1} \approx 1.54149. \tag{3.18}$$

The values $f_\gamma$ that satisfy the bound can be determined from

$$K_{\alpha\gamma} + K_{\gamma\alpha} - |f_\gamma - f_\alpha| = f_\alpha(1+f_\gamma) + f_\gamma(1+f_\alpha) - |f_\gamma - f_\alpha| = 0, \tag{3.19}$$

which is true only if $f_\gamma = 0$ or $f_\alpha = 0$. Since we already found the value for $f_\alpha$ to satisfy the FEB, we conclude,

$$S^{(\Sigma)}_{\alpha\alpha,\mathrm{cl}} + \frac{k_\mathrm{B}^2}{4} S^{(0)}_{\alpha\alpha,\mathrm{cl}} = 2k_\mathrm{B}\left|I^{(\Sigma)}_\alpha\right|, \tag{3.20}$$

if the two reservoirs have nonthermal average occupations which do not depend on energy

$$f_\alpha = \frac{1}{\sqrt{e}-1}, \quad f_\gamma = 0. \tag{3.21}$$

To gain further insight into how the bound behaves for thermal reservoirs, we plot it for the BE distribution, which is shown in Fig. (3.2) at the level of integrand. From this plot, it is clear that the bound becomes tight when $\frac{E-\mu_\alpha}{k_\mathrm{B}T_\alpha} = \frac{1}{2}$ and $\frac{E-\mu_\gamma}{k_\mathrm{B}T_\gamma} \gg 1$, which coincides with the result of Eq. (3.21).

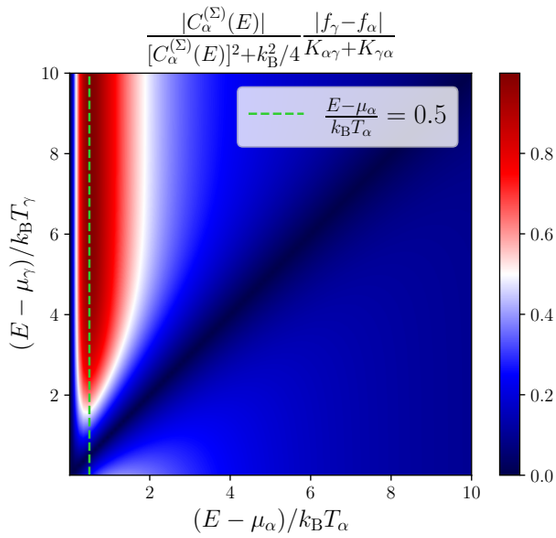


**Figure 3.2:** Figure displaying plot of the bound from Eq. (3.9) at the level of integrand, for thermal reservoirs. Here, the variables chosen are the arguments of the exponentials in the BE distributions: $f_\mathrm{BE}(x) = \frac{1}{e^x-1}$.

Following the same approach, we are able to establish similar bounds for the energy and particle currents using Eq. (3.7),

$$S^{(0)}_{\alpha\alpha,\mathrm{cl}} \geq 2|I^{(0)}_\alpha| \implies S^{(0)}_{\alpha\alpha} \geq 2|I^{(0)}_\alpha|, \tag{3.22}$$

$$S^{(E)}_{\alpha\alpha,\mathrm{cl}} + \frac{k_\mathrm{B}^2T^2}{4}S^{(0)}_{\alpha\alpha,\mathrm{cl}} \geq 2k_\mathrm{B}T|I^{(E)}_\alpha| \implies S^{(E)}_{\alpha\alpha} + \frac{k_\mathrm{B}^2T^2}{4}S^{(0)}_{\alpha\alpha} \geq 2k_\mathrm{B}T|I^{(E)}_\alpha|. \tag{3.23}$$

Here $k_\mathrm{B}T$ is chosen as an arbitrary constant with the unit of energy in Eq. (3.23), and in general, $T$ does not correspond to the temperature of a reservoir. As for the bound of Eq. (3.9) we are able to include the quantum part of the fluctuations for bosonic systems. In contrast to classical FEB the bounds in Eqs. (3.22, 3.23) are symmetric with respect to the exchange of $f_\alpha$ and $f_\gamma$, which stems from particle and energy conservation. This symmetry can be seen in Fig. (3.3), where the dependence on the average occupations of the classical bound of Eq. (3.22) at the integrand level is shown. Here we defined the ratio

$$Y_{\alpha\gamma} \equiv \frac{|f_\gamma - f_\alpha|}{K_{\alpha\gamma}+K_{\gamma\alpha}}. \tag{3.24}$$

From Eq. (3.19), we already know that the bound is saturated whenever $f_\gamma = 0$ or $f_\alpha = 0$, and $f_\gamma \neq f_\alpha$. This is illustrated in panels (b,c) of the figure, which display the ratio where one occupation is fixed. Letting the fixed reservoir have the occupation $f$ and the variable one have $f+\delta f$, we find that the ratios plotted in panels (b,c) reach the same values for large differences in occupations

$$\frac{|f_\gamma - f_\alpha|}{K_{\alpha\gamma}+K_{\gamma\alpha}} = \frac{\delta f}{\delta f + 2f\delta f + 2f(1+f)} \xrightarrow{\delta f\to\infty} \frac{1}{1+2f}. \tag{3.25}$$

It is again interesting to see how the classical current bound behaves for thermal reservoirs, which is plotted at the level of integrands in Fig. (3.4). Here we see that the bound is tight whenever there is a large difference in populations between the reservoirs. This is a natural result since, at equilibrium, there are only fluctuations and no average current.

To summarize, in this section, we successfully extended the previous fermionic results presented in Section 2.2.3.1 to bosonic systems. This establishes a trade-off relation between classical fluctuations and the local entropy production of a reservoir in Eq. (3.9), along with relations for the energy and particle currents. Furthermore, we managed to extend the bosonic bounds to include the full fluctuations without making the bound weaker. It is however possible to further improve the bound of Eq. (3.9) and this is the focus of the next section.

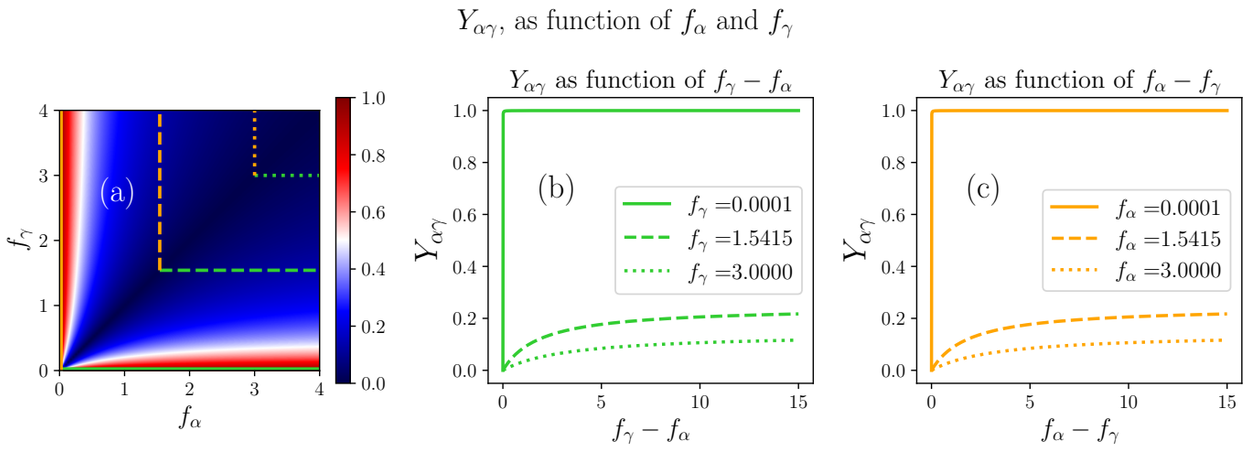


**Figure 3.3:** Figures displaying how the bound of Eq. (3.22) depends on the occupations of two reservoirs. Notice that the bound of Eq. (3.22) holds for every energy argument of the integrands. Here it is clear that this bound is symmetric with respect to exchanging the different occupations. This is illustrated in the two line plots, which display segments of the left plot where one of the occupations has been fixed. The bound saturates when $f_\alpha = 0$ or $f_\gamma = 0$.

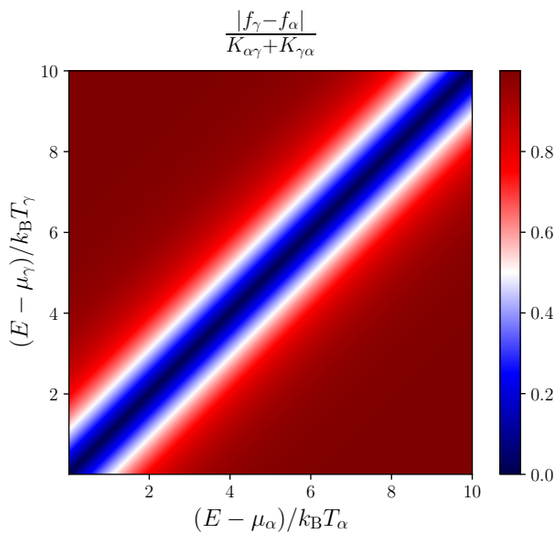


**Figure 3.4:** Figure displaying plot of the bound from Eq. (3.22) at the level of integrand, for thermal reservoirs. Here, the variables chosen are the arguments of the exponentials in the BE distributions: $f_{\mathrm{BE}}(x) = \frac{1}{e^x - 1}$.

### 3.1.3 Improved bosonic bounds set by classical fluctuations

In the last section, we derived bounds on the various currents set by fluctuations. In particular, the bounds of Eq. (3.9) and Eq. (3.23) can be improved by taking more care of how the particle current fluctuations are incorporated. To do this, we pick a real number $x$ with the same unit as $C_\alpha^{(\nu)}(E)$. In the case of $\nu = \Sigma$, $x$ has the dimension of energy over temperature, and in the case of $\nu = E$, the dimension of energy. Using the bounds of Eq.(3.7) we find

$$\left[\frac{C_\alpha^{(\nu)}(E)}{x}\right]^2 + \frac{1}{4} \geq \left|\frac{C_\alpha^{(\nu)}(E)}{x}\right|, \tag{3.26}$$

which implies

$$S_{\alpha\alpha,\mathrm{cl}}^{(\nu)} + \frac{x^2}{4} S_{\alpha\alpha,\mathrm{cl}}^{(0)} \geq 2x\left|I_\alpha^{(\nu)}\right|. \tag{3.27}$$

Up until now, there has been no real difference to the previous bounds, where we picked $x = k_\mathrm{B}$ for the FEB and $x = k_\mathrm{B}T$ for the bound on the energy current. This changes when we pick new values for $x$. We note that

$$S_{\alpha\alpha,\mathrm{cl}}^{(\nu)} + \frac{x^2}{4} S_{\alpha\alpha,\mathrm{cl}}^{(0)} - 2x\left|I_\alpha^{(\nu)}\right| \geq 0, \tag{3.28}$$

is a semidefinite positive quadratic form. We minimize this function with respect to the parameter $x$ by taking its derivative and find

$$\frac{x}{2} S_{\alpha\alpha,\mathrm{cl}}^{(0)} - 2\left|I_\alpha^{(\nu)}\right| = 0 \implies x = \frac{4\left|I_\alpha^{(\nu)}\right|}{S_{\alpha\alpha,\mathrm{cl}}^{(0)}}. \tag{3.29}$$

This is the value of $x$ that will yield the strictest possible bound between the current and its classical fluctuations, since it is minimizing the quadratic form. Inserting it into Eq. (3.27) we arrive at

$$S^{(\nu)}_{\alpha\alpha,\mathrm{cl}} + 4\frac{\left|I^{(\nu)}_\alpha\right|^2}{S^{(0)}_{\alpha\alpha,\mathrm{cl}}} \geq 8\frac{\left|I^{(\nu)}_\alpha\right|^2}{S^{(0)}_{\alpha\alpha,\mathrm{cl}}} \implies$$
$$S^{(\nu)}_{\alpha\alpha,\mathrm{cl}} \geq 4\frac{\left|I^{(\nu)}_\alpha\right|^2}{S^{(0)}_{\alpha\alpha,\mathrm{cl}}} \iff S^{(0)}_{\alpha\alpha,\mathrm{cl}} \geq 4\frac{\left|I^{(\nu)}_\alpha\right|^2}{S^{(\nu)}_{\alpha\alpha,\mathrm{cl}}}. \tag{3.30}$$

The second formulation of Eq. (3.30) has an interesting implication: the classical precision in a c-weighted current, e.g., entropy or energy current, is bounded by the classical fluctuations in the particle current. This means that, if one wants high precision in a c-weighted current, the particle current fluctuations have to be large. This might seem like a strange result, but it should be noted that particle current has special importance since the particle flow is mediating all other flows. This bound is reminiscent of the kinetic uncertainty relation, which can be understood by analyzing the expression for the classical current fluctuations in Eq. (3.4): this contribution to the fluctuations sums up all the transitions of particles between reservoirs, comparable to the dynamical activity of Markovian systems. However, to make this connection concrete, the dynamical activity in scattering theory should be properly derived from a microscopic picture. We denote the bound of Eq. (3.30) as the *Dynamical Fluctuation Bound*, or DFB for short. Note that for the particle current. i.e. $\nu = 0$, the DFB is equivalent to Eq. (3.22), since one can obtain it by squaring both sides of Eq. (3.22). Again, the bound of Eq. (3.30) extends to the full fluctuations for bosonic systems,

$$S^{(0)}_{\alpha\alpha} \geq S^{(0)}_{\alpha\alpha,\mathrm{cl}} \geq 4\frac{\left|I^{(\nu)}_\alpha\right|^2}{S^{(\nu)}_{\alpha\alpha,\mathrm{cl}}} \geq 4\frac{\left|I^{(\nu)}_\alpha\right|^2}{S^{(\nu)}_{\alpha\alpha}}. \tag{3.31}$$

If we pick a two-terminal system of bosonic reservoirs with nonthermal constant occupations $f_\alpha$ and $f_\gamma$, connected by an energy-independent scatterer in an energy window $B$ the DFB for the entropy current fluctuation becomes

$$S^{(0)}_{\alpha\alpha,\mathrm{cl}} = \frac{2}{h}D_{\alpha\gamma}B(K_{\alpha\gamma} + K_{\gamma\alpha}) \geq 4\frac{\left|\frac{1}{h}D_{\alpha\gamma}B[C^{(\Sigma)}]|f_\gamma - f_\alpha|\right|^2}{\frac{2}{h}D_{\alpha\gamma}B[C^{(\Sigma)}]^2(K_{\alpha\gamma} + K_{\gamma\alpha})}, \tag{3.32}$$

which, when simplified, reduces to

$$K_{\alpha\gamma} + K_{\gamma\alpha} \geq |f_\gamma - f_\alpha|. \tag{3.33}$$

This is the bound we plotted in Fig. (3.3). Interestingly, for this constant occupation case, the DFB for the local entropy production becomes symmetric with respect to exchanging the occupations of the reservoirs. Here we see that the bound is tight whenever the population difference between the reservoirs is large, in stark contrast to the FEB, which for this system is plotted in Fig. (3.1).

A difference from the earlier bounds of Eqs. (3.9, 3.22, 3.23) is that the DFB does not hold on the level of integrand, it concerns the full expressions. This means that if we want to plot its behaviour for thermal systems, we must calculate the currents and classical fluctuations. We do this for a system of two thermal reservoirs at the same temperature but different chemical potentials $\mu_\alpha = \bar{\mu} + \Delta\mu$, $\mu_\gamma = \bar{\mu} - \Delta\mu$ and a transmission probability defined through the Heaviside step function $\Theta(E)$,

$$D_{\alpha\gamma}(E; B_\alpha) = D[\Theta(E) - \Theta(E - B_\alpha)]. \tag{3.34}$$

We denote this type of energy dependence in the transmission probability as a *box transmission*, with a bandwidth of transport $B_\alpha$. The bandwidth of transport turns out to be an important parameter when treating the quantum noise. We will discuss the role of $B_\alpha$ in more detail later on, and define it in a general setting for any type of transmission probability. The DFB for entropy production can be seen in Fig. (3.5), plotted as a function of the chemical potential bias and the bandwidth of transport, where we defined the ratio

$$V^{(\nu)}_{\alpha,\mathrm{cl}} \equiv 4\frac{|I^{(\nu)}_\alpha|^2}{S^{(\nu)}_{\alpha\alpha,\mathrm{cl}}S^{(0)}_{\alpha\alpha,\mathrm{cl}}}. \tag{3.35}$$

In panel (b) we see that the bound looses symmetry with respect to flipping the sign of the chemical potential bias for larger bandwidths. We also see that for small $\Delta\mu$, close to equilibrium the bound is far from being saturated, which is expected since the average entropy current is small. The corresponding plot for the particle current version of the DFB is shown in Fig. (3.6). A difference

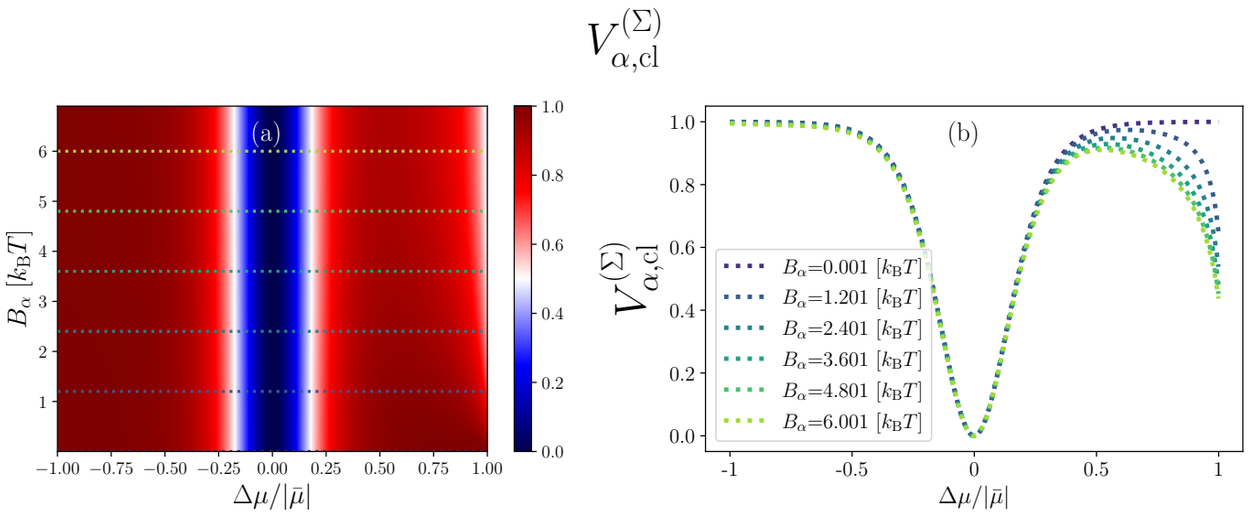


**Figure 3.5:** DFB for entropy production of Eq. (3.30), for a two-terminal system with thermal reservoirs at equal temperature, connected by a box transmission. Here, the bound is plotted as a function of the chemical potential bias and bandwidth. The bound is tighter for small values of $B_\alpha$ and asymmetric with respect to flipping the chemical potential bias. This is seen clearly in panel (b).

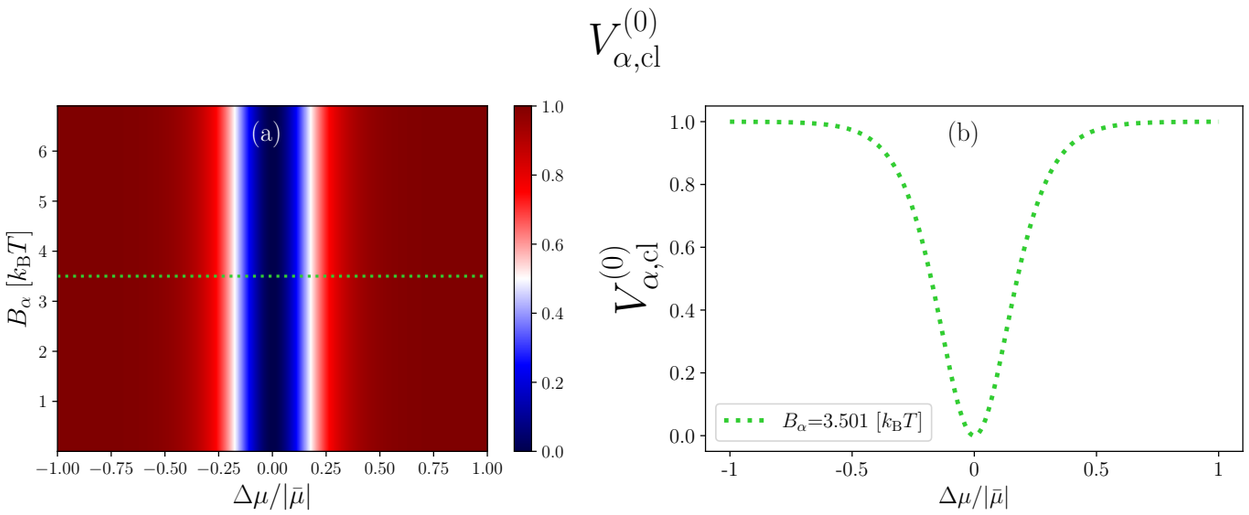


**Figure 3.6:** Figure displaying the DFB of Eq. (3.30) for the particle current in a two-terminal system with thermal reservoirs at equal temperature, connected by a box transmission. Here, the bound is plotted as a function of the chemical potential bias and bandwidth. This bound has a weak dependence on the bandwidth which can be seen in panel (a). This bound is again symmetric with respect to flipping the sign on the chemical potential bias which stems from particle current conservation.

to Fig. (3.5) is that this bound has a very weak dependence on the bandwidth. We also see that Fig. (3.6) remains symmetric with respect to flipping the sign of the chemical potential bias, which stems from particle-current conservation.

The DFB represents an improvement over the ones presented in the previous section, in the sense that Eq. (3.30) is a tighter bound on a current, set by the classical fluctuations. Furthermore, it includes the particle current in a clear way, reminiscent of a KUR. This new bound is also applicable to fermionic systems, and we show this in the next section.

### 3.1.4 Improved Fermionic bounds set by classical fluctuations

The derivation of the dynamical fluctuation bound for fermionic systems is analogous to the bosonic case of the previous section. We begin by defining the parameter $x$ as before and by using the bounds of Eq. (2.84) we find

$$\mathcal{S}^{(\nu)}_{\alpha\alpha,\mathrm{cl}} + \frac{x^2}{4}\mathcal{S}^{(0)}_{\alpha\alpha,\mathrm{cl}} \geq 2x\left|\mathcal{I}^{(\nu)}_\alpha\right|. \tag{3.36}$$

This again defines a positive quadratic form

$$\mathcal{S}^{(\nu)}_{\alpha\alpha,\mathrm{cl}} + \frac{x^2}{4}\mathcal{S}^{(0)}_{\alpha\alpha,\mathrm{cl}} - 2x\left|\mathcal{I}^{(\nu)}_\alpha\right| \geq 0. \tag{3.37}$$

We pick a value of $x$ by minimizing with respect to $x$ and find

$$\frac{x}{2}\mathcal{S}^{(0)}_{\alpha\alpha,\mathrm{cl}} - 2\left|\mathcal{I}^{(\nu)}_{\alpha}\right| = 0 \implies x = \frac{4\left|\mathcal{I}^{(\nu)}_{\alpha}\right|}{\mathcal{S}^{(0)}_{\alpha\alpha,\mathrm{cl}}}. \tag{3.38}$$

Inserting this value into Eq. (3.36), we arrive at the DFB for fermionic systems

$$\mathcal{S}^{(0)}_{\alpha\alpha,\mathrm{cl}} \geq 4\frac{\left|\mathcal{I}^{(\nu)}_{\alpha}\right|^2}{\mathcal{S}^{(\nu)}_{\alpha\alpha,\mathrm{cl}}}, \tag{3.39}$$

which we use to define the following ratio

$$\mathcal{V}^{(\nu)}_{\alpha,\mathrm{cl}} \equiv 4\frac{\left|\mathcal{I}^{(\nu)}_{\alpha}\right|^2}{\mathcal{S}^{(\nu)}_{\alpha\alpha,\mathrm{cl}}\mathcal{S}^{(0)}_{\alpha\alpha,\mathrm{cl}}}. \tag{3.40}$$

This bound again displays the same characteristics as the DFB for the bosonic systems and is a tighter bound than the one in Ref. [2]. A difference to the bosonic case is that we cannot extend Eq.(3.36) trivially, since for fermionic systems

$$\mathcal{S}^{(\nu)}_{\alpha\alpha,\mathrm{cl}} \geq \mathcal{S}^{(\nu)}_{\alpha\alpha,\mathrm{cl}} - \mathcal{S}^{(\nu)}_{\alpha\alpha,\mathrm{qu}} = \mathcal{S}^{(\nu)}_{\alpha\alpha}. \tag{3.41}$$

To be able to extend this bound to include the full fluctuations, we must first treat the quantum fluctuations separately. If we consider a system with constant average occupations and a box transmission, the bound of Eq. (3.39) for the particle current and entropy current reduces to

$$F_{\alpha\gamma} + F_{\gamma\alpha} \geq |f_\gamma - f_\alpha| \tag{3.42}$$

where $F_{\alpha\gamma} = f_\alpha(1 - f_\gamma)$ is the Pauli factor. This is simply the second bound of Eq. (2.84) and is plotted as function of the average occupation in Fig. (3.7). Here we defined the ratio

$$\mathcal{Y}_{\alpha\gamma} \equiv \frac{|f_\gamma - f_\alpha|}{F_{\alpha\gamma} + F_{\gamma\alpha}}. \tag{3.43}$$

By comparing panels (b, c), it is clear that the bound is symmetric with respect to exchanging the average occupations of the reservoirs, and the bound is far from being saturated when $f_\alpha \approx f_\gamma$, while being saturated when $f_\alpha \in \{0, 1\}$ [2].

As a next step we also plot the fermionic DFB for thermal reservoirs. To do this, we consider a two-terminal system with reservoirs at equal temperature but different chemical potentials $\mu_\alpha = \Delta\mu$, $\mu_\gamma = -\Delta\mu$ connected by a transmission probability

$$D_{\alpha\gamma}(E; B_\alpha) = \Theta(E - 2.5k_\mathrm{B}T) - \Theta(E - 2.5k_\mathrm{B}T + B_\alpha). \tag{3.44}$$

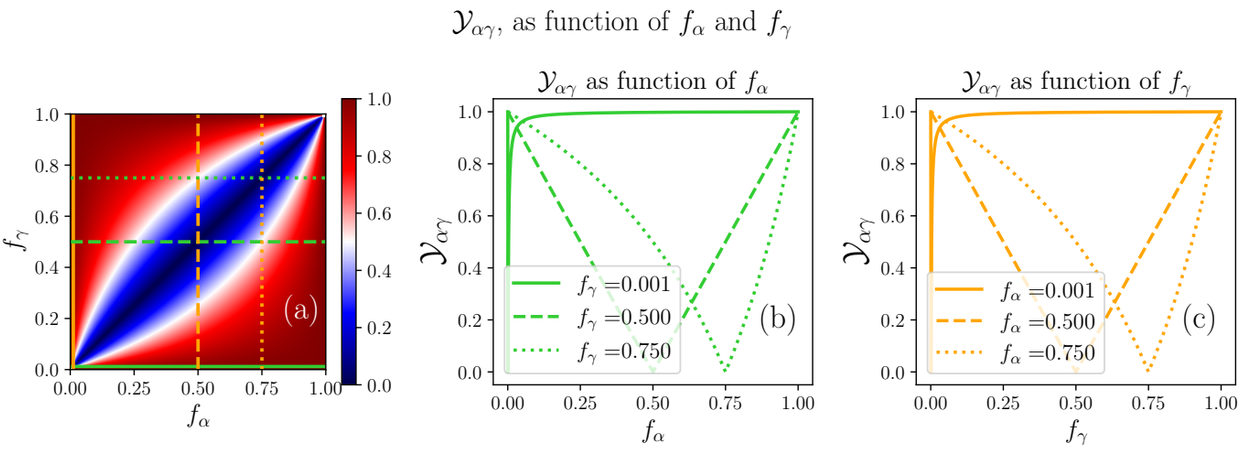


**Figure 3.7:** Figures displaying the bound of Eq. (3.39) for a two terminal system with constant average occupations and a box transmission. For this system, the bound corresponds to both the particle current and the entropy current version, as detailed by Eq (3.42). Here the bound is plotted as a function of the average occupations, and it is clear from comparing panels (b, c) that the bound is symmetric with respect to exchanging the average occupations. The bound is saturated when $f_\alpha \in \{0, 1\}$ [2].

It should be noted that the fermionic chemical potential can take any real value, so we allow for both positive and negative values, and the integration over energy goes from minus to plus infinity. The fermionic DFB of Eq. (3.39) is plotted in Fig. (3.8). This plot is quite different from the bosonic case shown in Fig. (3.5), showing a larger degree of asymmetry with respect to changing the sign of the chemical potential bias. A new feature of this bound is the blue region seen for negative chemical potential biases in panel (a). The bound losing saturation coincides with the condition

$$\mathcal{I}_\alpha^{(\Sigma)} = 0, \tag{3.45}$$

which for two bosonic reservoirs at equal temperature only occurs when there is no particle current flowing, i.e. $\Delta\mu = 0$. It is possible for the entropy production to cancel in the fermionic case when the contributions of particles entering the reservoir with energy below the average chemical potential cancel with the contributions of particles entering the reservoir with energy above. This is illustrated in Fig. (3.9), where the average occupations of the different reservoirs are displayed as functions of energy together with the transmission probability depicted as the shaded green region. The cancellation of the entropy production is possible when $\Delta\mu < 0$. The particle current version of the fermionic DFB is plotted in Fig. (3.10). This bound displays similar behaviour to the bosonic result shown in Eq. (3.6), notably being symmetric with respect to changing the sign of the chemical potential bias and having a weak dependence on the bandwidth. Here we also see that the bound is only far from being saturated when $\Delta\mu \approx 0$, as opposed to the bound for the entropy current.

We have now found multiple trade-off relations for bosonic systems involving the classical fluctua-

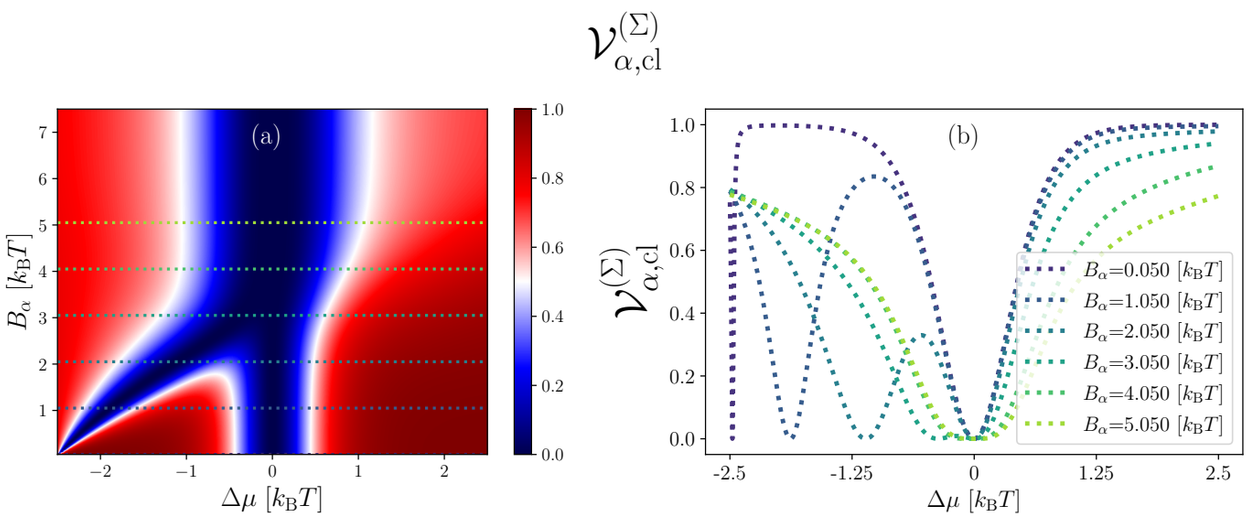


**Figure 3.8:** DFB for entropy production of Eq. (3.39), for a two-terminal system with thermal reservoirs at equal temperature, connected by a box transmission. Here, the bound is plotted as a function of the chemical potential bias and bandwidth. The bound is tighter for small values of $B_\alpha$ and asymmetric with respect to flipping the chemical potential bias.

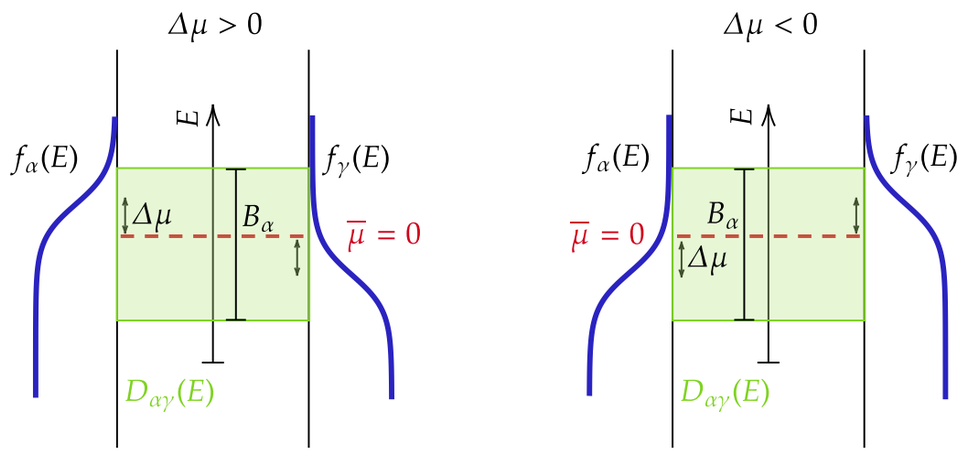


**Figure 3.9:** Figure displaying the average occupations given by the Fermi distribution of two thermal fermionic reservoirs. The shaded green region illustrates the transmission probability. When $\Delta\mu < 0$ it is possible for the particles flowing with energy above the average chemical potential to cancel the contribution of particles flowing with energy below. This is the cause of the blue region of the lower left corner in panel (a) of Fig. (3.8).

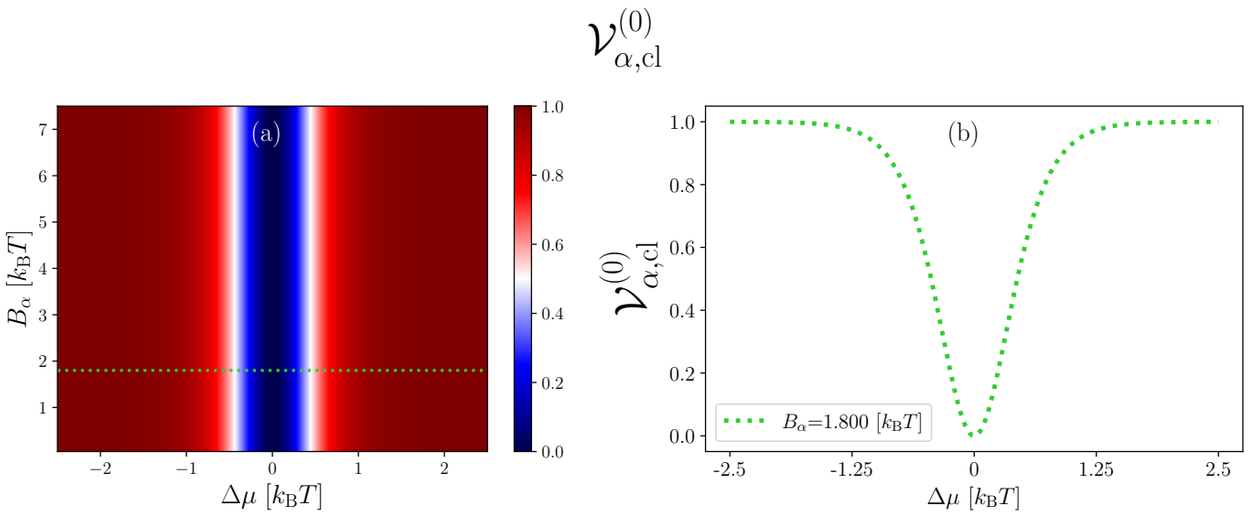


**Figure 3.10:** Figure displaying the DFB for the particle current of Eq. (3.39), for a two-terminal system with thermal reservoirs at equal temperature, connected by a box transmission. Here, the bound is plotted as a function of the chemical potential bias and bandwidth.

tions as well as the DFB, which applies to both bosonic and fermionic systems. We saw that we could trivially extend the bosonic bounds to include the quantum fluctuations, unlike the fermionic case. It is, however, desired to include more terms in the bound when doing this to ensure that it stays tight, and we must treat the quantum fluctuations separately if we want to extend the DFB to include the full fluctuations in the fermionic case. Therefore, in the coming sections, we will focus on finding relations between the quantum part of the fluctuations and currents.

### 3.1.5 Bosonic bounds set by quantum fluctuations

In the previous section, we saw that we were able to establish the previously set bound for fermions in the bosonic case. We also saw that we were able to extend this bound to include complete noise, unlike in the fermionic case, but it is desirable to improve the bound when including quantum noise to make it tighter. In this thesis, we show two ways of doing this for bosonic systems. First, we consider a situation when the population differences between reservoirs are large. After this, we find a more general trade-off relation for the bosonic quantum noise, which includes the effect of bunching.

#### 3.1.5.1 The strong current bound

We consider a situation where transport occurs in an energy window where the population in reservoir $\alpha$ is far from being equal to populations in the other reservoirs. We call this the *strong current regime*, and it could be achieved by having transport in a shorter, low energy window, with reservoir $\alpha$ having a different temperature, chemical potential, or otherwise different nonthermal distribution. This regime corresponds to a far-from-equilibrium situation for bosons outside of the tunneling regime. It is first noted that the factor

$$|s_{\alpha\gamma}(E)|^2|f_\alpha - f_\gamma|, \tag{3.46}$$

can be greater than one for bosonic reservoirs, unlike the fermionic case, where due to the Pauli exclusion principle, this factor is bounded by one. Then if $|s_{\alpha\gamma}(E)|^2|f_\alpha - f_\gamma| \geq 1$ it follows that

$$[|s_{\alpha\gamma}(E)|^2(f_\alpha - f_\gamma)]^2 \geq |s_{\alpha\gamma}(E)|^2|f_\alpha - f_\gamma|. \tag{3.47}$$

Turning our focus to the bound set for the entropy production and using Eq. (3.47) together with the first inequality of Eq. (3.7), we find

$$S^{(\Sigma)}_{\alpha\alpha,\mathrm{qu}} + \frac{k_\mathrm{B}^2}{4}S^{(0)}_{\alpha\alpha,\mathrm{qu}} \geq 2k_\mathrm{B}\left|I^{(\Sigma)}_\alpha\right| \tag{3.48}$$

if

$$\sum_{\gamma\neq\alpha}|s_{\alpha\gamma}(E)|^2|f_\alpha - f_\gamma| \geq 1, \quad \text{when} \quad \sum_{\gamma\neq\alpha}|s_{\alpha\gamma}(E)|^2|f_\alpha - f_\gamma| \neq 0. \tag{3.49}$$

The conditions of Eq. (3.49) we call the *strong current conditions*. One should note that the condition of Eq. (3.49) can be fulfilled for a fermionic system if it involves more than two reservoirs, since they are summed over. From this, it follows that in the strong current regime, the bosonic bound set by the full noise of Eq. (3.14) improves to

$$S^{(\Sigma)}_{\alpha\alpha} + \frac{k_\mathrm{B}^2}{4}S^{(0)}_{\alpha\alpha} \geq 4k_\mathrm{B}\left|I^{(\Sigma)}_\alpha\right|. \tag{3.50}$$

The same is true for the particle and energy currents, and in the strong current regime,

$$S^{(0)}_{\alpha\alpha} \geq 4|I^{(0)}_{\alpha}|, \tag{3.51}$$

$$S^{(E)}_{\alpha\alpha} + \frac{k_{\mathrm{B}}^2 T^2}{4} S^{(0)}_{\alpha\alpha} \geq 4k_{\mathrm{B}}T|I^{(E)}_{\alpha}|. \tag{3.52}$$

The strong current regime can also be implemented in the bosonic DFB. Beginning from

$$S^{(\Sigma)}_{\alpha\alpha,\mathrm{qu}} + \frac{x^2}{4} S^{(0)}_{\alpha\alpha,\mathrm{qu}} \geq 2x\left|I^{(\Sigma)}_{\alpha}\right|, \tag{3.53}$$

where $x$ is defined as before in section (3.1.3). By minimizing, we find,

$$S^{(0)}_{\alpha\alpha,\mathrm{qu}} \geq 4\frac{\left|I^{(\nu)}_{\alpha}\right|^2}{S^{(\nu)}_{\alpha\alpha,\mathrm{qu}}}. \tag{3.54}$$

Combining this with the classical DFB, we arrive at

$$S^{(0)}_{\alpha\alpha} \geq 8\frac{\left|I^{(\nu)}_{\alpha}\right|^2}{S^{(\nu)}_{\alpha\alpha}}, \tag{3.55}$$

in the strong current regime.

These bounds apply only in the strong coupling regime, but when the quantum fluctuations are large, they should be relevant, e.g., outside of the tunneling regime and far from equilibrium. It is, however, possible to find a trade-off relation for the quantum part of the fluctuations which is applicable in a more general situation. This is the focus of the next section.

#### 3.1.5.2 Bound from the Cauchy-Schwarz inequality

A more general way of treating the quantum part of the noise is by using the Cauchy-Schwarz Inequality (CSI) for integrals. The CSI states that for functions $y(x)$ and $c(x)$ that are square-integrable in an interval $x \in [a, b]$, the following inequality holds [17]:

$$\left(\int_a^b y(x)w(x)dx\right)^2 \leq \int_a^b (y(x))^2 dx \int_a^b (w(x))^2 dx. \tag{3.56}$$

We recall that for a c-weighted current, the integrand in the quantum part of the fluctuations is proportional to integrand in the c-weighted current itself. We can make this more clear by defining

$$g_{\alpha}(E) \equiv \sum_{\gamma\neq\alpha} |s_{\alpha\gamma}(E)|^2 |f_{\alpha} - f_{\gamma}|, \tag{3.57}$$

with which we can write

$$\left|I^{(\nu)}_{\alpha}\right| = \frac{1}{h}\int_0^{\infty} dE|C^{(\nu)}_{\alpha}(E)g_{\alpha}(E)|, \tag{3.58}$$

$$S^{(\nu)}_{\alpha\alpha,\mathrm{qu}} = \frac{2}{h}\int_0^{\infty} dE\left(C^{(\nu)}_{\alpha}(E)g_{\alpha}(E)\right)^2. \tag{3.59}$$

If we now consider the situation when the support of the integrand in Eq. (3.58) is finite: e.g. when transport occurs in some energy window with finite size, the CSI can be used to establish a bound between a c-weighted current and its quantum fluctuations. To use the CSI, we begin by defining a dimensionless filter function

$$\zeta_{\alpha}(E) = \begin{cases} 1 \text{ if } E \in \mathrm{supp}\left(C^{(\nu)}_{\alpha}(E)g_{\alpha}(E)\right), \\ 0 \text{ otherwise.} \end{cases} \tag{3.60}$$

This filter function has the following two properties: $\zeta_{\alpha}(E)^2 = \zeta_{\alpha}(E)$ and

$$\left|I^{(\Sigma)}_{\alpha}\right| = \frac{k_{\mathrm{B}}}{h}\int_0^{\infty} dE C^{(\Sigma)}_{\alpha}(E)g_{\alpha}(E)\zeta_{\alpha}(E). \tag{3.61}$$

Utilizing this, we apply the Cauchy-Schwarz inequality,

$$h^2\left|I^{(\nu)}_{\alpha}\right|^2 = \left(\int_0^{\infty} dE C^{(\nu)}_{\alpha}(E)g_{\alpha}(E)\zeta_{\alpha}(E)\right)^2 \leq \int_0^{\infty} dE\left(C^{(\nu)}_{\alpha}(E)g_{\alpha}(E)\right)^2 \int_0^{\infty} dE\left(\zeta_{\alpha}(E)\right)^2 = \\ = \frac{h}{2}S^{(\nu)}_{\alpha\alpha,\mathrm{qu}}\int_0^{\infty} dE\zeta_{\alpha}(E). \tag{3.62}$$

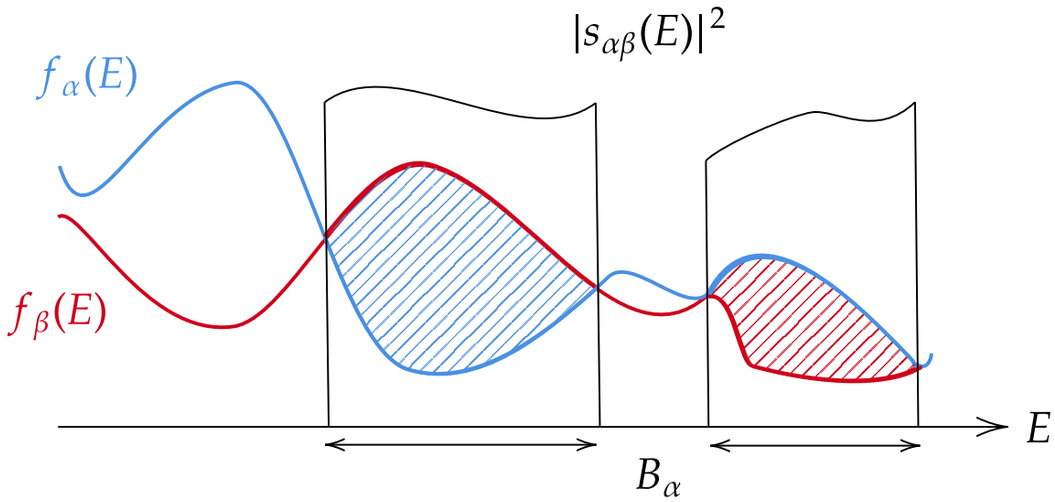


**Figure 3.11:** Diagrammatic representation of the bandwidth of transport. Here we see the average occupations of two reservoirs, $\alpha$ and $\gamma$, and the transmission probability between them. In this simple case, $B_\alpha$ would be the sum of the two energy intervals over witch the transmission probability is non-zero.

Here we define the *bandwidth of the transport* into and out of reservoir $\alpha$ as

$$B_\alpha = \int_0^\infty dE\zeta_\alpha(E). \tag{3.63}$$

We note that $B_\alpha$ has the unit of energy. The bandwidth quantifies how wide the energy interval is where transport is occurring, and it is illustrated in Fig. (3.11) for two reservoirs, $\alpha$ and $\beta$. Here, the bandwidth would be the sum of the two marked energy intervals. We use this to establish the following constraint between a c-weighted current and its quantum fluctuations:

$$S^{(\nu)}_{\alpha\alpha,\mathrm{qu}} \geq \frac{2h}{B_\alpha}\left|I^{(\nu)}_\alpha\right|^2. \tag{3.64}$$

This bound is another key result of this thesis, and it can naturally interpreted as how the effect of bunching in bosonic systems limits precision. To see this, we can reshuffle the terms in Eq. (3.64) to get

$$\frac{B_\alpha}{2h} \geq \frac{\left|I^{(\nu)}_\alpha\right|^2}{S^{(\nu)}_{\alpha\alpha,\mathrm{qu}}} \geq \frac{\left|I^{(\nu)}_\alpha\right|^2}{S^{(\nu)}_{\alpha\alpha}}. \tag{3.65}$$

Here we see that the precision in the coherent transport of bosons is fundamentally limited by the bandwidth of transport and we denote Eq.(3.65) as the *Quantum Precision Bound* or QPB for short. When the bandwidth is large, the bosons have the possibility of occupying different energy states and avoid bunching. In the extreme case when $B_\alpha \to \infty$, the quantum part of the fluctuations puts no limit on the achievable precision. On the other hand, when $B_\alpha$ is small, it isn't possible to achieve high precision. Physically, this can be interpreted as forcing the bosons to occupy the same energy state during transport and thus bunch together, which increases the fluctuations. Since the number of bosons occupying the same state is unbounded, one could, in principle, decrease the bandwidth while keeping the current constant. This would however force the quantum part of the fluctuations to become very large due to Eq. (3.64). To illustrate this, we consider a two-terminal system with nonthermal, constant average occupations in the transport window. Furthermore, we choose these occupations to depend on the bandwidth as $f_\alpha(B) = f_\alpha/B$ and a box transmission as in Eq. (3.34). For this system, the particle current becomes

$$I^{(0)}_\alpha(B) = \frac{1}{h}\int_0^\infty dED_{\alpha\gamma}\frac{f_\gamma - f_\alpha}{B} = \frac{1}{h}\int_0^B dED\frac{f_\gamma - f_\alpha}{B} = D[f_\gamma - f_\alpha] = \frac{1}{h}\int_0^{B'} dED\frac{f_\gamma - f_\alpha}{B'} = I^{(0)}_\alpha(B'). \tag{3.66}$$

Here we see that the current becomes independent for the choice of bandwidth, but the quantum part of the noise is strictly growing as the bandwidth decreases, as evident from Eq. (3.64). While this is a toy example of how bunching increases fluctuations, the bandwidth could still serve as a guiding parameter for an experimentalist designing some sort of device utilizing the transport of bosons.

It is again interesting to understand when these new bounds are saturated. This is the case when $C^{(\nu)}(E)g_\alpha(E)$ is constant, where one finds

$$S^{(\nu)}_{\alpha\alpha,\mathrm{qu}} = \frac{2}{h}B_\alpha[C^{(\nu)}g_\alpha]^2 = \frac{2h}{B_\alpha}\left|I^{(\nu)}_\alpha\right|^2. \tag{3.67}$$

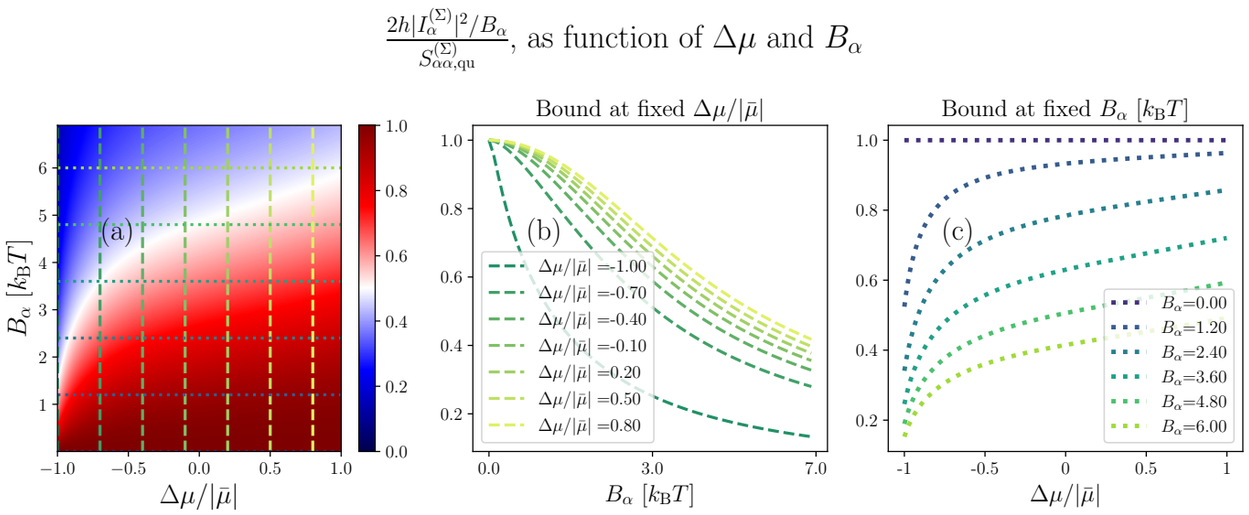


**Figure 3.12:** Figure displaying the QPB for entropy production of Eq. (3.65), for a two-terminal system with thermal reservoirs at equal temperature, connected by a box transmission. Here, the bound is plotted as a function of the chemical potential bias and bandwidth. The bound is tighter for small values of $B_\alpha$ and asymmetric with respect to flipping the chemical potential bias. This is seen clearly in panels (b, c), where one of the variables remains fixed while the other is varied.

For the entropy production and particle current, this can be fulfilled by picking a transmission probability like Eq. (3.34) and average occupations that are constant inside the transport window. For thermal systems, this approximately happens if one considers a constant transmission probability inside a small window at high temperatures, since the BE distributions could be approximated as constant. For the energy current, this would require more exotic transmission probabilities or average occupations, e.g., $f_\alpha(E) = \frac{k_\mathrm{B}T_\alpha}{E}$. To visualize the QPB of Eq. (3.64), we again pick a two-terminal system of thermal reservoirs with transmission probability of the same form as in Eq. (3.34). Here we are required to calculate the currents and fluctuations since the bounds concern the full expressions, not just the integrands. The QPB for the local entropy production is plotted in Fig. (3.12), where the potential bias is varied, $\mu_{\alpha/\gamma} = \bar{\mu} \pm \Delta\mu$ along with the bandwidth, which is displayed in units of $k_\mathrm{B}T$. Similarly to the classical FEB of Eq. (3.9), this bound is asymmetric, this time with respect to exchanging the chemical potentials. This is made clear in panels (a, b), where one of the variables remains fixed. It is also clear from this figure that the bound remains tighter for small values of the bandwidth. At larger bandwidths, the bound becomes less tight. This can be interpreted as the system not achieving the maximum possible precision that the QPB allows for with the given parameters. The corresponding plots for the particle current QPB are shown in Fig.(3.13). This bound displays similar characteristics to the entropy production version, with the difference that it is symmetric with respect to exchanging the chemical potentials. This is also reflected in the panel (c), where the bound is even around $\Delta\mu = 0$. This results from particle-current conservation. It is again a less tight bound for large bandwidths. With this understanding of the QBP, we are ready to combine these results with the trade-off relations from earlier chapters. We do this first for the bounds of section (3.1.3), which when combined with Eq. (3.64) gives us

$$S_{\alpha\alpha}^{(\Sigma)} + \frac{k_\mathrm{B}^2}{4} S_{\alpha\alpha}^{(0)} \geq 2k_\mathrm{B}\left|I_\alpha^{(\Sigma)}\right| + \frac{h}{B_\alpha}\left(2|I_\alpha^{(\Sigma)}|^2 + \frac{k_\mathrm{B}^2}{2}|I_\alpha^{(0)}|^2\right), \tag{3.68}$$

$$S_{\alpha\alpha}^{(0)} \geq 2|I_\alpha^{(0)}| + \frac{2h}{\mathcal{B}_\alpha}|I_\alpha^{(0)}|^2 = 2\left(1 + \frac{h}{B_\alpha}|I_\alpha^{(0)}|\right)|I_\alpha^{(0)}|, \tag{3.69}$$

$$S_{\alpha\alpha}^{(E)} + \frac{k_\mathrm{B}^2 T_\alpha^2}{4} S_{\alpha\alpha}^{(0)} \geq 2k_\mathrm{B}T_\alpha\left|I_\alpha^{(E)}\right| + \frac{h}{B_\alpha}\left(2|I_\alpha^{(E)}|^2 + \frac{k_\mathrm{B}^2 T_\alpha^2}{2}|I_\alpha^{(0)}|^2\right). \tag{3.70}$$

These bounds are key results of this thesis since they extend trade-off relations for the classical fluctuations to the full fluctuations while at the same time including more terms to make the bounds tighter. In this case, these additional terms include the effect bunching has on the fluctuations in the currents. We denote the bound of Eq. (3.68) as the full FEB. Importantly, in these bounds, the classical and quantum contributions scale differently with the transmission probabilities. Thus, in the tunneling regime, the classical part is the dominant contribution, while the quantum part is important when there is high transparency. To visualize this, we pick a two-terminal system with nonthermal, constant occupations $f_\alpha$ and $f_\gamma$ which do not depend on energy and a constant transmission probability. The saturation of the full FEB for this system is plotted for different transmission probabilities as a function of the average occupations in Fig. (3.14). All though this is a highly specific case, it still gives an intuitive understanding of how the full FEB behaves. One thing to note is that in the tunneling

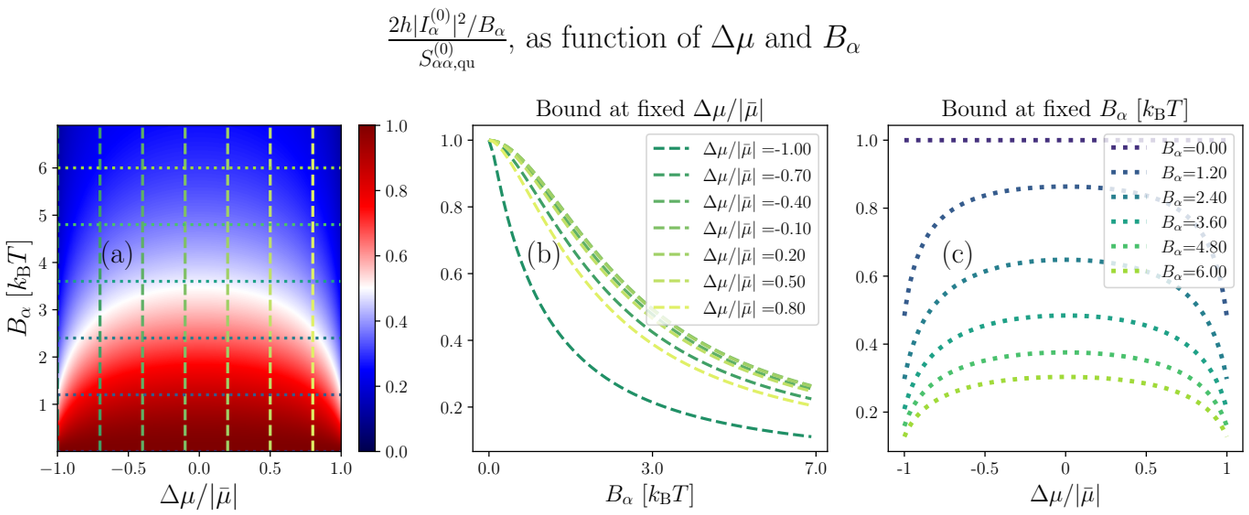


**Figure 3.13:** Figure displaying the QPB for particle current of Eq. (3.65), for a two-terminal system with thermal reservoirs at equal temperature, connected by a box transmission. Here, the bound is plotted as a function of the chemical potential bias and bandwidth. The bound is tighter for small values of $B_\alpha$ and symmetric with respect to flipping the chemical potential bias. This is seen clearly in panels (a, b), where one of the variables remains fixed while the other is varied.

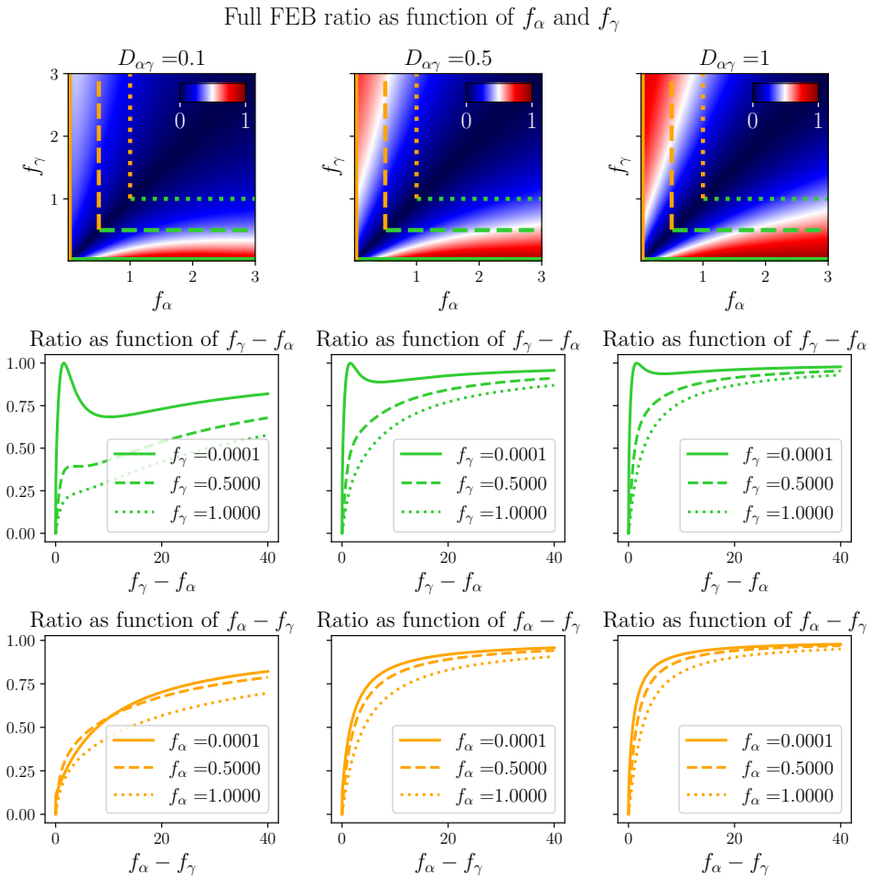


**Figure 3.14:** Figure displaying the full FEB of Eq. (3.68), for a two-terminal system with nonthermal reservoirs with energy-independent average occupations, connected by a box transmission. Here, the bound is plotted as a function of the average occupations for different transmission probabilities. We see that the plot becomes tighter and more symmetric when the transmission probability is high, as evident from the line plots included where one of the occupations is kept fixed while the other one is varied.

regime, the behaviour of the classical FEB is regained when $|f_\alpha - f_\gamma|$ is small, as expected from the scaling of the transmission probabilities. This is made clear by comparing this figure to Fig. (3.1). It should however be noted that with these specific nonthermal occupations, the full FEB always saturates as $|f_\alpha - f_\gamma| \to \infty$. We use the same system to visualize the current bound of Eq. (3.69) in Fig. (3.15). This bound is again symmetric with respect to the exchange of the particle current and otherwise displays the same general behavior as the full FEB.

While these bounds include full fluctuations, we also have derived another tighter bound concern-

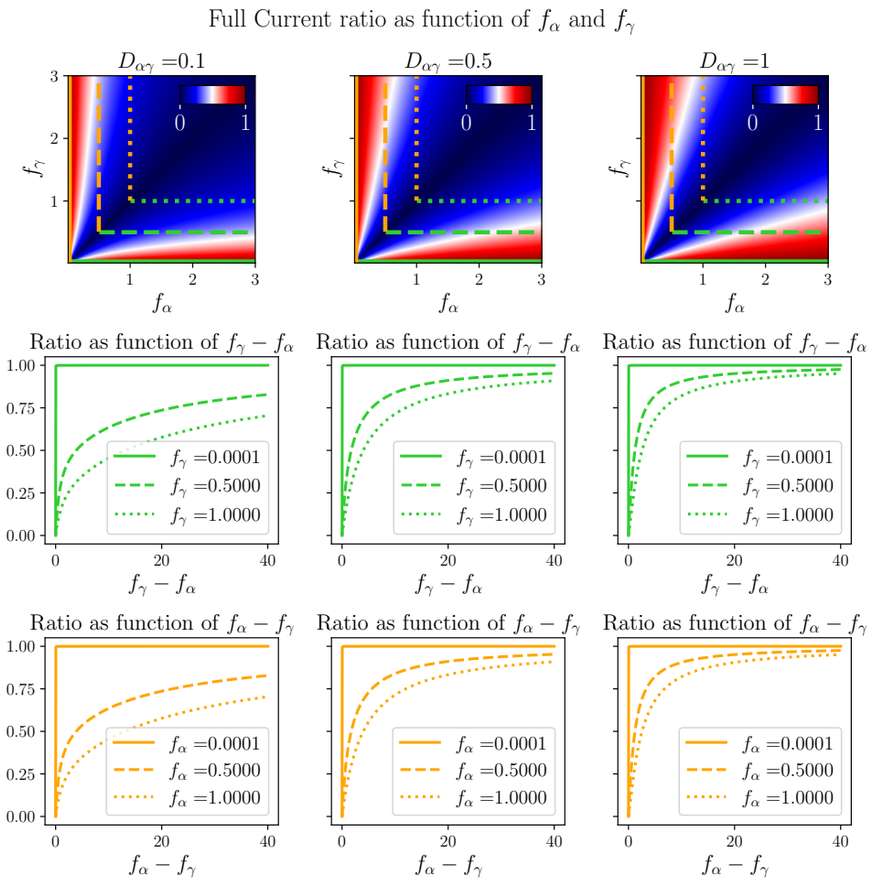


**Figure 3.15:** Figure displaying the current bound of Eq. (3.69), for a two-terminal system with non-thermal reservoirs with energy-independent average occupations, connected by a box transmission. Here, the bound is plotted as a function of the average occupations for different transmission probabilities. We see that the plot becomes tighter when the transmission probability is high, as evident from the line plots included where one of the occupations is kept fixed while the other one is varied.

ing the classical part of the fluctuations, the dynamical fluctuation bound. Combining the DFB of Eq. (3.30) with the QPB of Eq.(3.64) we find

$$\left(S^{(0)}_{\alpha\alpha} - \frac{2h}{B_\alpha}\left|I^{(0)}_\alpha\right|^2\right) \geq \frac{4\left|I^{(\nu)}_\alpha\right|^2}{\left(S^{(\nu)}_{\alpha\alpha} - \frac{2h}{B_\alpha}\left|I^{(\nu)}_\alpha\right|^2\right)}. \tag{3.71}$$

This bound is valid for an arbitrary c-weighted current that incorporates both classical and quantum fluctuations, and we denote it as the *Quantum Dynamical Fluctuation Bound* or QDFB for short. The structure of this relation can be made more clear by introducing the *bunching-compensated fluctuations*

$$\tilde{S}_{\alpha\alpha} = S^{(\nu)}_{\alpha\alpha} - \frac{2h}{B_\alpha}\left|I^{(\nu)}_\alpha\right|^2. \tag{3.72}$$

Using this, the QDFB can be compactly rewritten as

$$\tilde{S}^{(0)}_{\alpha\alpha} \geq \frac{4\left|I^{(\nu)}_\alpha\right|^2}{\tilde{S}^{(\nu)}_{\alpha\alpha}}. \tag{3.73}$$

The bunching-compensated fluctuations are not just a convenient way of writing down the QDFB; they also have a physical meaning. It can be interpreted as subtracting extra noise caused by bunching when extending the classical part of the fluctuations to the full fluctuations. If an experimentalist were to measure an average current and its fluctuations, calculating the bunching-compensated noise would be a way to estimate the classical fluctuations by finding a bound from above. With this, we interpret the right-hand side of Eq. (3.73) as a *bunching-compensated precision*. The QDFB is a central result of this thesis, and it tells us that the bunching-compensated particle current fluctuations limit the bunching-compensated precision in a c-weighted current. We also note that for systems where $C^\nu_\alpha(E)g_\alpha(E)$ is constant, the bunching-compensated fluctuations are exactly equal to the classical fluctuations: $\tilde{S}^{(\nu)}_{\alpha\alpha} = S^{(\nu)}_{\alpha\alpha,\mathrm{cl}}$ and the QDFB reduces to the classical DFB. To visualize the QDFB, we consider a two-terminal system of thermal reservoirs at equal temperature but different chemical potentials $\mu_\alpha = \bar{\mu} + \Delta\mu$, $\mu_\alpha = \bar{\mu} - \Delta\mu$ connected by a box transmission with high transperancy

$$D_{\alpha\gamma}(E; B_\alpha) = \Theta(E) - \Theta(E - B_\alpha). \tag{3.74}$$

The entropy current version of the QDFB as function of the chemical potential bias and bandwidth of transport is plotted in Fig. (3.16). Here we defined the ratio

$$\tilde{V}_\alpha^{(\nu)} \equiv 4\frac{|I_\alpha^{(\nu)}|^2}{\tilde{S}_{\alpha\alpha}^{(\nu)}\tilde{S}_{\alpha\alpha}^{(0)}}. \tag{3.75}$$

From panel (b), it is clear that the the bound is less tight for larger bandwidths, which we interpret as not reaching the maximum achievable precision for this particular system. It is also clear from panel (a) that there are three regions where the bound is not saturated when $\Delta\mu \approx 0$ and when $\Delta\mu \approx \pm 1$. The first region we recognize from the classical DFB plotted in Fig. (3.5), and stems from the fact that the average entropy current is small when the reservoirs are close to being at equilibrium. The two other regions are not present in the classical plot of Fig.(3.5). To interpret this, we notice that when $|\Delta\mu| = 1$, one of the reservoirs has a chemical potential with value of zero, which in turn means that the average occupation of that reservoir, given by the BE distribution, diverges, causing the quantum part of the fluctuations to blow up. In this situation, the average occupations varies strongly inside the region of integration, and the QPB of Eq. (3.58) is not tight. The particle current version of the QDFB for this system is plotted in Fig, (3.17) and displays similar features, with the difference that it is symmetric with respect to changing the sign of the chemical potential bias for all values of the bandwidth.

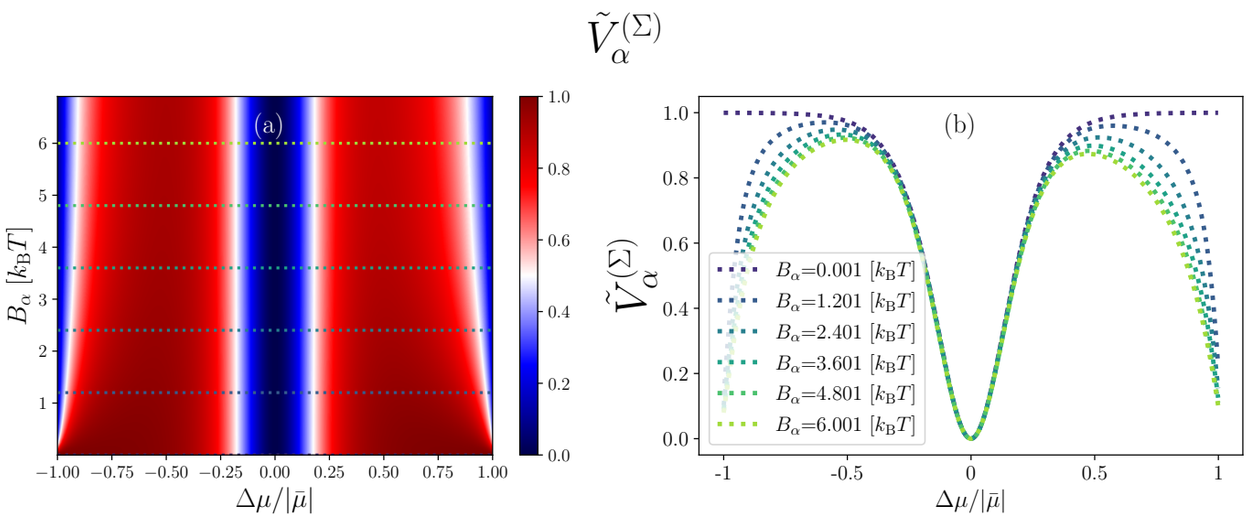


**Figure 3.16:** Figure displaying the DFB for entropy production of Eq. (3.30), for a two-terminal system with thermal reservoirs at equal temperature, connected by a box transmission. Here, the bound is plotted as a function of the chemical potential bias and bandwidth. The bound is tighter for small values of $B_\alpha$ and asymmetric with respect to changing the sign of the chemical potential bias. This is seen clearly in panel (b).

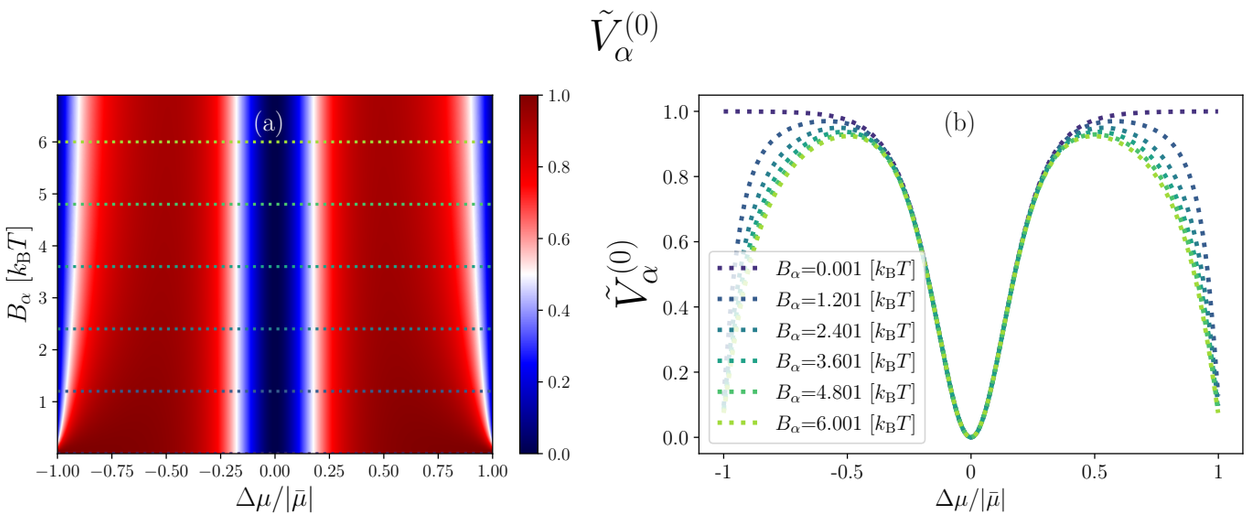


**Figure 3.17:** Figure displaying the DFB for the particle current of Eq. (3.30), for a two-terminal system with thermal reservoirs at equal temperature, connected by a box transmission. Here, the bound is plotted as a function of the chemical potential bias and bandwidth. The bound is tighter for small values of $B_\alpha$ and symmetric with respect to changing the sign of the chemical potential bias. This is seen clearly in panel (b).

In this section, we have seen how the quantum fluctuations include the effect of bunching in the bosonic case, which we have been able to reason from the structure of the QPB. This has allowed us to improve our previously derived trade-off when extending them to include the the quantum part of the fluctuations. We have, however, not been able to extend the DFB to include the full noise in the fermionic case, and doing this is the focus of the next section.

### 3.1.6 Fermionic bounds set by quantum fluctuations

In the previous section, we saw how we were able to improve the trade-off relations for bosonic systems by including the quantum part of the noise. In the fermionic case, this extension to full fluctuations is not as simple. Nonetheless, we will show two ways to extend the fermionic dynamical fluctuation bound of Eq.(3.39) to include the full fluctuations. The first way utilizes Eq. (2.86) together with the first inequality of Eq. (2.84), which allows us to write

$$\mathcal{S}^{(\nu)}_{\alpha\alpha} + \frac{x^2}{4}\mathcal{S}^{(0)}_{\alpha\alpha} \geq x 2k_{\mathrm{B}}\left|\mathcal{I}^{(\nu)}_{\alpha}\right| \inf_{E\in A} |s_{\alpha\alpha}(E)|^2, \tag{3.76}$$

where $x$ is defined as in Section 3.1.3. Using the same minimization scheme as earlier, we find the following bound:

$$\mathcal{S}^{(0)}_{\alpha\alpha} \geq \left[\inf_{E\in A} |s_{\alpha\alpha}(E)|^2\right]^2 4\frac{\left|\mathcal{I}^{(\nu)}_{\alpha}\right|^2}{\mathcal{S}^{(\nu)}_{\alpha\alpha}}. \tag{3.77}$$

Here we have extended the fermionic DFB to include the full fluctuations by utilizing results from Ref. [2]. When deriving the bosonic QDFB, we were able to gain insight into the role that bunching played in the noise of a current, and we are hoping to learn something similar from treating the fermionic case. We cannot use the Cauchy-Schwarz inequality in the fermionic case since the fermionic quantum noise is negative when included in the full fluctuations. We can, however, use a similar integral inequality, namely Pólya and Szegö's inequality (PSI). For two functions $y$ and $w$, which are bounded from below and above:

$$0 \leq m_y \leq y \leq M_y \leq \infty, \tag{3.78}$$

$$0 \leq m_w \leq w \leq M_w \leq \infty, \tag{3.79}$$

Pólya and Szegö's inequality states that [17, 30]

$$\phi\left(\int_A y\, w\, d\mu\right)^2 \geq \int_A (y)^2 d\mu \int_A (w)^2 d\mu. \tag{3.80}$$

where

$$\phi = \frac{1}{4}\left(\sqrt{\frac{M}{m}} + \sqrt{\frac{m}{M}}\right)^2, \tag{3.81}$$

or alternatively

$$\phi = \frac{1}{4}\frac{(m+M)^2}{mM}, \tag{3.82}$$

and

$$m = m_y m_w, \quad M = M_y M_w. \tag{3.83}$$

Here, the integration is done using Lebesgue integrals. The parameter $\phi$ can be thought of as encoding how strongly the integrands vary in the region of integration $A$. If $w$ and $y$ are constant functions, $\phi = 1$, and the PSI is trivially saturated. This parameter can, however, become large if the integrands vary strongly. To apply this inequality, we use the same definition of $g_\alpha(E)$ as in the bosonic case from Eq. (3.57) to write the fermionic currents and quantum fluctuations as

$$\mathcal{I}^{(\nu)}_{\alpha} = \frac{1}{h}\int_A dE C^{(\nu)}_{\alpha}(E) g_\alpha(E), \tag{3.84}$$

$$\mathcal{S}^{(\nu)}_{\alpha\alpha,\mathrm{qu}} = \frac{2}{h}\int_A dE \left(C^{(\nu)}_{\alpha}(E) g_\alpha(E)\right)^2. \tag{3.85}$$

Furthermore we restrict ourselves to treat the case when the integrand of Eq. (3.84) does not switch sign inside the region of integration, i.e. when

$$\left|\mathcal{I}^{(\nu)}_{\alpha}\right| = \frac{1}{h}\int_A dE |C^{(\nu)}_{\alpha}(E) g_\alpha(E)|. \tag{3.86}$$

We again use the same definition of the filter function $\zeta_\alpha(E)$ as from Eq. (3.60) and apply the PSI to find

$$\begin{aligned}\frac{h}{2}\mathcal{S}^{(\nu)}_{\alpha\alpha,\mathrm{qu}} B_\alpha &= \left(\int_A \left(C^{(\nu)}_{\alpha}(E) g_\alpha(E)\right)^2 dE\right)\left(\int_A \left(\zeta_\alpha(E)\right)^2 dE\right) \leq \\ &\leq \left(\int_A \left(C^{(\nu)}_{\alpha}(E) g_\alpha(E)\zeta_\alpha(E)\right) dE\right)^2 \phi = h^2\left|\mathcal{I}^{(\nu)}_{\alpha}\right|^2\phi.\end{aligned} \tag{3.87}$$

This implies that

$$\frac{2h\phi}{B_\alpha}\left|\mathcal{I}_\alpha^{(\nu)}\right|^2 \geq \mathcal{S}_{\alpha\alpha,\mathrm{qu}}^{(\nu)}, \tag{3.88}$$

where the bandwidth of transport $B_\alpha$ is defined in the same way as for the bosonic case in Eq. (3.63). Since we consider these integrals as Lebesgue integrals, we exclude any points where $\zeta_\alpha(E) = 0$, and the filter function is thus constant inside the region of integration. This means that

$$M = \sup_{E\in A}\left(|C_\alpha^{(\nu)}(E)g_\alpha(E)|\right), \tag{3.89}$$

$$m = \inf_{E\in A}\left(|C_\alpha^{(\nu)}(E)g_\alpha(E)|\right). \tag{3.90}$$

This new bound between a c-weighted current and its quantum fluctuations has similarities to the earlier bosonic bound derived using the CSI since it contains the bandwidth. One should, however, note that this inequality is "reversed" compared to the the bosonic QPB. Anyhow, this result allows us to extend the fermionic DFB to include the full fluctuations. We combine the result of Eq. (3.39) with the bound of Eq. (3.88) to obtain

$$\left(\mathcal{S}_{\alpha\alpha}^{(0)} + \frac{2h\phi}{B_\alpha}\left|\mathcal{I}_\alpha^{(0)}\right|^2\right) \geq \frac{4\left|\mathcal{I}_\alpha^{(\nu)}\right|^2}{\left(\mathcal{S}_{\alpha\alpha}^{(\nu)} + \frac{2h\phi}{B_\alpha}\left|\mathcal{I}_\alpha^{(\nu)}\right|^2\right)}, \tag{3.91}$$

which we denote as the fermionic quantum dynamical fluctuation bound. Unlike the bosonic case, where we had the freedom to include the QBP when extending the DFB to the full noise, we have no choice but to use the additional terms in the fermionic case. In the bosonic case, the bound was made tighter by the inclusion of the QPB, whereas here the bound becomes weaker. Specifically, the bound of Eq. (3.91) is made worse when the factor $\frac{\phi}{B_\alpha}$ is large, i.e., when the bandwidth is small or we are dealing with, for example, a peaked transmission probability causing a large $\phi$. This factor can be thought of as including the effect of anti-bunching on the precision of the coherent transport of fermionic particles. When $\frac{\phi}{B_\alpha}$ is large, more anti-bunching is occurring, which decreases fluctuations and allows for higher precision. The bound of Eq. (3.91) is not as widely applicable as its bosonic counter part, mainly due to the factor $\phi$ having the potential to become arbitrarily large. It should, however, be able to constrain precision in fermionic systems where one is using a roughly constant transmission probability in some energy window and zero-temperature reservoirs where the Fermi distribution becomes a step function. It could also be applicable in the high temperature limit, where the average occupations could be approximated as roughly constant in some energy window. With this intuition for these new fermionic results, we introduce the *anti-bunching compensated fluctuations* as

$$\tilde{\mathcal{S}}_{\alpha\alpha}^{(\nu)} = \left(\mathcal{S}_{\alpha\alpha}^{(\nu)} + \frac{2h\phi}{B_\alpha}\left|\mathcal{I}_\alpha^{(\nu)}\right|^2\right), \tag{3.92}$$

which allows us to write the fermionic QDFB as

$$\tilde{\mathcal{S}}_{\alpha\alpha}^{(0)} \geq \frac{4\left|\mathcal{I}_\alpha^{(\nu)}\right|^2}{\tilde{\mathcal{S}}_{\alpha\alpha}^{(\nu)}}. \tag{3.93}$$

This can be interpreted as the anti-bunching compensated fluctuations in the particle current putting a limit on the *anti-bunching compensated precision* of the right hand side, achievable for a fermionic c-weighted current. The fermionic QDFB is a key result of this thesis, as it is a bound on the precision of a c-weighted current in fermionic coherent transport. It can be interpreted as including the effect of anti-bunching, which allows for higher precision in fermionic systems for certain physical realizations. Interestingly, this bound is improved when the bandwidth $B_\alpha$ is large, unlike the bosonic case, where a large bandwidth caused the quantum fluctuations to not put a tight constraint on the achievable precision, as detailed in Eq.(3.64). This goes hand in hand in our interpretation of bunching and anti-bunching. For large bandwidths, bunching does not constrain precision in the bosonic case, while small bandwidths cause anti-bunching in fermionic devices, allowing for higher precision. A very important point is that any expression involving $\tilde{\mathcal{S}}_{\alpha\alpha}^{(\nu)}$ only holds when the integrand of $\mathcal{I}_\alpha^{(\nu)}$ does not change sign inside the region of integration, i.e. Eq. (3.86) holds true.

This concludes the first part of the results. We have found multiple trade-off relations, and our key results are the dynamical fluctuation bounds, the quantum precision bound and the extension of the DFBs to the QDFBs. By this analysis, we have gained insight into the role that the fundamental nature of bosons and fermions play in the precision of coherent transport. In the bosonic case, bunching allowed us to find a tighter bound on precision in Eq. (3.73), while we saw that anti-bunching caused our bounds to become less strict in the fermionic case of Eq. (3.93). In the next part of this chapter, we will focus on entropy production and derive a thermodynamic uncertainty relation for bosonic multi-terminal devices. We will also extend this bound to include the quantum fluctuations in both the bosonic and fermionic cases.

## 3.2 Thermodynamic uncertainty relations for coherent transport of particles.

In the previous part of the chapter, we were able to establish multiple bounds on currents set by fluctuations. By including the quantum part of the fluctuations, we have managed to improve the bosonic bounds and gain more insight into the role of bunching in the coherent transport of bosons. We also found new results applying to fermionic systems where the quantum part of the fluctuations could be interpreted as containing the effect of anti-bunching on precision. These bounds are applicable to systems where the reservoirs are possibly nonthermal. In this section, we take a different approach to finding relations between the currents and fluctuations, focusing on thermal reservoirs. Here we derive a thermodynamic uncertainty relation for strongly coupled bosonic systems, described by scattering theory. A TUR for fermionic systems described by scattering theory was derived by K. Brandner et. al. in Ref. [8], concerning the classical part of the particle current fluctuations of fermions. In Ref. [8], K. Brandner et. al. derived TURs for fermionic systems subject to chemical potential biases by constructing quadratic forms. In this thesis, we follow the same procedure, extending it to bosonic systems with time reversal symmetry, subject to both chemical potential biases and temperature biases. Furthermore, we are able to extend the bosonic TUR to the full fluctuations, unlike the fermionic case [8]. We are also able to extend the fermionic result of Ref. [8] to apply to reservoirs subject to both chemical potential biases and temperature biases, as well as including the quantum part of the fluctuations, using relations previously derived in this thesis.

We begin this part of the results by deriving a thermodynamic relation for the classical part of the bosonic fluctuations.

### 3.2.1 Thermodynamic uncertainty relations for bosonic systems, with time reversal symmetry

We start out by deriving a TUR for bosonic multiterminal devices where there is time reversal symmetry. To do this, we follow the same method as in Ref. [8]. After this, we will extend this TUR to include the quantum part of the fluctuations.

#### 3.2.1.1 Bosonic thermodynamic uncertainty relation for classical fluctuations

In this section, we focus on systems where the reservoirs are thermal, i.e., those described by the BE distribution of Eq. (2.24). This is an important point since the explicit form of the average occupation will be used multiple times in the following calculations. Since we are working with thermal reservoirs, the local entropy productions are simply given by Clausius' relation, and the total entropy production is calculated by summing the heat flows of Eq. (2.52) of each reservoir,

$$\sigma = \sum_{\alpha} \frac{J_\alpha}{T_\alpha} = \sum_{\alpha,\beta} \frac{k_\mathrm{B}}{h} \int_0^\infty dE D_{\alpha\beta}(E) \frac{E-\mu_\alpha}{k_\mathrm{B}T_\alpha}(f_\beta - f_\alpha). \tag{3.94}$$

For systems with time reversal symmetry, e.g a lack of magnetic fields, the transmission probabilities are symmetric: $D_{\alpha\beta}(E) = D_{\beta\alpha}(E)$. Using this and defining

$$\mathcal{F}_\alpha = \frac{\mu_\alpha - E}{k_\mathrm{B}T_\alpha}, \tag{3.95}$$

the entropy production can be rewritten as

$$\begin{aligned}
\sigma &= \frac{k_\mathrm{B}}{2h} \sum_{\alpha,\beta} \int_0^\infty dE D_{\alpha\beta}(E) \left(\mathcal{F}_\alpha - \mathcal{F}_\beta\right)\left(f_\alpha - f_\beta\right) \\
&= \frac{k_\mathrm{B}}{2h} \sum_{\beta,\gamma\neq\alpha} \left\{ \int_0^\infty dE D_{\beta\gamma}(E) \left(\mathcal{F}_\beta - \mathcal{F}_\gamma\right)\left(f_\beta - f_\gamma\right) \right\} \\
&\quad + \frac{k_\mathrm{B}}{h} \sum_{\beta\neq\alpha} \left\{ \int_0^\infty dE D_{\alpha\beta}(E) \left(\mathcal{F}_\alpha - \mathcal{F}_\beta\right)\left(f_\alpha - f_\beta\right) \right\}.
\end{aligned} \tag{3.96}$$

Now defining

$$\Lambda_{\alpha\beta} = \mathcal{F}_\alpha - \mathcal{F}_\beta, \tag{3.97}$$

we have the following identity for the BE distribution

$$(f_\alpha - f_\beta) = (1+f_\alpha) f_\beta (e^{\Lambda_{\alpha\beta}} - 1). \tag{3.98}$$

Using this together with the factor

$$\mathcal{W}_{\alpha\beta} = \frac{1}{h} D_{\alpha\beta}(E)(1 + f_\alpha) f_\beta \geq 0, \tag{3.99}$$

the total entropy production can be rewritten as

$$\sigma = \frac{k_\mathrm{B}}{2} \sum_{\beta,\gamma\neq\alpha} \int_0^\infty dE \left\{ \mathcal{W}_{\beta\gamma} \Lambda_{\beta\gamma} (e^{\Lambda_{\beta\gamma}} - 1) \right\} + k_\mathrm{B} \sum_{\beta\neq\alpha} \int_0^\infty dE \left\{ \mathcal{W}_{\alpha\beta} \Lambda_{\alpha\beta} (e^{\Lambda_{\alpha\beta}} - 1) \right\}. \tag{3.100}$$

In this form, it is clear that each term inside the two sums is strictly positive since the function $x(e^x - 1) \geq 0$. Following the same procedure as in Ref. [8], we define a quadratic form containing the entropy production, the particle current and its classical fluctuations,

$$A_\alpha^\mathrm{cl} = \frac{\sigma}{k_\mathrm{B}} - 2\psi x I_\alpha^{(0)} + \psi x^2 S_{\alpha\alpha,\mathrm{cl}}^{(0)}. \tag{3.101}$$

Here, $x$ and $\psi$ are real numbers parameterizing the quadratic form. We note that if we are able to find a value for $\psi$ such that the quadratic form is semipositive definite, $A_\alpha^\mathrm{cl} \geq 0$, we automatically obtain a TUR by minimizing $A_\alpha^\mathrm{cl}$ with respect to $x$:

$$\sigma \frac{S_{\alpha\alpha,\mathrm{cl}}^{(0)}}{\left| I_\alpha^{(0)} \right|^2} \geq \psi k_\mathrm{B}. \tag{3.102}$$

What remains now is to find a value of $\psi > 0$ such that the quadratic form is semipositive definite, and the larger the value of $\psi$, the stricter the resulting inequality will be. Using Eq. (3.98) and Eq. (3.99), the particle current can be rewritten as

$$I_\alpha^{(0)} = -\sum_{\beta\neq\alpha} \int_0^\infty dE \mathcal{W}_{\alpha\beta} (e^{\Lambda_{\alpha\beta}} - 1). \tag{3.103}$$

Similarly, using the following identity for the BE distribution

$$(f_\alpha + 1) f_\beta + (1 + f_\beta) f_\alpha = (1 + f_\alpha) f_\beta (e^{\Lambda_{\alpha\beta}} + 1), \tag{3.104}$$

the particle current fluctuations can be rewritten as

$$S_{\alpha\alpha,\mathrm{cl}}^{(0)} = \sum_{\beta\neq\alpha} \int_0^\infty dE \mathcal{W}_{\alpha\beta} (e^{\Lambda_{\alpha\beta}} + 1). \tag{3.105}$$

Altogether, this allows for the quadratic form to be expressed as

$$\begin{aligned} A_\alpha^\mathrm{cl} = \frac{1}{2} \sum_{\beta,\gamma\neq\alpha} \int_0^\infty dE \left\{ \mathcal{W}_{\beta\gamma} \Lambda_{\beta\gamma} (e^{\Lambda_{\beta\gamma}} - 1) \right\} + \\ \sum_{\beta\neq\alpha} \int_0^\infty dE \mathcal{W}_{\alpha\beta} \left\{ \Lambda_{\alpha\beta} (e^{\Lambda_{\alpha\beta}} - 1) + 2\psi x (e^{\Lambda_{\alpha\beta}} - 1) + \psi x^2 (e^{\Lambda_{\alpha\beta}} + 1) \right\}. \end{aligned} \tag{3.106}$$

As noted earlier, the first sum is strictly positive, and what remains to be found is a value for the parameter $\psi$ such that the second sum is strictly positive. The expressions in the second sum are on the same form as in Ref. [8], and it is possible to follow the same procedure used there. We begin by minimizing $A_\alpha^\mathrm{cl}$ with respect to $x$, which gives us

$$\begin{aligned} A_\alpha^\mathrm{cl} \geq & \frac{1}{2} \sum_{\beta,\gamma\neq\alpha} \left\{ \mathcal{W}_{\beta\gamma} \Lambda_{\beta\gamma} (e^{\Lambda_{\beta\gamma}} - 1) \right\} \\ & + \sum_{\beta\neq\alpha} \mathcal{W}_{\alpha\beta} \left\{ \Lambda_{\alpha\beta} (e^{\Lambda_{\alpha\beta}} - 1) - \psi \frac{(e^{\Lambda_{\alpha\beta}} - 1)^2}{(e^{\Lambda_{\alpha\beta}} + 1)} \right\}. \end{aligned} \tag{3.107}$$

Using the following inequality from Ref. [8]:

$$y(e^y - 1) \geq 2 \frac{(e^y - 1)^2}{(e^y + 1)}, \tag{3.108}$$

we find that for any $0 \leq \psi \leq 2$, the second sum in Eq. (3.107) is positive. Picking $\psi = 2$ to get the strictest inequality, we minimize the Eq. (3.101) with respect $x$ to obtain

$$\frac{\sigma S_{\alpha\alpha,\mathrm{cl}}^{(0)}}{\left| I_\alpha^{(0)} \right|^2} \geq 2k_\mathrm{B} \implies \sigma \geq 2k_\mathrm{B} \frac{\left| I_\alpha^{(0)} \right|^2}{S_{\alpha\alpha,\mathrm{cl}}^{(0)}}. \tag{3.109}$$

This is a TUR for strongly coupled bosonic systems with time-reversal symmetry, subject to both chemical potential and temperature biases. It is an analogous result to the one found by K. Brandner et. al. in Ref. [8]. The relation of Eq. (3.103) can be interpreted as quantifying a minimum thermodynamic cost of precision. For a certain precision in the particle current, a minimum entropy production is required. It can also be trivially extended to include the full noise since the bosonic quantum noise is positive:

$$\frac{\sigma S^{(0)}_{\alpha\alpha}}{\left|I^{(0)}_{\alpha}\right|^2} \geq \frac{\sigma S^{(0)}_{\alpha\alpha,\mathrm{cl}}}{\left|I^{(0)}_{\alpha}\right|^2} \geq 2k_{\mathrm{B}}. \tag{3.110}$$

An attempt at deriving a bosonic TUR for systems without time-reversal symmetry following the method used in Ref. [8] was made. This proved fruitless since it was not possible to find a value for $\psi > 0$ for which the quadratic form was semidefinite positive. This attempt is outlined in Appendix [C.1]. That this attempt failed is not a proof that it is impossible to derive the TUR. We where however able to find a counterexample allowing us to break the TUR to an arbitrary degree exploiting the broken time-reversal symmetry. We show this example now.

To find a counterexample, we need to perform calculations for a specific system, i.e. a specific scattering matrix. We only need to show that there exists a valid scattering matrix for which the TUR can be arbitrarily broken, but we do not need to have a specific physical realisation in mind. To do this, we make the following ansatz for a scattering matrix inspired by a classical Nernst engine [27, 8]:

$$s_{\alpha\beta}(E) = m(E)\delta_{\alpha\beta-1} + n(E)\delta_{\alpha\beta}, \tag{3.111}$$

where $m(E)$, $n(E)$ are complex numbers and $\alpha, \beta = 1, .., N$ are periodic indices [8]. We begin by enforcing unitarity

$$\sum_{\beta} s_{\alpha\beta}s^*_{\gamma\beta} = \tag{3.112}$$

$$= \sum_{\beta} |m(E)|^2\delta_{\alpha\beta-1}\delta_{\gamma\beta-1} + |n(E)|^2\delta_{\alpha\beta}\delta_{\gamma\beta} + m^*(E)n(E)\delta_{\alpha\beta}\delta_{\gamma\beta-1} + m(E)(n^*(E))\delta_{\alpha\beta-1}\delta_{\gamma\beta} \tag{3.113}$$

$$= |m(E)|^2\delta_{\alpha\gamma} + |n(E)|^2\delta_{\alpha\gamma} + m^*(E)n(E)\delta_{\alpha-1\gamma} + m(E)(n^*(E))\delta_{\alpha\gamma-1} = \delta_{\alpha\gamma}, \tag{3.114}$$

where the last inequality must hold true. This in turn means that either $m(E) = 0$ or $n(E) = 0$; we pick the latter and find

$$s_{\alpha\beta}(E) = m(E)\delta_{\alpha\beta-1} = e^{i\theta}\delta_{\alpha\beta-1}, \tag{3.115}$$

where $m(E)$ is a complex phase. We modify this scattering matrix by using an energy filter

$$W(E, \epsilon, B) = \Theta(E + \epsilon) - \Theta(E + \epsilon + B), \tag{3.116}$$

and write

$$s_{\alpha\beta}(E) = W(E, \epsilon, B)\delta_{\alpha\beta-1} + (1 - W(E, \epsilon, B))\delta_{\alpha\beta}. \tag{3.117}$$

This is the scattering matrix we will use to find our counterexample. We do this by considering a system of $N$ reservoirs at equal temperature but different chemical potential biases. Transport occurs in an energy window, where each reservoir is injecting particles into the next reservoir, and the $N^{\mathrm{th}}$ reservoir is sending particles into the first reservoir in a similar fashion as to the classical Nernst engine of Refs. [27, 8]. The reservoirs have different chemical potentials

$$\mu_{\alpha} = \frac{\alpha\mu}{N}, \tag{3.118}$$

where $\mu$ is negative. Using this the particle current becomes

$$I^{(0)}_{\alpha} = \frac{1}{h}\int_{\epsilon}^{B+\epsilon} dE f_{\mathrm{BE}}(E, \mu_{\alpha-1}) - f_{\mathrm{BE}}(E, \mu_{\alpha}) = \left[\frac{\log\left(e^{(\mu_{\alpha-1}-E)/k_{\mathrm{B}}T} - 1\right)}{k_{\mathrm{B}}Th} - \frac{\log\left(e^{(\mu_{\alpha}-E)/k_{\mathrm{B}}T} - 1\right)}{k_{\mathrm{B}}Th}\right]^{B+\epsilon}_{\epsilon}, \tag{3.119}$$

unless $\alpha = 1$, where we instead have

$$I^{(0)}_{1} = \left[\frac{\log\left(e^{(\mu_{N}-E)/k_{\mathrm{B}}T} - 1\right)}{k_{\mathrm{B}}Th} - \frac{\log\left(e^{(\mu_{1}-E)/k_{\mathrm{B}}T} - 1\right)}{k_{\mathrm{B}}Th}\right]^{B+\epsilon}_{\epsilon}. \tag{3.120}$$

The classical particle current fluctuations becomes

$$S^{(0)}_{\alpha\alpha,\mathrm{cl}} = \frac{2}{h}\int_{\epsilon}^{\epsilon+B} dE f_{\mathrm{BE}}(E, \mu_{\alpha-1}) + f_{\mathrm{BE}}(E, \mu_{\alpha}) + 2f_{\mathrm{BE}}(E, \mu_{\alpha})f_{\mathrm{BE}}(E, \mu_{\alpha-1}) \tag{3.121}$$

$$= \frac{2}{h}\left[\frac{e^{k_{\mathrm{B}}T\mu_{\alpha}}\log\left(e^{k_{\mathrm{B}}T\mu_{\alpha-1}} - e^{k_{\mathrm{B}}TE}\right)}{k_{\mathrm{B}}T\left(e^{k_{\mathrm{B}}T\mu_{\alpha-1}} - e^{k_{\mathrm{B}}T\mu_{\alpha}}\right)} - \frac{e^{k_{\mathrm{B}}T\mu_{\alpha-1}}\log\left(e^{k_{\mathrm{B}}T\mu_{\alpha}} - e^{k_{\mathrm{B}}TE}\right)}{k_{\mathrm{B}}T\left(e^{k_{\mathrm{B}}T\mu_{\alpha-1}} - e^{k_{\mathrm{B}}T\mu_{\alpha}}\right)} + E\right]^{\epsilon+B}_{\epsilon}, \tag{3.122}$$

unless $\alpha = 1$, where we instead have

$$S^{(0)}_{1,1,\mathrm{cl}} = \frac{2}{h}\left[\frac{e^{k_\mathrm{B}T\mu_1}\log\left(e^{k_\mathrm{B}T\mu_N} - e^{k_\mathrm{B}TE}\right)}{k_\mathrm{B}T\left(e^{k_\mathrm{B}T\mu_N} - e^{k_\mathrm{B}T\mu_1}\right)} - \frac{e^{k_\mathrm{B}T\mu_N}\log\left(e^{k_\mathrm{B}T\mu_1} - e^{k_\mathrm{B}TE}\right)}{k_\mathrm{B}T\left(e^{k_\mathrm{B}T\mu_N} - e^{k_\mathrm{B}T\mu_1}\right)} + E\right]_{\epsilon}^{\epsilon+B}. \tag{3.123}$$

Since all reservoirs are at equal temperatures, the total entropy production is simply given by

$$\sigma = \sum_{\alpha=1}^{N} \frac{-\mu_\alpha}{T} I^{(0)}_\alpha. \tag{3.124}$$

With these expression in place, we define the ratio

$$Q^{\mathrm{cl}}_\alpha = \sigma \frac{S^{(0)}_{\alpha\alpha,\mathrm{cl}}}{|I^{(0)}_\alpha|^2}. \tag{3.125}$$

If we can find values for our parameters such as $Q^{\mathrm{cl}}_\alpha$ for a reservoir that become arbitrarily close to zero, this means that we have found an example proving that it is not possible to derive a bosonic TUR with respect to the classical fluctuations for a general system described by scattering theory with broken time reversal symmetry. Note that the ratio of Eq. (3.125) is bounded by 2 from below for systems with time reversal symmetry since the TUR holds for these as shown in Eq. (3.103) and any value of $Q^{\mathrm{cl}}_\alpha < 2$ is a sign of TUR violation. We set $\epsilon = 10^{-4}k_\mathrm{B}T$, $B = 10^{-5}k_\mathrm{B}T$ and plot the ratio for the first reservoir $Q^{\mathrm{cl}}_1$, which can be seen for different numbers of reservoirs $N$ in Fig. (3.18). Here we notice that when we increase the number of reservoirs, $Q^{\mathrm{cl}}_1$ can get arbitrarily close to zero, which in turn means that it is not possible to derive the TUR in general for systems with broken time reversal symmetry.

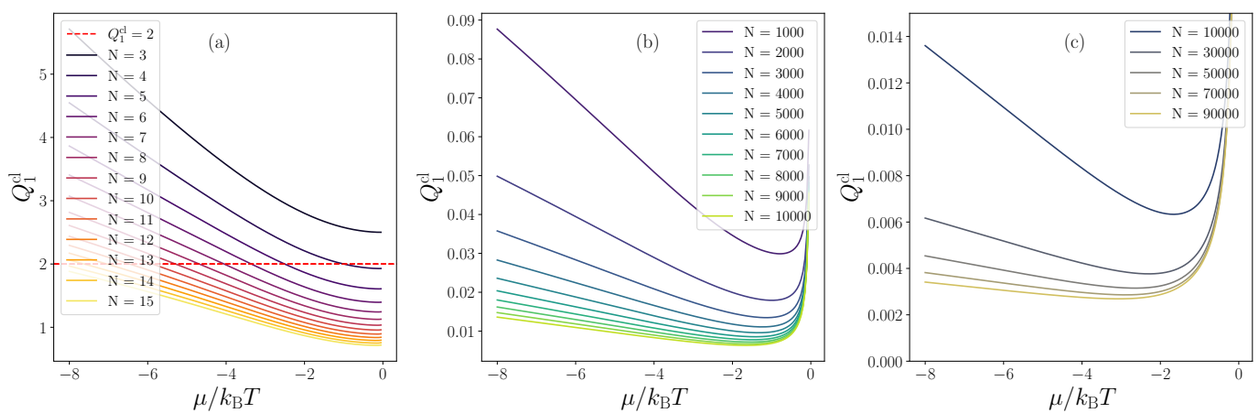


**Figure 3.18:** Plot of the ratio of Eq. (3.125) for the first reservoir of our setup as a function of the chemical potential parameter in Eq. (3.118). Notice that for all values we show in panels (b,c), $Q^{\mathrm{cl}}_1$ is far below 2, which indicates rather strong violation of the TUR. Specifically for systems with a large number of reservoirs $N$, the ratio can get arbitrarily close to zero.

These TURs are key results of this thesis, extending this type of trade-off relation to strongly coupled bosonic systems. We can, however, improve this bound by including the quantum precision bound of Eq. (3.65), in a similar way as in the previous part of the results. This will be the focus of the next section.

#### 3.2.1.2 Bosonic thermodynamic uncertainty relation for the full fluctuations

In the previous section, we derived a TUR for bosonic systems with time-reversal symmetry. This trade-off relation included the classical precision and total entropy production. We now extend it by combining Eq. (3.65) and Eq. (3.103) to find

$$\sigma \geq 2k_\mathrm{B}\frac{|I^{(0)}_\alpha|^2}{S^{(0)}_{\alpha\alpha} - \frac{2h}{B_\alpha}|I^{(0)}_\alpha|^2} = 2k_\mathrm{B}\frac{|I^{(0)}_\alpha|^2}{\tilde{S}^{(0)}_{\alpha\alpha}}. \tag{3.126}$$

Here we again encounter the bunching-compensated fluctuation and precision. We have already analyzed the meaning behind these expressions in section (3.1.5) and conclude that this bound can be interpreted as the total entropy production bounding the bunching-compensated precision in the particle current from above. If we want to have high bunching-compensated precision in the particle current, we have to pay the thermodynamic cost of having large entropy production. This is another key result of this thesis, and it is valid for thermal systems with time-reversal symmetry. We denote

the bound of Eq. (3.126) as the bosonic quantum thermodynamic uncertainty relation, or QTUR for short. This result shows us that bunching *increases* the thermodynamic cost of precision in the coherent transport of bosons.

We have previously shown that we can include the quantum fluctuations for our fermionic bounds with the introduction of the anti-bunching compensated fluctuations. In the next section, we apply these results to the fermionic TURs derived in Ref. [8] to extend them to the full fluctuations.

### 3.2.2 Extending the fermionic thermodynamic uncertainty relation to the full fluctuations

As discussed in Section 2.2.3.2, K. Brandner et. al. derived TURs for fermionic systems subject to chemical potential biases [8]. These included the classical part of the fluctuations. To extend it to the full fluctuations, we can use the fermionic quantum dynamical fluctuation bound of Eq. (3.88) in combination with the TUR of Eq. (2.90) to find

$$\sigma \geq \psi k_{\mathrm{B}} \frac{|\mathcal{I}_\alpha^{(0)}|^2}{\mathcal{S}_{\alpha\alpha}^{(0)} + \frac{2h\phi}{B_\alpha}|\mathcal{I}_\alpha^{(0)}|^2} = \psi k_{\mathrm{B}} \frac{|\mathcal{I}_\alpha^{(0)}|^2}{\tilde{\mathcal{S}}_{\alpha\alpha}^{(0)}}, \tag{3.127}$$

where $\psi = 2$ for systems with time reversal symmetry and $\psi \approx 0.89612$ for systems without [8]. This bound has a natural interpretation as the total entropy production limiting the anti-bunching compensated precision in the particle current. Here we see that the effect of anti-bunching allows for a lower thermodynamic cost of precision in comparison to bosonic systems. This is a key result of this thesis and we denote Eq. (3.127) as the fermionic quantum thermodynamic uncertainty relation. An important point is that since this bound involves the anti-bunching-compensated fluctuations it is only valid when the integrand of the particle current does not switch sign inside the region of integration, i.e. Eq. (3.86) holds true for the particle current.

To summarize, we were able to find a TUR for bosonic systems described by scattering theory. Furthermore, we were able to include the quantum part of the fluctuations in this trade-off relation, which encoded the added cost of precision when bunching is occurring. After this, we extended the previously derived fermionic TUR of Ref.[8] to include the full fluctuations as well. By doing this, we saw that the effect of anti-bunching decreased the thermodynamic cost of precision.

In the third and final part of the results, we will combine the bounds of Section 3.1 with the TURs to be able to bound entropy production from both below and above.

## 3.3 Bounding entropy production from below and above

In the previous Section 3.1, we derived multiple trade-off relations for c-weighted currents. What all these bounds have in common is that the precision or strength of a current is limited by fluctuations from above. This is fundamentally different statements to the TURs of Section 3.2, where the precision of the particle current is limited by the total entropy production. In fact, if we change perspective on the TUR, we can interpret it as the precision in the particle current limiting the entropy production from below. We can thus combine it with our bounds in Section 3.1 to find bounds on the total entropy production for thermal reservoirs from both below and above at the same time. We begin by doing this for bosonic systems.

### 3.3.1 Bosonic systems

In this section, we consider bosonic multiterminal devices where each reservoir is thermal. In addition, we only consider systems with time-reversal symmetry, which allows us to use the TURs we have derived for bosonic systems in the previous part of the results.

#### 3.3.1.1 Constraints set by classical fluctuations

In Section 3.1, we found two bounds, constraining the local entropy production from above. The first one of these is the FEB of Eq. (3.9), and it can be related to the total entropy production by summing over reservoirs. By letting $N$ equal the number of reservoirs, we find

$$\sum_{\alpha=1}^{N} R_{\alpha,\mathrm{cl}} \geq 2k_{\mathrm{B}} \sum_{\alpha=1}^{N} |I_\alpha^{(\Sigma)}| \geq 2k_{\mathrm{B}}\sigma\,. \tag{3.128}$$

For bosonic systems with time-reversal symmetry, we can combine this result with the TUR of Eq. (3.103) to find

$$\sum_{\alpha=1}^{N} R_{\alpha,\mathrm{cl}} \geq 2k_{\mathrm{B}}\sigma \geq 4k_{\mathrm{B}}\frac{|I_{\alpha}^{(0)}|^2}{S_{\alpha\alpha,\mathrm{cl}}^{(0)}}, \tag{3.129}$$

thus bounding the total entropy production from both below and above. However, the FEB is not the tightest bound on the local entropy production set by the classical fluctuations at our disposal. This is the DFB of Eq. (3.30). Using this bound and summing over reservoirs, we find

$$\sum_{\alpha=1}^{N}\sqrt{S_{\alpha\alpha,\mathrm{cl}}^{(0)}S_{\alpha\alpha,\mathrm{cl}}^{(\Sigma)}} \geq 2\sum_{\alpha=1}^{N}|I_{\alpha}^{(\Sigma)}| \geq 2\sigma\,. \tag{3.130}$$

Combining it in the same manner as before with Eq. (3.103) we find

$$\sum_{\alpha=1}^{N}\sqrt{S_{\alpha\alpha,\mathrm{cl}}^{(0)}S_{\alpha\alpha,\mathrm{cl}}^{(\Sigma)}} \geq 2\sigma \geq 4k_{\mathrm{B}}\frac{|I_{\alpha}^{(0)}|^2}{S_{\alpha\alpha,\mathrm{cl}}^{(0)}}. \tag{3.131}$$

Both of these bounds extend to the full fluctuations $S_{\alpha\alpha}^{(\nu)}$ trivially. The bound of Eq.(3.131) is a central result of this thesis, since we show that the entropy production in bosonic systems is limited both from above and below by the fluctuations present in the system. If we desire high precision in the particle current, the entropy production must be large, which in turn forces the fluctuations in the system to become large. We can also sum over reservoirs in the left-hand side, which gives us

$$\sum_{\alpha=1}^{N}\sqrt{S_{\alpha\alpha,\mathrm{cl}}^{(0)}S_{\alpha\alpha,\mathrm{cl}}^{(\Sigma)}} \geq 2\sigma \geq 4k_{\mathrm{B}}\frac{\sum_{\alpha=1}^{N}|I_{\alpha}^{(0)}|^2}{\sum_{\alpha=1}^{N}S_{\alpha\alpha,\mathrm{cl}}^{(0)}}, \tag{3.132}$$

or alternatively

$$\sum_{\alpha=1}^{N}\sqrt{S_{\alpha\alpha,\mathrm{cl}}^{(0)}S_{\alpha\alpha,\mathrm{cl}}^{(\Sigma)}} \geq 2\sigma \geq \frac{4k_{\mathrm{B}}}{N}\sum_{\alpha=1}^{N}\frac{|I_{\alpha}^{(0)}|^2}{S_{\alpha\alpha,\mathrm{cl}}^{(0)}}. \tag{3.133}$$

These bounds extend to the full fluctuations as well. We are, however, interested in employing the quantum precision bound to achieve a tighter overall bound. This is the focus of the next section.

#### 3.3.1.2 Constraints set by full fluctuations

At this point, we have already seen how to include the limits on precision set by the classical quantum fluctuations in the classical trade-off relations multiple times. To use the full FEB of Eq. (3.68) we first use the discrete version of the Cauchy-Schwarz inequality [17] to find

$$\sum_{\alpha=1}^{N}S_{\alpha\alpha,\mathrm{qu}}^{(\Sigma)} \geq \sum_{\alpha=1}^{N}\frac{2h}{B_{\alpha}}|I_{\alpha}^{(\Sigma)}|^2 \geq 2h\frac{\left(\sum_{\alpha=1}^{N}|I_{\alpha}^{(\Sigma)}|\right)^2}{\sum_{\alpha=1}^{N}B_{\alpha}} \geq \frac{2h}{N\mathbb{B}}\sigma^2, \tag{3.134}$$

where we defined the *total bandwidth*

$$\mathbb{B} = \sum_{\alpha=1}^{N}B_{\alpha}. \tag{3.135}$$

Using this, we find

$$\sum_{\alpha=1}^{N}\left\{S_{\alpha\alpha}^{(\Sigma)} + \frac{k_{\mathrm{B}}^2}{4}\tilde{S}_{\alpha\alpha}^{(0)}\right\} \geq 2\sigma\left(k_{\mathrm{B}} + \frac{h}{N\mathbb{B}}\sigma\right) \geq 4k_{\mathrm{B}}\frac{|I_{\alpha}^{(0)}|^2}{\tilde{S}_{\alpha\alpha}^{(0)}}\left(k_{\mathrm{B}} + \frac{k_{\mathrm{B}}2h}{N\mathbb{B}}\frac{|I_{\alpha}^{(0)}|^2}{\tilde{S}_{\alpha\alpha}^{(0)}}\right), \tag{3.136}$$

limiting entropy production from both below and above. Instead using the QDFB of Eq. (3.126) and by summing over reservoirs, we find

$$\sum_{\alpha=1}^{N}\sqrt{\tilde{S}_{\alpha\alpha}^{(0)}\tilde{S}_{\alpha\alpha}^{(\Sigma)}} \geq 2\sigma \geq 4k_{\mathrm{B}}\frac{|I_{\alpha}^{(0)}|^2}{\tilde{S}_{\alpha\alpha}^{(0)}}. \tag{3.137}$$

This bound is a central result of this thesis, and it can be interpreted as the total entropy production being constrained by the bunching compensated noise, both from below and above. If we have high bunching-compensated precision in the particle current, the total entropy production becomes large. This then forces the bunching-compensated noise to become large in turn. This shows us that entropy production and fluctuations are fundamentally linked in scattering theory for bosonic systems.

We have now bounded entropy production from both sides for bosonic thermal systems with time reversal symmetry. We also managed to incorporate the effect of bunching when extending these bounds to the full fluctuations, constraining the total entropy production tighter. We now perform the corresponding procedure for fermionic systems.

### 3.3.2 Fermionic systems

In Ref. [8], TURs for fermionic systems were derived, and the parameter $\psi$ as shown to be $\psi = 2$ for time-reversal symmetric systems and $\psi \approx 0.89612$ otherwise. We now combine this TUR with the DFB derived in Section 3.1 to find both an upper and lower limit on the entropy production for fermionic systems.

#### 3.3.2.1 Constraints set by classical fluctuations

We begin by considering the classical fluctuations and follow the same procedure as in Section 3.3.1.1. Starting from the constraint of Eq. (3.39) on the local entropy production, we find a bound on the total entropy production by summing over all reservoirs,

$$\sum_{\alpha=1}^{N} \sqrt{\mathcal{S}^{(0)}_{\alpha\alpha,\mathrm{cl}} \mathcal{S}^{(\Sigma)}_{\alpha\alpha,\mathrm{cl}}} \geq 2 \sum_{\alpha=1}^{N} |\mathcal{I}^{(\Sigma)}_{\alpha}| \geq 2\sigma \,. \tag{3.138}$$

combining this with the TURs of Ref. [8], we find

$$\sum_{\alpha=1}^{N} \sqrt{\mathcal{S}^{(0)}_{\alpha\alpha,\mathrm{cl}} \mathcal{S}^{(\Sigma)}_{\alpha\alpha,\mathrm{cl}}} \geq 2\sigma \geq 2\psi k_{\mathrm{B}} \frac{|\mathcal{I}^{(0)}_{\alpha}|^2}{\mathcal{S}^{(0)}_{\alpha\alpha,\mathrm{cl}}}. \tag{3.139}$$

This shows us that the fermionic entropy production is constrained from both sides by the classical parts of the fluctuations. It is however not possible to extend this bound to the full fluctuations without using the results dealing with the quantum part of the noise, in contrast to the bosonic systems. This will be the focus of the next section.

#### 3.3.2.2 Constraints set by full fluctuations

To constrain the fermionic entropy production from below and and above using the full fluctuations, we utilize the fermionic QDFB of Eq. (3.93) together with the quantum TUR of Eq. (3.141). By summing over reservoirs, we find

$$\sum_{\alpha=1}^{N} \sqrt{\tilde{\mathcal{S}}^{(0)}_{\alpha\alpha} \tilde{\mathcal{S}}^{(\Sigma)}_{\alpha\alpha}} \geq 2 \sum_{\alpha=1}^{N} |\mathcal{I}^{(\Sigma)}_{\alpha}| \geq 2\sigma. \tag{3.140}$$

Having an upper limit on the total entropy production set by the anti-bunching compensated fluctuations, we continue to use the QTUR to find

$$\sum_{\alpha=1}^{N} \sqrt{\tilde{\mathcal{S}}^{(0)}_{\alpha\alpha} \tilde{\mathcal{S}}^{(\Sigma)}_{\alpha\alpha}} \geq 2\sigma \geq 2\psi k_{\mathrm{B}} \frac{|I^{(0)}_{\alpha}|^2}{\tilde{\mathcal{S}}^{(0)}_{\alpha\alpha}}. \tag{3.141}$$

With this bound, we have been able to constrain the total entropy production in fermionic systems by the anti-bunching-compensated noise. Here again we notice a difference to the bosonic case, see Eq. (3.137). The quantum part of the fluctuations causes the bound to become less tight from both sides, not constraining the entropy production as tightly as in the bosonic case. This is due to anti-bunching decreasing the noise in fermionic systems and allowing for higher precision. An important point is that since this bound involves the anti-bunching-compensated fluctuations it is only valid when the integrand of the particle current does not switch sign inside the region of integration, i.e. Eq. (3.86) holds true for the particle current.

With this, we finish presenting the results derived during this master's project. We have been able to find trade-off relations for the coherent transport of weakly interacting particles. These are quite general results, and the only time we made an additional assumption apart from standard on the scattering matrix and thus the device investigated was when we assumed time reversal symmetry when deriving the bosonic TUR. We now move on to the conclusions of this thesis.

# 4
# Conclusion

In this thesis, we have investigated the relationship between noise and currents in nanoscale devices modelled by scattering theory. We found multiple trade-off relations for precision for both fermionic and bosonic systems with possibly strong coupling and nonthermal resources. In Chapter 1, we introduced the fundamental concepts that this work has been examining. We motivated using entropy production as the fundamental way of characterizing a thermodynamic process. Additionally, we discussed the notion of performance and how it has to be modified when studying the thermodynamics of nanoscale devices. In this context, we introduced the notion of fluctuations and precision in an output, which are central concepts of this thesis. The presence of fluctuations is not the only difference between large and small-scale devices; so are quantum effects. Specifically, the two types of indistinguishable quantum particles, fermions and bosons, have different transport properties. We examined these differences by studying the fluctuations in a Hong-Ou-Mandel setup where bosons are observed to bunch increasing fluctuations, whereas fermions anti-bunch decreasing fluctuations. These effects are important for understanding our results later on. Finally, we motivated the use of scattering theory to model nanoscale devices to be able to make general statements about precision in the coherent transport of weakly interacting particles.

In Chapter 2, we introduced the theory needed to describe the thermodynamics of nanoscale devices in greater detail. First, we discussed the role of entropy and how its notion differs in quantum mechanical systems. In particular, we showed that the quantum mechanical von Neumann entropy reduces to the classical Gibbs entropy when describing states diagonal in the number basis, which we focus on in this thesis. After this, we introduced two important trade-off relations valid for classical Markovian systems: the thermodynamic and kinetic uncertainty relations. To understand whether these relations are valid also for quantum transport, we first introduce the theoretical framework used in this thesis: scattering theory. We utilize this framework to calculate different kinds of currents and their fluctuations and discuss trade-off relations involving them [2, 8]. We introduced the notion of a c-weighted current, which we showed could be used to describe particle, energy, heat, and entropy currents within a common formula. We concluded Chapter 2 by investigating the thermodynamics of two reservoirs connected by a central scattering region and showed some differences in working with fermionic and bosonic systems.

Our results are presented in Chapter 3, where we derived numerous trade-off relations for systems described by scattering theory. Here we summarize our main results:

- We showed that the bosonic fluctuations could be decomposed into the same division of classical and quantum fluctuations as used in Refs. [2, 8]. Here we saw that the bosonic *quantum* fluctuations gave a positive contribution to the total noise, unlike the fermionic case [Section 3.1.1].

- We extended the trade-off relation concerning the classical fluctuations for nonthermal fermionic systems of Ref. [2] to bosonic systems with the fluctuation entropy production bound of Eq. (3.9). We found similar bounds for other c-weighted currents, and a key result is that all these bounds could be trivially extended to the full fluctuations, namely the quantum fluctuations unlike the fermionic case [Section 3.1.2].

- We found tighter bounds than the ones presented in Section 3.1.1 involving classical fluctuations and a c-weighted current, namely the dynamical fluctuation bound. This bound applied to both bosonic and fermionic system, as shown in Eq. (3.30) and Eq. (3.39). Both of these bounds bear a resemblance to the kinetic uncertainty relation. However, to make this connection concrete, further research is needed. In the bosonic case, it was straightforward to extend the DFB to include the full noise unlike in the fermionic case [Section 3.1.3, Section 3.1.4].

- We analyzed the bosonic quantum noise to find multiple new bounds on precision, with the central one being the quantum precision bound in Eq. (3.64). This bound showed us how the precision in a bosonic c-weighted current was inherently limited by the bandwidth, which could be interpreted as bunching, limiting precision. We also incorporated the QPB into our classical noise bounds of the FEB and DFB, which allowed us to find the full FEB in Eq. (3.68) and the

QDFB in Eq. (3.71). These bounds are key results of the thesis, providing bounds between full physical fluctuations and a current while at the same time including the effect of bunching in a clear way [Section 3.1.5].

- We extended the fermionic dynamical fluctuation bound to include the quantum fluctuations in two ways. The first way resulted in the bound of in Eq. (3.77), which holds in a general setting. The second way included the effect of anti-bunching, allowing for a higher precision in a c-weighted current in the fermionic QDFB of Eq. (3.91). It however required the integrand in the currents to not change sign inside the region of integration. This is a central result of this thesis, allowing us to compare the trade-off relations for precision in bosonic and fermionic systems [Section 3.1.6].

- We extended the thermodynamic uncertainty relation derived in Ref. [8] for thermal fermionic systems to bosonic systems with time-reversal symmetry in Eq. (3.109). This is a key result of this thesis, establishing a TUR for strongly coupled bosonic systems. It was possible to trivially extend the bosonic TUR to include the full fluctuations, unlike the fermionic case [Section 3.2.1.1].

- We extended both the bosonic and fermionic TURs to include the full fluctuations, which incorporated the effects of bunching in Eq. (3.126) and anti-bunching in Eq. (3.127), respectively. By doing this, we saw that the thermodynamic cost of precision was increased for bosonic systems while it was decreased for fermionic systems [Section 3.2.1.2, Section 3.2.2].

- For thermal bosonic systems with time-reversal symmetry, we found both upper and lower bounds on the total entropy production by combining our results from Section 3.1 and Section 3.2. This is a central result of this thesis, where we showed that fluctuations limit the possible entropy production fundamentally. We also managed to incorporate the effect of bunching in these bounds, making them tighter. This is made clear by the bound of Eq. (3.137), where we saw that the total entropy production is limited from above by bunching-compensated fluctuations, while being limited from below by the bunching-compensated precision in the particle current.

- For thermal fermionic systems, we managed to find both upper and lower bounds on the total entropy production by combining our results from Section 3.1 and Section 3.2. This is a central result of this thesis, where we showed that fluctuations limit the possible entropy production fundamentally. We also managed to incorporate the effect of anti-bunching in these bounds, making them less tight. This is made clear by the bound of Eq. (3.141), where we saw that the total entropy production is limited from above by anti-bunching-compensated fluctuations, while being limited from below by the anti-bunching-compensated precision in the particle current.

In conclusion, these new trade-off relations for coherent transport of weakly interacting particles offer new insights in the understanding of fluctuations in nanoscale devices. In particular, they highlight the role that bunching and anti-bunching play in the precision of a current and in the relation between entropy production and fluctuations.

# 5
# Outlook

In this thesis, we have derived trade-off relations valid for any coherent conductor described by scattering theory. In addition, we allowed for the reservoirs to have arbitrary temperatures and chemical potentials, or even to be nonthermal. However, we restricted ourselves to working with "semi-classical" states, which are diagonal in the number basis. How precision is affected by more exotic quantum states is, however, very interesting, especially in the bosonic case where there can be, e.g., coherent and squeezed states [9]. It is worth noting that the entropy production could become more complicated to calculate because of decoherence.

Furthermore, we focused on c-weighted currents in stationary systems. Adding external drives to the system opens up the possibility of studying more devices, e.g. heat or particle pumps and even collective excitations.

Moreover, there are other interesting types of currents to investigate which are not c-weighted currents. This is the case in spintronics, where spin currents and their precision play a crucial role [22, 19, 20].

Finally, while we are able to treat strong coupling between the leads and the scattering region using scattering theory, we are restricted to treat only weak particle-particle interactions. Strong interactions can, in principle, have important effects on precision. However, extending the trade-off relations derived here to the strongly interacting would require different approaches like Green's functions and would require other types of approximations e.g. weak coupling.

# Bibliography


[1] Mohammed Ali Aamir et al. *Thermally driven quantum refrigerator autonomously resets superconducting qubit*. arXiv:2305.16710 [cond-mat, physics:quant-ph]. May 2023. DOI: 10.48550/arXiv.2305.16710. URL: http://arxiv.org/abs/2305.16710 (visited on 05/22/2024).

[2] Matteo Acciai et al. *Constraints between entropy production and its fluctuations in nonthermal engines*. arXiv:2309.11570 [cond-mat]. Dec. 2023. DOI: 10.48550/arXiv.2309.11570. URL: http://arxiv.org/abs/2309.11570 (visited on 02/01/2024).

[3] Hans-Albert Bachor and Timothy C. Ralph. *A guide to experiments in quantum optics*. eng. Third edition. Weinheim: Wiley-VCH, 2019. ISBN: 9783527411931.

[4] Andre C. Barato and Udo Seifert. "Thermodynamic uncertainty relation for biomolecular processes". In: *Physical Review Letters* 114.15 (Apr. 2015). arXiv:1502.05944 [cond-mat, physics:physics], p. 158101. ISSN: 0031-9007, 1079-7114. DOI: 10.1103/PhysRevLett.114.158101. URL: http://arxiv.org/abs/1502.05944 (visited on 05/16/2024).

[5] Felix Binder et al., eds. *Thermodynamics in the Quantum Regime: Fundamental Aspects and New Directions*. en. Vol. 195. Fundamental Theories of Physics. Cham: Springer International Publishing, 2018. ISBN: 9783319990453 9783319990460. DOI: 10.1007/978-3-319-99046-0. URL: http://link.springer.com/10.1007/978-3-319-99046-0 (visited on 06/22/2024).

[6] Ya. M. Blanter and M. Büttiker. "Shot noise in mesoscopic conductors". In: *Physics Reports* 336.1 (Sept. 2000), pp. 1–166. ISSN: 0370-1573. DOI: 10.1016/S0370-1573(99)00123-4. URL: https://www.sciencedirect.com/science/article/pii/S0370157399001234 (visited on 02/01/2024).

[7] E. Bocquillon et al. "Coherence and Indistinguishability of Single Electrons Emitted by Independent Sources". In: *Science* 339.6123 (Mar. 2013). arXiv:1301.7093 [cond-mat], pp. 1054–1057. ISSN: 0036-8075, 1095-9203. DOI: 10.1126/science.1232572. URL: http://arxiv.org/abs/1301.7093 (visited on 06/20/2024).

[8] Kay Brandner, Taro Hanazato, and Keiji Saito. "Thermodynamic Bounds on Precision in Ballistic Multiterminal Transport". en. In: *Physical Review Letters* 120.9 (Mar. 2018), p. 090601. ISSN: 0031-9007, 1079-7114. DOI: 10.1103/PhysRevLett.120.090601. URL: https://link.aps.org/doi/10.1103/PhysRevLett.120.090601 (visited on 02/07/2024).

[9] Heinz-Peter Breuer and Francesco Petruccione. *The theory of open quantum systems*. eng. Repr. Oxford: Clarendon Press, 2010. ISBN: 9780199213900.

[10] G. Cook and R. H. Dickerson. "Understanding the chemical potential". en. In: *American Journal of Physics* 63.8 (Aug. 1995), pp. 737–742. ISSN: 0002-9505, 1943-2909. DOI: 10.1119/1.17844. URL: https://pubs.aip.org/ajp/article/63/8/737/1054734/Understanding-the-chemical-potential (visited on 01/23/2024).

[11] Sebastian E. Deghi and Raúl A. Bustos-Marún. "Entropy current and efficiency of quantum machines driven by nonequilibrium incoherent reservoirs". In: *Physical Review B* 102.4 (July 2020). arXiv:2006.16397 [cond-mat], p. 045415. ISSN: 2469-9950, 2469-9969. DOI: 10.1103/PhysRevB.102.045415. URL: http://arxiv.org/abs/2006.16397 (visited on 02/01/2024).

[12] Ivan Di Terlizzi and Marco Baiesi. "Kinetic uncertainty relation". In: *Journal of Physics A: Mathematical and Theoretical* 52.2 (Jan. 2019). arXiv:1809.06410 [cond-mat, q-bio], 02LT03. ISSN: 1751-8113, 1751-8121. DOI: 10.1088/1751-8121/aaee34. URL: http://arxiv.org/abs/1809.06410 (visited on 05/16/2024).

[13] J. Dubois et al. "Minimal-excitation states for electron quantum optics using levitons". en. In: *Nature* 502.7473 (Oct. 2013), pp. 659–663. ISSN: 1476-4687. DOI: 10.1038/nature12713. URL: https://www.nature.com/articles/nature12713 (visited on 06/20/2024).

[14] Ian Duck, Wolfgang Pauli, and E. C. G. Sudarshan. *Pauli and the spin-statistics theorem*. Singapore ; River Edge, NJ: World Scientific, 1997. ISBN: 9789810231149.

[15] *Focus on Thermoelectric Effects in Nanostructures - New Journal of Physics - IOPscience*. URL: https://iopscience.iop.org/journal/1367-2630/page/Focus%20on%20Thermoelectric%20Effects%20in%20Nanostructures (visited on 05/22/2024).

[16] Charles Coulston Gillispie and Theodore M. Porter. *The edge of objectivity: an essay in the history of scientific ideas*. New paperback edition. OCLC: ocn959958002. Princeton, New Jersey: Princeton University Press, 2016. ISBN: 9780691172521.

[17] Godfrey H. Hardy, John Edensor Littlewood, and George Pólya. *Inequalities*. eng. 1. paperback ed., repr., transferred to digital printing. Cambridge mathematical library. Cambridge: Cambridge Univ. Press, 2001. ISBN: 9780521358804 9780521052061.

[18] C. K. Hong, Z. Y. Ou, and L. Mandel. "Measurement of subpicosecond time intervals between two photons by interference". In: *Physical Review Letters* 59.18 (Nov. 1987), pp. 2044–2046. DOI: 10.1103/PhysRevLett.59.2044. URL: https://link.aps.org/doi/10.1103/PhysRevLett.59.2044 (visited on 05/15/2024).

[19] M. Matsuo et al. "Spin Current Noise of the Spin Seebeck Effect and Spin Pumping". In: *Physical Review Letters* 120.3 (Jan. 2018), p. 037201. DOI: 10.1103/PhysRevLett.120.037201. URL: https://link.aps.org/doi/10.1103/PhysRevLett.120.037201 (visited on 05/21/2024).

[20] Jonathan Meair, Peter Stano, and Philippe Jacquod. "Measuring spin accumulations with current noise". In: *Physical Review B* 84.7 (Aug. 2011), p. 073302. DOI: 10.1103/PhysRevB.84.073302. URL: https://link.aps.org/doi/10.1103/PhysRevB.84.073302 (visited on 05/21/2024).

[21] Michael V. Moskalets. *Scattering matrix approach to non-stationary quantum transport*. OCLC: ocn730403761. London : Singapore ; Hackensack N.J: Imperial College Press ; World Scientific Publishing [distributor], 2012. ISBN: 9781848168343.

[22] S. Omar et al. "Spin relaxation 1/f noise in graphene". In: *Physical Review B* 95.8 (Feb. 2017), p. 081403. DOI: 10.1103/PhysRevB.95.081403. URL: https://link.aps.org/doi/10.1103/PhysRevB.95.081403 (visited on 05/21/2024).

[23] Michael Edward Peskin and Daniel V. Schroeder. *An introduction to quantum field theory*. eng. The advanced book program. Boca Raton London New York: CRC Press, Taylor & Francis Group, 2019. ISBN: 9780367320560 9780201503975.

[24] L. E. Reichl. *A modern course in statistical physics*. 2nd ed. New York: Wiley, 1998. ISBN: 9780471595205.

[25] J J. Sakurai and Jim Napolitano. *Modern quantum mechanics*. eng. Third edition. OCLC: 1156991840. Cambridge ; New York: Cambridge University Press, 2021. ISBN: 9781108473224.

[26] Rafael Sánchez, Janine Splettstoesser, and Robert S. Whitney. "Non-equilibrium System as a Demon". In: *Physical Review Letters* 123.21 (Nov. 2019). arXiv:1811.02453 [cond-mat, physics:physics, physics:quant-ph], p. 216801. ISSN: 0031-9007, 1079-7114. DOI: 10.1103/PhysRevLett.123.216801. URL: http://arxiv.org/abs/1811.02453 (visited on 02/01/2024).

[27] Julian Stark et al. "Classical Nernst engine". In: *Physical Review Letters* 112.14 (Apr. 2014), p. 140601. DOI: 10.1103/PhysRevLett.112.140601. URL: https://link.aps.org/doi/10.1103/PhysRevLett.112.140601 (visited on 06/17/2024).

[28] Ludovico Tesser. "Fluctuations and nonequilibrium thermodynamics in electronic nanosystems". In: *Chalmers University of Technology* ().

[29] Van Tuan Vo, Tan Van Vu, and Yoshihiko Hasegawa. "Unified thermodynamic-kinetic uncertainty relation". In: *Journal of Physics A: Mathematical and Theoretical* 55.40 (Oct. 2022). arXiv:2203.11501 [cond-mat, physics:quant-ph], p. 405004. ISSN: 1751-8113, 1751-8121. DOI: 10.1088/1751-8121/ac9099. URL: http://arxiv.org/abs/2203.11501 (visited on 05/13/2024).

[30] Gu Zhang, Igor V. Gornyi, and Christian Spånslätt. "Does delta-$T$ noise probe quantum statistics?" In: *Physical Review B* 105.19 (May 2022). arXiv:2201.13174 [cond-mat], p. 195423. ISSN: 2469-9950, 2469-9969. DOI: 10.1103/PhysRevB.105.195423. URL: http://arxiv.org/abs/2201.13174 (visited on 02/27/2024).

# A

# Appendix 1

## A.1 The chemical potential

In this section the role of the chemical potential for bosonic systems is discussed. For a system that can exchange energy and particles with its surrounding a change in internal energy $U$ is written as

$$dU = Td\Sigma + \mu dN, \tag{A.1}$$

where $T$ is the temperature, $d\Sigma$ is the change in entropy, $\mu$ is the chemical potential and $dN$ is the change in number of particles [10]. From this it follows that

$$\mu = \left.\frac{\partial U}{\partial N}\right|_{\Sigma}. \tag{A.2}$$

Using this equation, the chemical potential can be interpreted as the amount of energy needed to keep the entropy constant in the system when a particle is added. In principle, $\mu$ can be both negative and positive. In fermionic systems, the chemical potential can be positive due to the Pauli exclusion principle, since if all states are occupied, there is not room for adding a particle without supplying enough energy to reach an unoccupied state. Then the chemical potential is interpreted as the fermi level, and the energy needed is exactly the energy it takes for a particle to enter the next highest energy state, yielding a positive chemical potential [10]. This can, of course, not happen for non-interacting bosons since the particle could always enter the ground state. The chemical potential for a reservoir of non interacting bosonic particles is $\mu \leq 0$ and is equal to zero for a Bose Einstein Condensate (BEC) [10]. This is because when adding a bosonic particle to a BEC it enters the ground state, not increasing the multiplicity of microstates. If we instead add it to a reservoir of bosons, not in a BEC, the number of microstates increases, yielding an increase in entropy. Then the internal energy has to be decreased to ensure that the entropy remains constant, resulting in a negative chemical potential.

In Ref. [10], an elegant illustration of this is made using a simple reservoir of bosonic particles that can each take energies in quantas of $\epsilon$. Here we use the same example to gain intuition for the chemical potential in bosonic systems, but we emphasize that this argument was made in Ref. [10]. Initially, two particles, $R$ and $B$, are in a reservoir with an internal energy of $U = 2\epsilon$ and an entropy of $S = k_{\mathrm{B}} \ln 3$. A third particle $G$ is added to the reservoir. If the internal energy is kept constant, the entropy is increased to $S = k_{\mathrm{B}} \ln 6$. If the energy is decreased by $-\epsilon$, the entropy remains constant. Thus, the chemical potential is $\mu = -\epsilon$. An illustration of this argument made in Ref. [10] can be seen in Fig (A.1). This view also allows for a natural interpretation of a chemical potential bias for

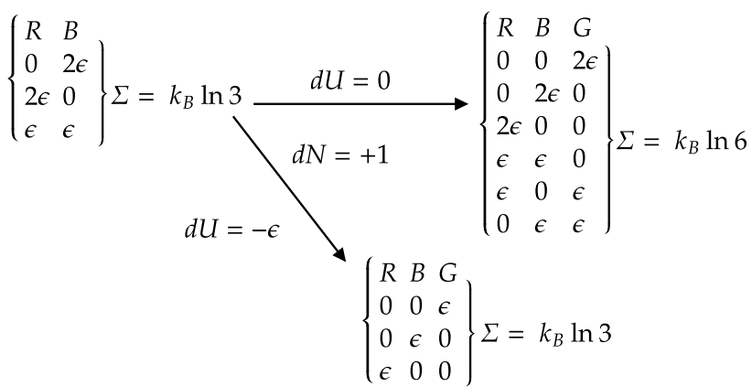


**Figure A.1:** States of a two-particle reservoir when a third particle with zero energy is added. The particles in the reservoir can take on energies in quanta of $\epsilon$. If the third particle is added without removing internal energy, the entropy increases from $\Sigma = k_{\mathrm{B}} \ln 3$ to $\Sigma = k_{\mathrm{B}} \ln 6$ due to an increase in microstates. If we instead remove the internal energy $dU = -\epsilon$, the entropy stays constant, thus the chemical potential is negative with the value $\mu = -\epsilon$.

bosons. When allocating particles into a reservoir with bosons, the more negative $\mu$ is, the more the

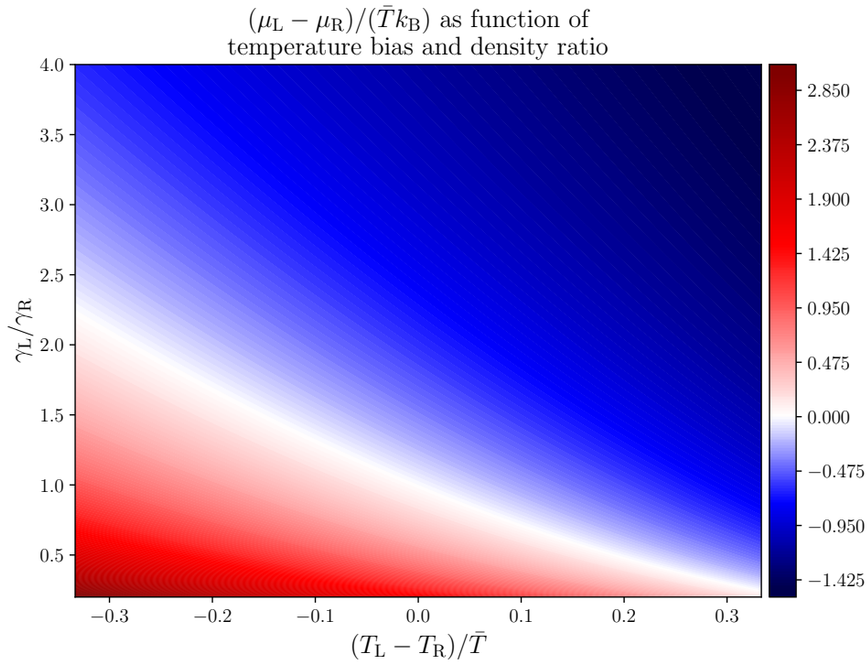


**Figure A.2:** Chemical potential bias between two bosonic reservoirs as functions of particle densities $\gamma_R$, $\gamma_L$ and temperatures $T_R$, $T_L$. By changing the ratio of densities in the two reservoirs, it is possible to achieve both positive and negative chemical potential biases for both positive and negative temperature biases.

entropy is increased. Therefore, if a flow of particles is allowed between two reservoirs at the same temperature but different chemical potentials, the flow of particles will be into the reservoir with the most negative chemical potential since this produces entropy,

$$d\Sigma = \Delta\mu dN. \tag{A.3}$$

As discussed in Section 2.3, one might achieve a thermoelectric effect using a temperature bias to drive a particle current against a chemical potenial bias. This hinges on the fact that it is possible to achieve a positive chemical potential bias and a negative temperature bias at the same time. That this is possible is not instantly clear since the chemical potential for a reservoir described by a BE distribution depends strongly on temperature. In Ref. [30], the chemical potential is calculated by integrating the BE distribution and setting a constant density of states $g$ and number of particles $N$,

$$g\int_0^\infty dE f_{\mathrm{BE}}(E) = N \implies \mu(T,\gamma) = T\ln\left(1 - e^{-\gamma/T}\right), \tag{A.4}$$

where $\gamma = N/g$ is a parameter determining the density of particles in a reservoir. Following from this, it is not possible to have a positive potential bias and a negative temperature bias while having the two reservoirs at the same densities. This can however be achieved by keeping the reservoirs at different densities, which is illustrated in Fig. (A.2). Here $\gamma_{L/R}$ are the density parameters of a left and right reservoir, $T_{L/R}$ the temperatures, $\bar{T}$ the average temperature and $\mu_{L/R}$ the chemical potentials as functions of the previously mentioned variables.

# B

# Appendix 2

## B.1 Derivation of bosonic classical and quantum fluctuations

In this section, we show how we split the bosonic zero-frequency noise of Eq. (2.75) into a classical part, quadratic in the scattering matrix, and a quantum part, quartic in the scattering matrix, which has been used before for fermionic systems [2, 8]. We drop all energy arguments for brevity and define

$$K_{\alpha\beta} \equiv f_\alpha(E)(1+f_\beta(E)), \tag{B.1}$$

which allows us to write the cross-correlators as

$$S^{(\nu)}_{\alpha\beta} = \frac{1}{2h}\sum_{\gamma\delta}\sum_{ij}\sum_{mn}\int dE \boldsymbol{\mathcal{A}}^{E,E}_{\alpha i,\gamma m,\delta n}\boldsymbol{\mathcal{A}}^{E,E}_{\beta j,\delta n,\gamma m}C^{(\nu)}_\alpha C^{(\nu)}_\beta \left\{K_{\gamma\delta}+K_{\delta\gamma}\right\}. \tag{B.2}$$

We begin by treating

$$\begin{aligned}
&\sum_{\gamma\delta}\sum_{mn}\boldsymbol{\mathcal{A}}^{E,E}_{\alpha i,\gamma m,\delta n}\boldsymbol{\mathcal{A}}^{E,E}_{\beta j,\delta n,\gamma m}C^{(\nu)}_\alpha C^{(\nu)}_\beta \left\{K_{\gamma\delta}+K_{\delta\gamma}\right\} = \\
&\sum_{\gamma\delta}\sum_{mn}\left(s^*_{\alpha i\gamma m}s_{\alpha i\delta n}-\delta_{\alpha i\gamma m}\delta_{\alpha i\delta n}\right)\left(s^*_{\beta j\delta n}s_{\beta j\gamma m}-\delta_{\beta j\delta n}\delta_{\beta j\gamma m}\right) = \\
&M_1+M_2+M_3+M_4,
\end{aligned} \tag{B.3}$$

where we defined

$$M_1 \equiv \sum_{\gamma\delta}\sum_{mn}[s^\dagger]_{\gamma m\alpha i}s_{\alpha i\delta n}[s^\dagger]_{\delta n\beta j}s_{\beta j\gamma m}(K_{\gamma\delta}+K_{\delta\gamma}), \tag{B.4}$$

$$M_2 \equiv -\sum_{\gamma\delta}\sum_{mn}s^*_{\alpha i\gamma m}s_{\alpha i\delta n}\delta_{\beta j\delta n}\delta_{\beta j\gamma m}(K_{\gamma\delta}+K_{\delta\gamma}), \tag{B.5}$$

$$M_3 \equiv -\sum_{\gamma\delta}\sum_{mn}\delta_{\alpha i\gamma m}\delta_{\alpha i\delta n}s^*_{\beta j\delta n}s_{\beta j\gamma m}(K_{\gamma\delta}+K_{\delta\gamma}), \tag{B.6}$$

$$M_4 \equiv \sum_{\gamma\delta}\sum_{mn}\delta_{\alpha i\gamma m}\delta_{\alpha i\delta n}\delta_{\beta j\delta n}\delta_{\beta j\gamma m}(K_{\gamma\delta}+K_{\delta\gamma}). \tag{B.7}$$

Performing the sum in $M_2$, $M_3$ and $M_4$, we find

$$-M_2 = s^*_{\alpha i\beta j}s_{\alpha i\beta j}(K_{\beta\beta}+K_{\beta\beta}) = 2|s_{\alpha i\beta j}|^2K_{\beta\beta}, \tag{B.8}$$

$$-M_3 = s^*_{\beta j\alpha i}s_{\beta j\alpha i}(K_{\alpha\alpha}+K_{\alpha\alpha}) = 2|s_{\beta j\alpha i}|^2K_{\alpha\alpha}, \tag{B.9}$$

$$M_4 = 2\delta_{\alpha i\beta j}K_{\alpha\alpha}. \tag{B.10}$$

To treat $M_1$ we split it into different parts $M_1 = M_1' + M_1'' + M_1'''$ and use

$$K_{\gamma\delta}+K_{\delta\gamma} = K_{\gamma\gamma}+K_{\delta\delta}-(f_\gamma-f_\delta)^2, \tag{B.11}$$

together with the unitarity of the scattering matrix to find

$$\begin{aligned}
M_1' &\equiv \sum_{\gamma\delta}\sum_{mn}[s^\dagger]_{\gamma m\alpha i}s_{\alpha i\delta n}[s^\dagger]_{\delta n\beta j}s_{\beta j\gamma m}K_{\gamma\gamma} \\
&= \sum_{\gamma m}[s^\dagger]_{\gamma m\alpha i}s_{\beta j\gamma m}\delta_{\alpha i\beta j}K_{\gamma\gamma} = \delta_{\alpha i\beta j}\sum_{\gamma m}|s_{\alpha i\gamma m}|^2K_{\gamma\gamma},
\end{aligned} \tag{B.12}$$

and

$$\begin{aligned}
M_1'' &\equiv \sum_{\gamma\delta}\sum_{mn}[s^\dagger]_{\gamma m\alpha i}s_{\alpha i\delta n}[s^\dagger]_{\delta n\beta j}s_{\beta j\gamma m}K_{\delta\delta} \\
&= \sum_{\delta m}[s^\dagger]_{\delta n\beta j}s_{\alpha i\delta n}\delta_{\alpha i\beta j}K_{\delta\delta} = \delta_{\alpha i\beta j}\sum_{\gamma m}|s_{\alpha i\gamma m}|^2K_{\gamma\gamma},
\end{aligned} \tag{B.13}$$

which gives us

$$M_1' + M_1^{ii} = 2\delta_{\alpha i\beta j}\sum_{\gamma m}|s_{\alpha i\gamma m}|^2K_{\gamma\gamma}. \tag{B.14}$$

Using

$$(f_\gamma - f_\delta)^2 = (f_\gamma - f_\alpha)^2 + (f_\alpha - f_\delta)^2 + 2(f_\gamma - f_\alpha)(f_\alpha - f_\delta), \tag{B.15}$$

together with the unitarity of the scattering matrix, we find

$$\begin{aligned} M_1''' \equiv & -\sum_{\gamma\delta}\sum_{mn}\left(s^*_{\alpha i\gamma m}s_{\beta j\gamma m}(f_\gamma - f_\delta)\right)\left(s^*_{\beta j\delta n}s_{\alpha i\delta n}(f_\gamma - f_\delta)\right) \\ = & \sum_{\gamma\delta}\sum_{mn}\Big\{ -\delta_{\alpha i\beta j}|s_{\alpha i\delta n}|^2(f_\alpha - f_\delta)^2 - \delta_{\alpha i\beta j}|s_{\alpha i\gamma m}|^2(f_\alpha - f_\gamma)^2 \\ & + 2s^*_{\alpha i\gamma m}s_{\alpha i\delta n}s^*_{\beta j\delta n}s_{\beta j\gamma m}(f_\alpha - f_\gamma)(f_\alpha - f_\delta)\Big\}. \end{aligned} \tag{B.16}$$

Combining $M_4$ with $M_1'$, $M_1''$ and using Eq. (3.125) we get

$$M_4 + M_1' + M_1'' = 2\delta_{\alpha i\beta j}\sum_{\gamma m}|s_{\alpha i\gamma m}|^2(K_{\alpha\gamma +}K_{\gamma\alpha}) + 2\delta_{\alpha i\beta j}\sum_{\gamma m}|s_{\alpha\gamma}|^2(f_\alpha - f_\gamma)^2. \tag{B.17}$$

Defining

$$M^r \equiv 2\delta_{\alpha i\beta j}\sum_{\gamma m}|s_{\alpha\gamma}|^2(f_\alpha - f_\gamma)^2, \tag{B.18}$$

we find

$$\begin{aligned} M_1''' + M^r = & \sum_{\delta n\gamma m} 2s^*_{\alpha i\gamma m}s_{\alpha i\delta n}s^*_{\beta j\delta n}s_{\beta j\gamma m}(f_\alpha - f_\gamma)(f_\alpha - f_\delta) \\ = & \, 2\,\mathrm{Re}\left\{\sum_{\delta n\gamma m} s^*_{\alpha i\gamma m}s_{\alpha i\delta n}s^*_{\beta j\delta n}s_{\beta j\gamma m}(f_\alpha - f_\gamma)(f_\alpha - f_\delta)\right\}. \end{aligned} \tag{B.19}$$

Using these calculations, we define the classical part of the correlator as

$$\begin{aligned} S^{(\nu)}_{\alpha\beta,\mathrm{cl}} \equiv & \frac{1}{2h}\sum_{ij}\int dE C^{(\nu)}_\alpha C^{(\nu)}_\beta \left\{M_1' + M_1'' + M_3 + M_4 - M^r\right\} \\ = & \frac{2}{h}\sum_{ij}\int dE C^{(\nu)}_\alpha C^{(\nu)}_\beta \left\{ -K_{\alpha\alpha}|s_{\beta j\alpha i}|^2 - K_{\beta\beta}|s_{\alpha i\beta j}|^2 + \delta_{\alpha i\beta j}\sum_{\gamma m}|s_{\alpha i\gamma m}|^2[K_{\alpha\gamma} + K_{\gamma\alpha}]\right\}, \end{aligned} \tag{B.20}$$

and the quantum part as

$$\begin{aligned} S^{(\nu)}_{\alpha\beta,\mathrm{qu}} \equiv & \frac{1}{2h}\sum_{ij}\int dE C^{(\nu)}_\alpha C^{(\nu)}_\beta \left\{M_1''' + M^r\right\} \\ = & \frac{2}{h}\int dE C^{(\nu)}_\alpha C^{(\nu)}_\beta \,\mathrm{Re}\left\{\sum_{ij\gamma m\delta n} s^*_{\alpha i\gamma m}s_{\beta j\gamma m}s_{\alpha i\delta n}s^*_{\beta j\delta n}(f_\alpha - f_\gamma)(f_\beta - f_\delta)\right\}. \end{aligned} \tag{B.21}$$

The autocorrelators become

$$S^{(\nu)}_{\alpha\alpha,\mathrm{cl}} = \frac{2}{h}\sum_i\int_0^\infty dE[C^{(\nu)}_\alpha(E)]^2\left\{\sum_{\gamma m\neq\alpha i}|s_{\alpha i\gamma m}|^2(K_{\alpha\gamma} + K_{\gamma\alpha})\right\}, \tag{B.22}$$

$$S^{(\nu)}_{\alpha\alpha,\mathrm{qu}} = \frac{2}{h}\sum_i\int_0^\infty dE[C^{(\nu)}_\alpha(E)]^2\left\{\sum_{\gamma m\neq\alpha i}|s_{\alpha i\gamma m}|^2(f_\alpha - f_\gamma)\right\}^2, \tag{B.23}$$

which concludes our derivations of the expression for the fluctuations used in this thesis.

# C
# Appendix 3

## C.1 Bosonic thermodynamic uncertainty relation without time reversal symmetry

In this section, we outline a failed attempt at deriving a TUR for bosonic systems without time reversal symmetry. This attempt followed the same approach as used by K. Brandner et. al. in Ref. [8], but as we will see, it does not yield a TUR for bosonic systems with broken time reversal symmetry. We begin from the quadratic form

$$A_\alpha^{\mathrm{cl}} = \frac{\sigma}{k_{\mathrm{B}}} - 2\psi x I_\alpha^{(0)} + \psi x^2 S_{\alpha\alpha,\mathrm{cl}}^{(0)}, \tag{C.1}$$

where $\sigma$ is defined as in Eq. (3.94), $I_\alpha^{(0)}$ is the expectation value of the particle current operator, and $S_{\alpha\alpha,\mathrm{cl}}^{(0)}$ is the classical part of its fluctuations. Since we are dealing with systems without time reversal symmetry, the scattering matrix and transmission probabilities are not symmetric, and we are restricted to using unitarity. We define

$$L[\mathcal{F}_\alpha] = \log[f[\mathcal{F}_\alpha]] - \mathcal{F}_\alpha, \tag{C.2}$$

where $\mathcal{F}_\alpha$ is defined as in Eq. (3.95) and $f[\mathcal{F}_\alpha]$ is the BE distribution

$$f[\mathcal{F}_\alpha] = \frac{1}{e^{-\mathcal{F}_\alpha} - 1}. \tag{C.3}$$

We note that

$$\frac{\partial}{\partial y} L[y] = \frac{1}{e^y - 1} = f[y], \tag{C.4}$$

and

$$\frac{\partial^2}{\partial^2 y} L[y] = \frac{e^y}{(e^y - 1)^2} \geq 0, \tag{C.5}$$

meaning that $L[\mathcal{F}_\alpha]$ is a convex function [8]. Furthermore, by using the unitarity of the scattering matrix together with renaming summation indices, we find

$$\sum_{\alpha\beta} D_{\alpha\beta}(E)(-L[\mathcal{F}_\alpha]+L[\mathcal{F}_\beta]) = \sum_{\alpha\beta} -D_{\beta\alpha}(E)L[\mathcal{F}_\alpha]+D_{\alpha\beta}(E)L[\mathcal{F}_\beta] = \sum_{\alpha\beta} D_{\alpha\beta}(E)(-L[\mathcal{F}_\beta]+L[\mathcal{F}_\beta]) = 0. \tag{C.6}$$

Using this we are able to rewrite the entropy production as

$$\sigma = \frac{k_{\mathrm{B}}}{h} \int dE \sum_{\alpha\beta} D_{\alpha\beta}(E) \left\{ f[\mathcal{F}_\beta](\mathcal{F}_\beta - \mathcal{F}_\alpha) + L[\mathcal{F}_\alpha] - L[\mathcal{F}_\beta] \right\}. \tag{C.7}$$

We note that due to Eq. (C.4) and the convexity of $L[y]$, that all terms inside the sum of Eq. (C.7) are positive [8]:

$$\begin{aligned} & f[\mathcal{F}_\beta](\mathcal{F}_\beta - \mathcal{F}_\alpha) + L[\mathcal{F}_\alpha] - L[\mathcal{F}_\beta] \\ \geq & f[\mathcal{F}_\beta](\mathcal{F}_\beta - \mathcal{F}_\alpha) + L[\mathcal{F}_\beta] - L[\mathcal{F}_\beta] + \left( \frac{\partial}{\partial \mathcal{F}_\beta} L[\mathcal{F}_\beta] \right) (\mathcal{F}_\alpha - \mathcal{F}_\beta) \\ = & f[\mathcal{F}_\beta](\mathcal{F}_\beta - \mathcal{F}_\alpha) + f[\mathcal{F}_\beta](\mathcal{F}_\alpha - \mathcal{F}_\beta) = 0. \end{aligned} \tag{C.8}$$

Rewriting $A_\alpha^{\mathrm{cl}}$ we find

$$\begin{aligned} A_\alpha^{\mathrm{cl}} = & \frac{1}{h} \int dE \sum_{\beta\neq\alpha} \sum_\gamma D_{\beta\gamma}(E) \Big\{ f[\mathcal{F}_\gamma](\mathcal{F}_\gamma - \mathcal{F}_\beta) - L[\mathcal{F}_\gamma] + g[\mathcal{F}_\beta] \Big\} \\ & + \frac{1}{h} \int dE \sum_\beta D_{\alpha\beta}(E) \Big\{ f[\mathcal{F}_\beta](\mathcal{F}_\beta - \mathcal{F}_\alpha) - L[\mathcal{F}_\beta] + g[\mathcal{F}_\alpha] \\ & + 2\psi x (f[\mathcal{F}_\alpha] - f[\mathcal{F}_\beta]) + \psi x^2 (f[\mathcal{F}_\alpha] + f[\mathcal{F}_\beta] + 2f[\mathcal{F}_\alpha] f[\mathcal{F}_\beta]) \Big\}. \end{aligned} \tag{C.9}$$

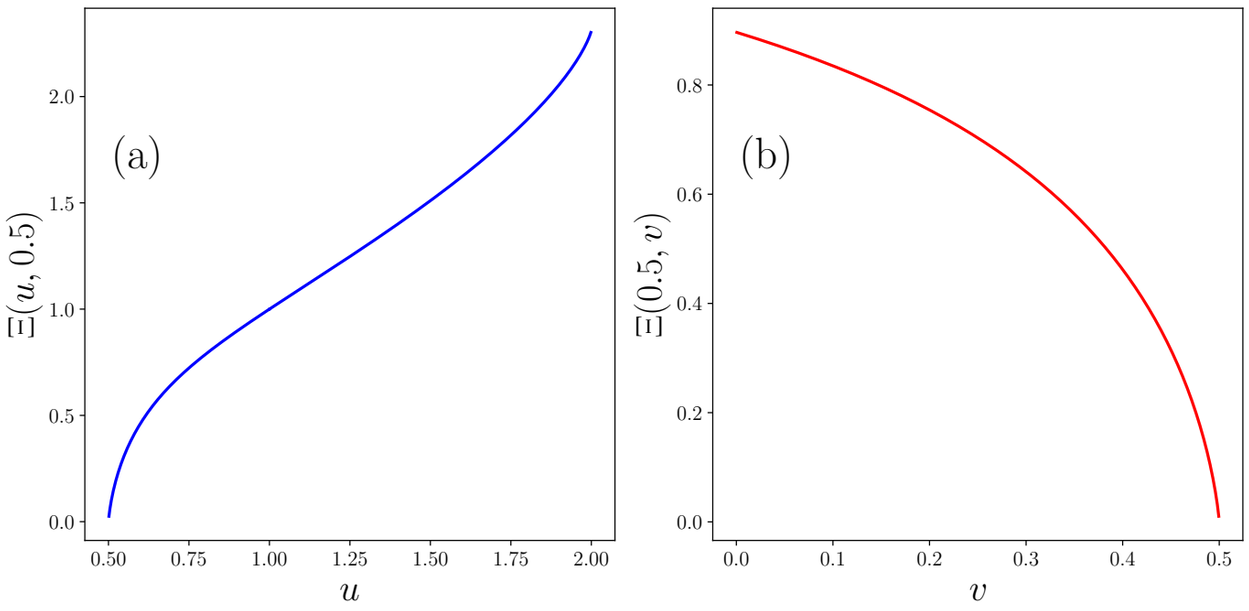


**Figure C.1:** Plots of the function $\Xi[u, v]$ where either $u$ or $v$ is kept fixed while the other one varies. It is clear from both plots that $\Xi[u, v]$ can get arbitrarily close zero, which in turn means that we cannot find a value of $\psi \geq 0$ such that $A_\alpha^{\mathrm{cl}} \geq 0$ for all $x$.

By defining

$$c_1 = (f[\mathcal{F}_\alpha] - f[\mathcal{F}_\beta]), \quad c_2 = (f[\mathcal{F}_\alpha] + f[\mathcal{F}_\beta] + 2f[\mathcal{F}_\alpha]f[\mathcal{F}_\beta]), \tag{C.10}$$

and minimizing Eq. (C.9) with respect to $x$, we find the following condition, which must be fulfilled for $A_\alpha^{\mathrm{cl}} \geq 0$ to hold:

$$f[\mathcal{F}_\beta](\mathcal{F}_\beta - \mathcal{F}_\alpha) - L[\mathcal{F}_\beta] + g[\mathcal{F}_\alpha] - \psi\frac{c_1^2}{c_2} \geq 0 \tag{C.11}$$

$$\implies \Xi \equiv \left\{f[\mathcal{F}_\beta](\mathcal{F}_\beta - \mathcal{F}_\alpha) - L[\mathcal{F}_\beta] + g[\mathcal{F}_\alpha]\right\}\frac{c_2}{c_1^2} \geq \psi. \tag{C.12}$$

Thus, we need to find the minimum of the function $\Xi$, which we do by introducing the variables $u$ and $v$ in analogy to Ref. [8]

$$u = e^{\mathcal{F}_\beta - \mathcal{F}_\alpha}, \quad v = e^{\mathcal{F}_\alpha + \mathcal{F}_\beta}, \tag{C.13}$$

which allows us to write

$$uv = e^{\mathcal{F}_\beta}, \quad \frac{v}{u} = e^{\mathcal{F}_\alpha}, \quad f[\mathcal{F}_\alpha] = \frac{1}{\frac{u}{v} - 1}, \quad f[\mathcal{F}_\beta] = \frac{1}{\frac{1}{uv} - 1}. \tag{C.14}$$

Importantly, these variables fulfill

$$u > v \geq 0, \quad 1 > uv, \tag{C.15}$$

due to requiring the BE distribution to be positive. Expressing $\Xi$ in terms of $u$ and $v$, we find

$$\Xi[u, v] = \frac{(u^2 + 1)\,(u - v)\left(-\log\left[\frac{v}{u}\right] + \log[uv] - (uv - 1)\left(\log\left[\frac{v}{u - v}\right] - \log\left[\frac{uv}{1 - uv}\right]\right)\right)}{(u^2 - 1)^2\, v}, \tag{C.16}$$

which can be seen plotted in Fig. (C.1) as a function of $u$ for a fixed $v$ in panel (a) and as function $v$ for a fixed $u$ in panel (b). It is clear from both panels that $\Xi[u, v]$ can get arbitrarily close zero, which in turn means that we cannot find a value of $\psi \geq 0$ such that $A_\alpha^{\mathrm{cl}} \geq 0$ for all $x$. In particular, we have that

$$\lim_{u \to v} \Xi[u, v] = 0, \quad \lim_{v \to u} \Xi[u, v] = 0. \tag{C.17}$$

While it should be noted that $u = v$ is problematic since

$$\lim_{u \to v} f[\mathcal{F}_\alpha] = \lim_{u \to v} \frac{1}{\frac{u}{v} - 1} \to \infty, \tag{C.18}$$

this still ultimately leads to us not being able to find a value for $\psi > 0$, which means that our derivation of a bosonic TUR for systems without time reversal symmetry has failed. It is, however, important to note that we have not disproved the viability of finding a TUR for these systems. To do this, we would need to find a concrete example where the TUR for the classical fluctuations is violated arbitrarily. We show this in Section. 3.2.1.1.

**DEPARTMENT OF SOME SUBJECT OR TECHNOLOGY**
**CHALMERS UNIVERSITY OF TECHNOLOGY**
Gothenburg, Sweden
www.chalmers.se


CHALMERS
UNIVERSITY OF TECHNOLOGY